

SAFETY EVALUATION BY THE OFFICE OF NUCLEAR REACTOR REGULATION

NEDC-33083P, "TRACG APPLICATION FOR ESBWR"

GE NUCLEAR ENERGY

PROJECT 717 - ESBWR PREAPPLICATION REVIEW

1.0 INTRODUCTION

By letter dated April 18, 2002, General Electric Nuclear Energy (GENE) requested a preapplication review of the economic simplified boiling water reactor (ESBWR) advanced passive reactor design. The ESBWR is a 4000 MWth (1390 MWe), natural circulation, boiling water reactor design, which utilizes passive safety systems. The staff has held several public meetings, including meetings with the Advisory Committee on Reactor Safeguards, to discuss the preapplication review scope and schedule, and the ESBWR design and technology basis. The staff documented the scope, schedule, and cost for the preapplication review in a letter to GENE dated December 19, 2002.

The preapplication review is focused on the TRACG thermal-hydraulic analysis computer code and the testing and scaling programs relevant to assessment of the computer code. The scope of the preapplication review does not address the design of the ESBWR. The scope of this safety evaluation report (SER) is limited to the application of TRACG to ESBWR loss-of-coolant accident (LOCA) analyses and the relevant testing programs and scaling analyses. The NRC's Offices of Nuclear Reactor Regulation and Nuclear Regulatory Research, and their contractors, performed this review.

2.0 REGULATORY BASIS

2.1 Regulatory Basis for Loss-of-Coolant Accidents

The requirements of 10 CFR 50.46 specify that each boiling or pressurized light-water cooled nuclear power reactor fueled with uranium oxide pellets within cylindrical zircaloy or ZIRLO cladding must be provided with an emergency core cooling system (ECCS) that must be designed so that its calculated cooling performance following a postulated LOCA conforms to the criteria contained in that section.

Section 50.46 states further that this requirement can be met through an evaluation model for which an uncertainty analysis has been performed, specifically, section 50.46(a) states that:

the evaluation model must include sufficient supporting justification to show that the analytical technique realistically describes the behavior of the reactor system during a loss-of-coolant accident. Comparisons to

applicable experimental data must be made and uncertainties in the analysis method and inputs must be identified and assessed so that the uncertainty in the calculated results can be estimated. This uncertainty must be accounted for, so that, when the calculated ECCS cooling performance is compared to the criteria set forth in paragraph (b) of this section, there is a high level of probability that the criteria would not be exceeded.

Section 50.46(b) specifies that the calculated peak cladding temperature (PCT) must not exceed 2200 EF, the maximum cladding oxidation must not exceed 0.17 times the total cladding thickness before oxidation, the maximum hydrogen generation must not exceed 0.01 times the hypothetical amount that would be generated if all of the metal in the cladding surrounding the fuel pellets were to react, the core must remain in a coolable geometry, and, after calculated successful ECCS initiation, the core temperature shall be maintained at an acceptably low level and decay heat shall be removed for the extended period of time required by the long-lived radioactivity remaining in the core.

2.2 Containment Regulatory Basis

The staff reviews the containment design to ensure compliance with the relevant requirements of General Design Criteria (GDC) 4, "Environmental and Dynamic Effects Design Bases," GDC 16, "Containment Design," GDC 38, "Containment Heat Removal," GDC 50, "Containment Design Basis," and GDC 53, "Provisions for Containment Testing and Inspection." The relevant requirements for this review are as follows.

GDC 16, insofar as it requires that reactor containment be provided to establish an essentially leak-tight barrier against the uncontrolled release of radioactivity to the environment;

GDC 38, insofar as it requires that a system to remove heat from the containment be provided, and that the system's safety function be to reduce rapidly, consistent with the functioning of other associated systems, the containment pressure and temperature following any LOCA and maintain them at acceptably low levels; and

GDC 50, insofar as it requires that the containment structure be designed so that it and its internal compartments can accommodate, without exceeding the design leakage rate and with sufficient margin, the calculated pressure and temperature conditions resulting from any LOCA.

Unlike the transient response for other containment designs where the containment pressure peaks rapidly, the ESBWR pressure transient does not rapidly increase to a peak value from which it must be rapidly reduced. The pressure increases slowly over several hours and is expected to remain well below the design limits for the duration of the transient (72 hours). The passive containment cooling system (PCCS) removes the decay heat from the containment and the containment pressure is determined by the transport of noncondensibles into the wetwell and the heat input to the containment. GENE concluded that the intent of GDC 38 can be satisfied by the use of a decay heat removal system that maintains the containment pressure

below the design pressure at all times. ESBWR calculations for radiological releases from the containment will be based on the assumption that the containment remains at the design pressure throughout the 72 hours, and no credit for pressure reduction will be used for design basis analyses during design certification.

The Standard Review Plan (SRP) for the Review of Safety Analysis Reports for Nuclear Power Plants, draft NUREG-0800, June 1996, describes the responsibilities and guidelines for the staff's review. The section of the SRP that is relevant to the TRACG analysis for the ESBWR is Section 6.2.1, "Containment Functional Design." Two statements from the introduction of SRP Section 6.2.1 relate directly to the staff's review of the use of the TRACG code for the analysis of the ESBWR Containment/LOCA response:

- *The containment structure must be capable of withstanding, without loss of function, the pressure and temperature conditions resulting from postulated loss-of-coolant, steam line, or feedwater line break accidents.*
- *GDC 50, among other things, requires that consideration be given to the potential consequences of degraded engineered safety features, such as the containment heat removal system and the emergency core cooling system, the limitations in defining accident phenomena, and the conservatism of calculational models and input parameters, in assessing containment design margins.*

Guidelines specific to boiling water reactor (BWR) pressure suppression containments are contained in SRP Section 6.2.1.1.C, "Pressure-Suppression Type BWR Containments." This SRP addresses GENE Mark I, II, and III pressure-suppression containments, and was also used by the staff as the basis for the review of the Advanced Boiling Water Reactor (ABWR) containment design. The ESBWR containment design has developed from the Mark III and ABWR containments. Therefore, these guidelines are considered by the staff to be an applicable basis for the review of the ESBWR containment analysis.

The SRP, developed prior to the promulgation of 10 CFR Part 52, provides a two-step approach to acceptance of calculated containment pressure and drywell/containment [wetwell] pressure differential. At the construction permit stage, the containment design pressure should provide at least a 15 percent margin above the peak calculated containment pressure, and the design differential pressure between drywell and containment [wetwell] should provide at least a 30 percent margin above the peak calculated differential pressure. At the operating license stage, the peak calculated containment pressure and the differential pressure between the drywell and the containment [wetwell] should be less than their respective design values.

The other containment acceptance criteria are related to missile and pipe whip protection (GDC 4), periodic inspections (GDC 53), containment dynamic loads, allowable bypass leakage rates, design leakage rate, containment negative pressures, external pressures, safety relief valve (SRV) in-plant tests, local suppression pool (SP) temperature limits during SRV discharges, and instrumentation for post-accident monitoring. These criteria are not relevant to

this TRACG application method review and they will be addressed by other analytical methods or procedures in the design certification application.

2.3 Standard Design Regulatory Basis

The Commission promulgated specific regulatory requirements for the acceptance, review, and approval of standardized nuclear power plant designs. Those requirements are found in 10 CFR Part 52. Specifically applicable to the review of the TRACG analysis methodology, 10 CFR 52.47(b), "Contents of Applications," requires the following:

(2)(i) Certification of a standard design which differs significantly from the light water reactor designs described in paragraph (b)(1) of this section or utilizes simplified, inherent, passive, or other innovative means to accomplish its safety functions will be granted only if

(A)(1) The performance of each safety feature of the design has been demonstrated through either analysis, appropriate test programs, experience, or a combination thereof;

(2) Interdependent effects among the safety features of the design have been found acceptable by analysis, appropriate test programs, experience, or a combination thereof; [and]

(3) Sufficient data exist on the safety features of the design to assess the analytical tools used for safety analyses over a sufficient range of normal operating conditions, transient conditions, and specified accident sequences, including equilibrium core conditions[.]

For the qualification of TRACG, GENE used a broad range of tests that span and bound the important ESBWR parameters and passive safety features. In particular, a full-scale prototype of the isolation condenser (IC) and a near-full scale PCCS were tested at PANTHERS. The various test programs are discussed in Section 3.7.1 of this report. Reduced scale PCCS units were tested at GIRAFFE (3 tubes) and PANDA (20 tubes), which confirmed the scaling basis for the PCCS. Integral tests were performed at the GIRAFFE and PANDA tests facilities. Both were full height simulations of the Simplified Boiling Water Reactor (SBWR), with different aspect ratios. PANDA is scaled to a system scale of 1:25 and GIRAFFE to a system scale of 1:400; that is, the volumes, flow areas, and power are scaled by these ratios for the SBWR. PANDA also simulated possible asymmetrical effects within the drywell and wetwell with two vessels for each region, situated a distance apart, corresponding to the diameter of the SBWR wetwell annulus. The ESBWR/SBWR relationship is discussed in Section 3.0 of this report.

For this phase of the ESBWR preapplication review, the staff's assessment of compliance with Section 52.47(b)(2)(i)(A)(3) is limited to the TRACG code for LOCAs only. The above regulations require that GENE provide data sufficient to assess the TRACG computer code, which is used to analyze ESBWR plant behavior in LOCAs. The staff expects GE to submit

additional topical reports related to the applicability of TRACG to ESBWR transients, including anticipated transient without scram (ATWS) and stability in October and November 2004. These topics are excluded from the scope of this review.

3.0 TECHNICAL EVALUATION

The GENE TRACG code is a proprietary methodological development based on the TRAC-BD1 code developed jointly by the NRC and GENE at the Idaho National Engineering Laboratory. The code has models and correlations that were developed at the commercial expense of GENE and are, thus, considered to be proprietary. The staff reviewed and approved the TRACG code for application to anticipated operational occurrences (AOO) in the current operating fleet of BWR/2-6s. The AOOs include the increase and decrease in heat removal by the secondary system, decrease in reactor coolant flow rate, reactivity and power distribution anomalies, and increase and decrease in reactor coolant inventory, all with reactor scram. The TRACG code was also reviewed and approved for application to prediction of the initial peak pressure for ATWS in the current operating fleet of BWRs.

The requirements for a realistic methodology in 10 CFR 50.46 are somewhat different than those for a prescriptive methodology in that more realistic models can be used and a measure of the uncertainty in the code must be determined. Various means of achieving an estimate of uncertainty are available. GENE has chosen to follow the basic Code Scaling Applicability and Uncertainty (CSAU) approach outlined in NUREG/CR-5249, Reference 5. While the CSAU approach defines the process by which uncertainty analysis is performed, it leaves room for the applicant to determine the exact statistical methodology to be applied. In both the AOO application of TRACG and the ATWS application, GENE chose to apply a Normal Distribution One-Sided Upper Limit statistical methodology. The approach taken for application of TRACG to the ESBWR LOCA event is somewhat different. A description of the methodology will be found in Section 3.14 of this SER.

ESBWR Safety System Overview

GENE submitted the ESBWR design description, Reference 15, in support of the review of the applicability of TRACG to ESBWR. The staff did not perform a detailed review of this document. The following descriptions are offered due to the unique nature of the systems and equipment not in use in the current commercial fleet of BWRs in the United States. The layout of the ESBWR safety systems are illustrated in Figure 3.0.1 in Section 8 of this report.

Editorial Note: In this report numerical values and their units are reported as received from the applicant. Conversions of units are provided for the convenience of the reader.

3.0.1 Gravity-Driven Cooling System

The Gravity-Driven Cooling System (GDCCS) is a low-pressure coolant injection system. The GDCCS and the Automatic Depressurization System (ADS) comprise the ECCS for the ESBWR. The GDCCS consists of three separate GDCCS pools, which are located in the upper containment

(with the pool bottom at about 33 ft above the top of active fuel), and piping with squib valves and check valves to connect the pools to the reactor pressure vessel (RPV). The gas space of each GDCS pool is individually connected to the wetwell (WW) gas space above the SP via a pipe, and the GDCS pools are completely isolated from the drywell (DW).

During a LOCA, cooling water drains from the GDCS pools to the RPV when it is nearly depressurized, so that the gravity driving head of the GDCS pools is sufficient to overcome the pressure difference between the RPV and the wetwell. The RPV depressurization is initially due to the break flow and is further enhanced by the ADS actuation (which by itself is a large-break LOCA), which occurs when the water level in the downcomer drops to 5.547 m (18.2 ft) above the top of active fuel (TAF).

The GDCS is passive in its actions in that no external alternating current (AC) electrical power source or operator action is necessary. Once the injection valves have opened, they remain open and are not capable of being closed or overridden by operator action.

An additional function of the GDCS is to provide cooling water to the drywell floor during a hypothetical severe accident. Note that the evaluation of severe accidents is outside the scope of the ESBWR preapplication review.

3.0.2 Passive Containment Cooling System

The PCCS is the ultimate heat sink of the reactor and containment systems during a design-basis accident (DBA), such as a LOCA. It maintains containment cooling for up to 72 hours after initiation of a LOCA, in which core decay heat arrives in the containment in the form of steam. The PCCS keeps the containment pressure below its design pressure of 413.7 kPa (60 psia) without using active safety systems. The PCCS consists of four low-pressure condensers submerged in a large pool of water (IC/PCCS pool) located outside and above the drywell. The inlet of the condensers is always open to the drywell. Steam or a steam/nitrogen mixture (the ESBWR containment is nitrogen-inerted during normal operation) enters a PCCS condenser via a steam inlet line in the drywell and the steam is condensed inside the vertical tubes of the condenser. Pool water outside of the condenser tubes boils off and the steam produced is vented to the atmosphere. Condensate inside the condenser tubes drains into a condensate drain tank that is connected to the RPV with a check valve and a squib valve in between. Noncondensable gas (which may include some uncondensed steam) is vented below the surface of the SP. The PCCS inlet lines, drain lines, and vent lines are always open.

3.0.3 Isolation Condenser System

The Isolation Condenser System (ICS) removes decay heat for the transients involving main steam line isolation and reactor scram. It is a passive, high-pressure system that has four isolation condenser loops as part of the reactor coolant pressure boundary. Each loop has an isolation condenser submerged in a large pool of water (IC/PCCS pool) located outside and above the drywell. Steam produced by the core decay heat rises in the core and flows through the chimney region and steam separators and dryers before it enters the ICS supply lines. The

steam is condensed inside the vertical condenser tubes, and the condensate drains into the RPV downcomer annulus and flows into the core to repeat the cycle. As the pool water outside the condenser tubes boils off, the steam produced is vented to the atmosphere. During normal operation, the ICS is in a ready-standby mode with all the steam supply lines fully open and all the drain lines closed with valves. When the main steam lines are isolated and the reactor is scrammed, the ICS is activated by the opening of the valves on the condensate drain lines. Each ICS condenser also has a vent line that is automatically operated to vent the noncondensable gas (produced by radiolytic decomposition of water) below the SP surface. The vent line can also be opened manually by the operator.

Unlike the GDACS, the ICS is not part of the ECCS and is the only safety related system that is not an engineered safety feature. As a result, no credit is taken in GE's analyses for ICS operation during a LOCA. Some of the integral system tests involving the concurrent operation of ICS and PCCS indicate that ICS operation tends to reduce the peak pressures of the RPV and containment. However, the design and testing of the ICS are not part of the ESBWR preapplication review.

3.0.4 Automatic Depressurization System

The ADS provides a rapid depressurization of the RPV. Activation allows the GDACS to provide coolant injection into the RPV during a LOCA. The ADS activates automatically when the water level in the downcomer drops to 5.547 m (18.2 ft) above the TAF by opening the SRVs and Depressurization Valves (DPVs) in groups. The only difference between the ESBWR ADS and the ADS of current operating BWRs is that the ESBWR DPVs discharge into the drywell.

3.0.5 Depressurization Valve

A DPV is a squib-type valve that remains fully open after the activation. Full-size testing of the DPV was successfully conducted by GENE to demonstrate its operation and reliability. However, the design and testing of the DPV are not part of the ESBWR preapplication review.

3.0.6 Vacuum Breaker

The Vacuum Breaker (VB) prevents the wetwell pressure from exceeding the drywell pressure by a specified value. It is a large check valve located between the drywell and the wetwell gas space. The VB is normally closed and will open only when the wetwell pressure has exceeded the drywell pressure by the specified value. GENE has conducted full-size VB tests to demonstrate its operation and reliability. However, technical evaluation of the VB testing program is not part of the ESBWR preapplication review.

3.0.7 Biased-Open Check Valve

A biased-open check valve is installed on each of the GDACS injection lines to the RPV. This type of check valve is designed to remain slightly open when there is no pressure difference across it. In addition, it can be magnetically opened or closed by an external direct current

(DC)-driven torque motor (for testing valve operation). The biased-open check valve by itself is not unique, but magnetically linking to a DC-torque motor is a unique design. However, technical evaluation of the check valve design and operation is not part of the ESBWR preapplication review.

3.0.8 Squib Valve

A squib valve is installed on each of the GDCS injection lines to the RPV. The valve is leakproof during normal ESBWR operation. After opening, the squib valve will remain fully open. This kind of squib valve is similar to, but smaller than, the DPV (which has been tested at full size). Technical evaluation of the squib valve design and operation is not part of the ESBWR preapplication review.

ESBWR/SBWR Relationship

The ESBWR design relies heavily on the integral systems and component test data developed for the SBWR. Justification is therefore needed for using the SBWR test data to qualify the TRACG code for ESBWR applications.

The ESBWR is basically a larger (4000 MWth) version of the SBWR (2000 MWth). Both designs have passive safety systems and components that will activate in a LOCA. Designs of the IC, DPV, VB, biased-open check valve, and squib valve are identical for both ESBWR and SBWR. However, a PCCS condenser in the ESBWR has about 35 percent more condenser tubes (at the same tube diameter, length, and pitch) and capacity than the PCCS in the SBWR.

From a LOCA perspective, the major difference between these two designs is that in the ESBWR, the GDCS pool gas space is connected to the wetwell gas space, while it is connected to the drywell in the SBWR. This design change provides additional gas space (during and after GDCS draining to the RPV) to accommodate the wetwell pressure in the ESBWR during a LOCA. As a result, the overall wetwell and drywell pressures may be lower in the ESBWR than in the SBWR for the same LOCA. There are also other differences. The ESBWR has a 10 foot active core compared to a 9 foot core in the SBWR. The ESBWR has a condensate drain tank in the drywell to collect condensate from the PCCS condenser, and the drain tank is connected to the RPV. In the SBWR, the PCCS condensate drains to the RPV via the GDCS pools in the drywell. The ESBWR has four larger (35 percent more tubes and capacity) PCCS condensers compared to three PCCS condensers in the SBWR. The ESBWR has four IC units (same size) compared to three IC units in the SBWR.

No new phenomena are expected to be introduced from the design differences between the ESBWR and SBWR.

CSAU Based Technical Evaluation

The CSAU methodology, discussed in References 5 through 8, consists of 14 steps contained within three elements. The first element include steps 1 through 6 and determines the event

specifications and code capabilities. The scenario modeling specifications are identified and compared against code capabilities to evaluate the applicability of the code to the specific plant and accident scenario. Code limitations are noted during Element 1.

The second element in the methodology includes steps 7 through 10 and assesses the capabilities of the code by comparison of calculations against experimental data to determine code accuracy, scale-up capability, and appropriate ranges over which parameter variations need to be considered in sensitivity studies.

The third element in the methodology consists of steps 11 through 14 and individual contributors to uncertainty, such as plant input parameters, state, and sensitivities, are calculated, collected, and combined with biases and uncertainties into a total uncertainty.

Element 1— Event Specifications and Code Capability

3.1 Step 1—Scenario Selection

The processes and phenomena that can occur during an accident or transient vary considerably depending on the specific event being analyzed. GENE has identified the LOCA and containment response in the ESBWR as the events to which the methodology under review will be applied. Application of the methodology to transients has not been considered in this review.

Reference 11, Table 2.4-2 indicates that the GDCS line break (GDLB) results in the lowest static head in the chimney of the three break locations examined, i.e., in the GDCS line, the main steam line, and the bottom drain line. At the design certification stage, GENE will need to provide supporting analyses for a spectrum of break locations to demonstrate that there is no core uncover for the possible break locations. Should core uncover occur, review of the TRACG code will be revisited to determine the adequacy of the applicable models and correlations.

The staff notes this is the first application that has been reviewed in which one single code is used to analyze the entire reactor coolant system/safety systems/containment as a single calculation.

GENE is consistent with this step in the CSAU approach.

3.2 Step 2—Nuclear Power Plant Selection

The dominant phenomena and timing for an event can vary significantly from one nuclear power plant design to another. GENE has specified the nuclear power plant (NPP) applicability for the methodology under review to be the advanced passive BWR design ESBWR.

GENE is consistent with this step in the CSAU approach.

3.3 Step 3—Phenomena Identification and Ranking

The behavior of an NPP undergoing an accident or transient is not influenced in an equal manner by all phenomena that occur during the event. A determination needs to be made to establish those phenomena that are important for each event and various phases within an event. Development of a Phenomena Identification and Ranking Table (PIRT) establishes those phases and phenomena that are significant to the progress of the event being evaluated.

Important phenomena for LOCAs in the ESBWR have been identified in two PIRTS—LOCA/ECCS and LOCA/containment. The PIRT for LOCA/ECCS includes all the high-ranked and medium-ranked phenomena in the RPV, main steam lines, and ICS, including system interactions. The PIRT for LOCA/Containment covers all the high-ranked and medium-ranked phenomena in the drywell, wetwell, GDCS, PCCS, DPVs, VBs, main vents (between the drywell and wetwell), and SRV quenchers. Both top-down and bottom-up processes were conducted by a team of experts to obtain these phenomena, which were later used for TRACG assessment. A diagram of these processes is shown in Figure 3.3.1.

The two PIRTS were further evaluated and revised according to the results of the scaling analysis. The revision either confirmed or downgraded, with few exceptions, the ranking of some high-ranked phenomena. The exceptions were the addition of the mass flow through the break during the GDCS injection phase and long-term cooling phase of the LOCA, mass flow through the SRVs/DPVs during the GDCS injection phase of the LOCA, flashing/redistribution in the control rod guide tube region, and flashing in the downcomer annulus during the GDCS injection phase of the LOCA to the high-ranked phenomena.

The staff identified a weakness in the PIRT that needs to be corrected in the ESBWR design certification application. The PIRT in the application needs to include the long-term cooling phase of the LOCA. Since the long-term cooling phase is not expected to introduce any new phenomena that were not reviewed at the preapplication phase, and since the long-term cooling phase is highly design dependent, the staff concluded that the addition of the long-term cooling phase to the LOCA/ECCS PIRT is not necessary at the preapplication phase. Should new phenomena be found to occur during the long-term cooling phase, the appropriate models and correlations in the TRACG code will be revisited by the staff.

GENE is consistent with this step in the CSAU approach, but needs to include the long-term cooling phase in the PIRT for the ESBWR design certification review.

3.4 Step 4—Frozen Code Version Selection

The version of a code, or codes, reviewed for acceptance should be “frozen” to ensure that after an evaluation has been completed, changes to the code do not impact the conclusions and that changes occur in an auditable and traceable manner. GENE has specified that the TRACG04 code, which is under configuration control, was used for the ESBWR LOCA application. GENE performed the initial assessments with the TRACG02A code and then transitioned to the TRACG04 code. GENE submitted all affected assessment cases using the

TRACG04 code. The staff has reviewed the assessment cases and has determined that they are acceptable.

GENE is consistent with this step in the CSAU approach.

3.5 Step 5—Provision of Complete Code Documentation

This step is to provide documentation on the frozen code version such that evaluation of the code's applicability to postulated transient or accident scenarios for a specific plant design can be performed through a traceable record. GENE has provided the necessary documentation through submittal of ESBWR-specific documentation, SBWR-specific documentation, and reference to code documentation in the possession of the staff from the previous review of the TRACG code reported in References 1 and 2. The staff reviews of References 1 and 2 are discussed in References 3 and 4.

The staff review of the documentation, most notably References 9 and 10, disclosed numerous errors and omissions which GENE has committed to address in a revised TRACG model description topical report. This should be submitted prior to submission of the design certification application for the ESBWR design. The documentation supporting the application of TRACG to the ESBWR design, the scaling, and the testing programs is found in References 11 through 17.

GENE is consistent with this step in the CSAU approach.

3.6 Step 6—Determination of Code Applicability

An analysis code used to calculate a scenario in an NPP should use many models to represent the thermal-hydraulics and components. Those models should include the following four elements:

1. *Field equations*—provide code capability to address global processes.
2. *Closure equations*—provide code capability to model and scale particular processes.
3. *Numerics*—provide code capability to perform efficient and reliable calculations.
4. *Structure and Nodalization*—address code capability to model plant geometry and perform efficient and accurate plant calculations.

The TRACG code application to the ESBWR plant design is in two areas—the reactor coolant system response to a LOCA, and the containment system response to the LOCA. The use of a single thermal-hydraulic computer code for both simulations couples the two systems. Previous analyses of NPP response to LOCAs have made use of separate, independent computer codes for these two systems. The staff review and evaluation of the TRACG code will address the

application of the code to each of these systems. In each case, the appropriateness of the code modeling of the above elements will be addressed.

3.6.1 ESBWR TRACG LOCA Applicability

TRACG employs a two-fluid model for two-phase flow. It solves six conservation equations for both the liquid and gas phases, along with phasic constitutive relations for closure. In addition, a boron transport equation and a noncondensable gas mass equation are solved. The spatially discretized equations are solved by donor-cell differencing in staggered meshes in one, two, or three dimensions.

TRACG employs basic component models as building blocks to construct physical models for intended applications. Such an approach renders it a very general and flexible tool to simulate a wide variety of systems. The components that are modeled include pipe, pump, valve, tee, channel, jet pump, steam separator, steam dryer, vessel, upper plenum, heat exchanger, and break and fill as boundary conditions.

3.6.1.1 Thermal-Hydraulics Model

TRACG employs a two-fluid model for two-phase flow. It solves six conservation equations for both the liquid and gas phases, along with phasic constitutive relations for closure. In addition, a boron transport equation and a noncondensable gas mass equation are solved. The spatially discretized equations are solved by donor-cell differencing in staggered meshes in one, two, or three dimensions. TRACG is used for both reactor vessel and containment. However, the current version of the model description report, Reference 10, does not address the phenomena occurring in the containment making it necessary to also use Reference 9 for that material.

The model equations are presented with assumptions. The three dimensional formulation has mixing terms to account for turbulent mixing and molecular diffusion. This is a good feature, but the mixing model is qualitative and has not been qualified. The critical flow model and counter-current flow limit (CCFL) models are applied to the velocity field calculated from the field equations. The code formulation resets the velocities to conform to these models. It is important that when velocities are reset, the mass balance is maintained.

The action of steam flowing upward can impede the downward flow of cooling water and lead to the counter-current flow condition. GENE has assessed the TRACG CCFL model with data from the CSHT test facility. Comparisons, Reference 34, for liquid temperatures near saturation, versus TRACG demonstrate that the code provides excellent agreement for saturated liquid. Agreement with subcooled liquid is excellent with steam flow rates which are less than the condensation capacity. For flow rates greater than the condensation capacity, the average deviation between liquid downflow predicted by TRACG is within the measurement error. Accordingly, the staff concludes that TRACG adequately predicts saturated CCFL and subcooled CCFL breakdown.

3.6.1.2 Heat Conduction

TRACG solves the heat conduction equation for the fuel rods (in cylindrical geometry) and for structural materials (in slab geometry) in the system. The latter has either a lumped slab model or a one-dimensional slab model.

The strengths of the TRACG heat conduction model are the sophisticated transient gap conductance model and the implicit solution method that couples the heat transfer between the fuel rod and the coolant by iteration. The staff concludes that TRACG appropriately provides for solution of heat conduction.

3.6.1.3 Flow Regime Maps

A two-fluid formulation relies upon models for estimating interfacial transfer rates for mass, momentum, and energy. The models for interfacial processes, in turn, rely on the shape and size of the interface. The common practice is to develop flow regime maps to identify the distinct regime for two-phase distribution. The knowledge of the flow regime allows the code to select applicable correlations for transport processes.

The flow regime maps are generally two-dimensional maps between void fraction and mass flux. TRACG has used this approach to identify the two-phase flow regimes. It also has correlations for entrainment for dispersed flow regimes.

The staff questioned a lack of definitions and GENE has committed to incorporate the missing definition for E_p , and new equations for the transition criterion between churned turbulent and annular flow, including the drift velocity term, in the next revision of Reference 10.

3.6.1.4 Models and Correlations

The list of constitutive models covers all important phenomena that may occur in a BWR, SBWR, or ESBWR. The unified flow regime map is a strong point. TRACG models and correlations consist of models for interfacial shear, wall friction and form losses, critical flow, two-phase level tracking, interfacial heat transfer, and wall heat transfer.

The interfacial shear model was derived from the drift flux model using available experimental data at steady state. The models are based on current state-of-the-art technology and have been assessed with a large database covering the range of conditions that are expected in the reactor. The code uses a critical Weber number criterion for estimating interfacial area density or bubble/droplet diameter. However, there are differences in the way this approach is used for interfacial momentum and heat transfer in bubbly flow and droplet flow. The interfacial shear is assessed, Reference 34, through the capability of TRACG to predict void fraction data including single tube data, rod bundle data, and data for large hydraulic diameters. The test conditions used in assessment cover both adiabatic tests, where there is no effect of heat transfer on the void fraction, and heated tests. The tests cover a wide range of flow conditions with pressure, flow rate, and inlet subcooling varied. Comparisons between TRACG and test data from

sources such as the FRIGG and Christensen tests show calculations to be within the measurement error for the tests. The staff concludes this demonstrates acceptable capability to predict interfacial shear.

The wall friction and form losses are important for predicting single- and two-phase flows. The code has standard models consisting of Moody curves for single-phase flow and a two-phase multiplier based on the Chisholm correlation. Similarly, there is a standard model for form losses for abrupt area changes. The staff recognizes that simplifying assumptions are often necessary or expedient in computer code simulation of two-phase flow phenomena. However, the induced errors due to simplifying assumptions should be understood. GENE has determined those errors in the assumption of consistent wall friction and form loss partitioning between phases through code assessments using data from the FRIGG, Christensen, Wilson, and Bartolomei test programs, Reference 34. In all assessment cases, the prediction-measurement standard deviation was shown to be on the order of the measurement error. In addition, wall friction assessments have been performed using data from the ATLAS facility over a range of flow conditions. The prediction-measurement comparisons show a calculated error rate on the order of the measurement error. The staff concludes these assessments demonstrate acceptable capability to predict wall friction and form loss.

Critical flow is calculated using coarse-mesh nodalization and semi-empirical approximation for choking criteria. The critical flow model also allows for choking in the presence of noncondensable gases. The critical flow model in TRACG has been assessed against data from the Marviken critical flow tests, Pressure Suppression Test Facility (PSTF), and the Edwards test. The Edwards test and the PSTF tests are small scale tests and the Marviken tests are large scale tests. Comparisons of TRACG versus the Marviken tests showed a distinct drop in discharge flow at the transition from liquid blowdown to two-phase blowdown. In each blowdown period the measured and predicted mass flows were in good agreement, with the predicted bounding the measured. Timing of the transition were also in good agreement. The predicted mass flows were generally conservative compared with the data in the smaller scale tests. Comparison of TRACG predictions versus data from tests in different scale test facilities show that TRACG generally overpredicts the data and is therefore conservative. The critical flow model is detailed, well defined, and acceptable for predicting choked flow.

A two-phase level may exist in the bypass, lower plenum, downcomer, chimney, drywell, and wetwell. The two-phase level-tracking model invokes some approximations for the void fraction above and below the mixture level that may not be accurate if significant voiding occurs below the mixture level. Furthermore, the model uses an arbitrary cutpoint α_{cut} and $\Delta_{\alpha_{cut}}$ for level detection. A level is detected when the $[\alpha_{cut} - \Delta_{\alpha_{cut}}]$. It is further assumed that void fraction above the level is the same as the void fraction in the cell above the level, and the void fraction below the level is the same as that of the cell below the cell with the level. Level position can then be computed. The model has been assessed with Pressure Suppression Test Facility (PSTF) level swell tests. Comparisons of predicted versus measured level indicate that TRACG was generally able to predict the measured level to an accuracy consistent with the measurement uncertainty. Sensitivity studies were also performed on nodalization, convergence ratio, and time step size.

Little sensitivity was found in the studies. The staff concludes that level swell is adequately modeled in TRACG as evidenced by the code predictions falling within the experimental measurement uncertainty.

Vapor generation or flashing is an important phenomenon for any depressurization transient such as a LOCA. The vapor generation is predicted by energy balance at the interface, where the differences in heat fluxes result in phase change. TRACG has a mechanistic model for interfacial heat transfer that depends upon interfacial area and the shape of the interface. The interface is defined on the basis of flow regime. The model has been assessed with a variety of tests. TRACG predictions were reasonable, indicating that the models are applicable to LOCAs. Staff request for additional information (RAI 54) concerns limits on different characteristics in bubbly flow (and also droplet flows), such as the upper limit on bubble size and number density. RAI 57 concerns interfacial area in stratified flows for which TRACG predicts a much larger interfacial area than the smooth interface. As is the case with all thermal-hydraulic system codes today, there is an inconsistency in interfacial area used for momentum transfer and heat transfer in bubbly and droplet flows.

Wall heat transfer was rated high in many components during a LOCA in the GENE PIRT. TRACG has a very detailed model based on the boiling curve. The model has standard heat transfer regimes—single-phase liquid or vapor, nucleate boiling, critical heat flux, transition boiling, film boiling, and condensation with and without the effect of noncondensibles. There are correlations for transitions between different heat transfer regimes, such as the minimum stable film boiling temperature. The correlations for different regimes are standard correlations from the literature. However, for critical heat flux, TRACG has a proprietary correlation, the General Electric Critical Quality Boiling Length correlation (GEXL), based on the critical quality concept for normal flows, and which uses a modified Zuber correlation for low flows and flow reversal. The GEXL correlation has been approved by NRC for specific fuel designs. The GEXL correlation is expected to be qualified through experimental data for the ESBWR-specific fuel bundle. The code has been assessed with a variety of tests that have become the standards for assessing wall heat transfer. The assessments include THTF tests for film boiling heat transfer, CSHT tests that include thermal radiation heat transfer, and THTF tests for boiling transition, as well as ATLAS critical power data. The staff concludes the breadth and accuracy of the assessment cases demonstrates acceptable capability for TRACG to predict wall heat transfer.

TRACG has a rewet model for post-critical heat flux (CHF) heat transfer. The rewet model is not well described and should be expanded in the revised report.

3.6.1.5 Component Models

TRACG employs basic component models as building blocks to construct physical models for intended applications. Such an approach renders it a very general and flexible tool to simulate a wide variety of systems. The components that are modeled include pipe, pump, valve, tee, fuel channel, jet pump, steam separator, steam dryer, vessel, upper plenum, heat exchanger, and break and fill as boundary conditions. However, a turbine model for balance of plant (BOP)

simulation is missing. The heat exchanger model contains some simplifying approximations that may not be appropriate for simulating the isolation condenser or the condenser in BOP. However, GENE is not using the heat exchanger model for simulating either the PCCS or the ICS. On the positive side, TRACG has very sophisticated upper plenum, steam separator, and steam dryer models.

However, since the steam separator is not considered important in the GENE PIRT, it is modeled by a simple semi-empirical model. The model is based on the assumption that the vapor core has solid body rotation and the thin film has azimuthal velocity decaying as the inverse of the square root of the radial position. The model has four constants that are determined by comparing the prediction with the full-scale performance data.

3.6.1.6 Gap Conductance

All section and equation references in the following discussion of Gap Conductance are found in Reference 10.

Section 7.5.2, Fuel Pellet Gap Conductance, describes the thermal conductance model for the gap between the fuel pellet and the cladding of a fuel rod. Section 7.5.3, Cladding Perforation, describes the model that predicts the perforation of the fuel rod cladding.

The review of Sections 7.5.2 and 7.5.3 has resulted in a number of RAIs (68-87). This is due mainly to insufficient documentation of model descriptions in Reference 10. It is understood that the dynamic gap models in TRACG are consistent and similar to the SAFER/GESTR models previously approved by the NRC and also reviewed in the TRACG application for AOOs, Reference 3. The scope of Reference 10, in terms of documentation, is clear from the statement in Section 1.2 of the report that says, "This document is intended to be a complete, stand-alone description of TRACG." The main objective of the review of Sections 7.5.2 and 7.5.3 is not to reevaluate the technical validity of the dynamic gap models, but rather to evaluate the adequacy of the model description and the implementation and integration of the models in TRACG.

The review has resulted in a number of RAIs that suggest the need to provide more detailed description of the models. The following is a list of areas that need better documentation.

1. proper identification of reference for each equation
2. provide basis for determining the values of model constants
3. more detailed description of model parameters
4. proper identification and definition of variables in model equations.

The TRACG transient gap conductance model is comparable to the model in SAFER, Reference 30, that has been reviewed and approved by NRC. The TRACG gap conductance

model is also consistent with another NRC-reviewed and approved code, GESTR-LOCA. The initialization of the TRACG gap conductance model is done by retrieving data calculated by GESTR-LOCA using fuel pellet exposure and power as inputs. The model equations are presented in Section 7.5.2 without reference to their sources. An example is Equation (7.5-7) that is similar to the Ross and Stoute model and yet no reference was cited for the model.

The gap conductance is modeled as the sum of the contributions from radiation heat transfer (Section 7.5.2.1), thermal conduction through the gas mixture in the asymmetric radial gap (Section 7.5.2.2), and conduction through the fuel/cladding contact spots (Section 7.5.2.3). The conductance of the gas in the radial gap depends on the effective gap size, and accounts for the asymmetric radial displacement of cracked pellet wedges (Section 7.5.2.4). The contact conductance depends on the size of the gap after accounting for fuel and cladding thermal expansion (Section 7.5.2.5). Section 7.5.2.6 discusses the implementation and initialization of the gap conductance model, including the determination of the gap gas composition (Section 7.5.2.6.1) and the initial gap size (Section 7.5.2.6.2). The assessment of the gap conductance models is briefly described in Section 7.5.2.7.

The radiation heat transfer between the fuel pellet and cladding is modeled by a conventional radiation heat transfer coefficient with separate thermal emissivities for the pellet and clad surface.

The conductance across the gas gap is calculated as the gas gap thermal conductivity divided by an effective gap modified for temperature jump at the gas-solid interface and the effect of discontinuous gas gap due to contact spots. The gas in the gap is composed of helium and fission gas. An effective thermal conductivity is calculated for the gap gas. The helium pressure, composition of the fission gas, and the relative amount of xenon and krypton in the fission gas are all obtained from the GESTR fuel files.

After cladding perforation, the gas conductivity is adjusted to reflect the presence of a stoichiometric mixture of steam and hydrogen from metal-water reaction. The constants in the equation for the gas conductivity in a perforated fuel rod are TRACG input constants.

The contact pressure (P_c) is zero when the hot gap size is greater than or equal to zero. In this context the hot gap size is defined as,

$$\text{Hot gap size} = R_{ci} - R_{fo}$$

The initial interaction (I_i) is determined from Equation 7.5-30, while the hot outer fuel radius (R_{fo}) and the hot cladding inner radius (R_{ci}) are calculated from Equations 7.5-25 and 7.5-26, respectively.

The model for the effective gap size (R_{eff}) accounts for the thermal expansion of the fuel pellet and the cladding. It also takes into consideration the effects of cladding hoop stress and plastic strain on the gap size.

The R_{f_0} is calculated as the sum of the reference fuel outer radius (R_{ref}) and differential growth from thermal expansion. R_{ref} is calculated as a function of the exposure history and the linear heat generation rate (LHGR) used to accumulate that exposure. It does not vary with time during the transient and is evaluated in Equation 7.5-31 at an initial reference temperature (T_{ref}).

The calculation of the hot clad inner radius considers the effects of thermal expansion and hoop stress. Different models are used if the cladding has begun to yield or has perforated.

The interface between GESTR-LOCA and TRACG is discussed in relation to the initialization of the transient gap model implemented in TRACG. TRACG depends on GESTR-LOCA to provide the steady-state conditions for the dynamic gap model. The documentation did not discuss the variables that are passed from the TRACG thermal-hydraulic and neutronic calculations to the gap model. A brief discussion of the coupling between the gap model and the rest of TRACG was provided by GENE.

The ratio of krypton to xenon (F_{kx}) is a built-in constant in the GESTR model and cannot be set through input. For typical TRACG applications, the fraction of additional fission gas released F_r is selected to have a value of [[]]. If a prolonged temperature increase were expected, a larger fraction would be appropriate.

Given the initial total gap conductance (h_g) from the GESTR-LOCA output, the initial gap size ($R_{eff, i}$) and the initial contact pressure (P_{ci}) are calculated by solving Equation 7.5-7 [[]].

GENE's response to RAI 79 is the only documented information provided that verifies the TRACG implementation of the gap model against the SAFER model. This comparison of gap conductance calculated by TRACG and SAFER shows that the results are indeed comparable.

The TRACG cladding perforation model needs cladding hoop stress and cladding temperature inputs from the code calculation. The fuel rod cladding hoop stress is a function of the difference between the fuel rod internal gas pressure and the external coolant pressure. Section 7.5.3.1 discusses the calculation of the cladding hoop stress and the internal gas pressure. The contribution of the plenum gas temperature to the overall internal gas pressure is discussed in Section 7.5.3.2. The utilization of the hoop stress and cladding temperature in the rod perforation model is outlined in Section 7.5.3.3. The assessment of the perforation model is discussed in Section 7.5.3.4.

The internal gas pressure is calculated by considering gas in the volume along the length of the fuel column and the gas in the fuel rod plenum. Outputs from GESTR-LOCA are used to calculate the initial fuel column volume to temperature ratio. [[

]]. The perforation model applies to any point along the length of the fuel rod and is not limited just to the point of peak LHGR (RAI 80). The use of [[

]] is explained in the response to

RAI 82 as leading to a conservative overestimation of the cladding hoop stress. The staff concludes that this use of the NRC-approved GESTR-LOCA method to set initial steady-state conditions is acceptable. In addition, the resulting cladding hoop stress is conservatively predicted.

The use of the same subscript 'f' in Equation 7.5-35 to refer to two different materials, gas in fuel column and fuel pellet, is confusing. In response, GENE has agreed to update the next version of the documentation.

The cladding average temperature at the maximum LHGR axial position is used in calculating the growth in the volume of the fuel gas plenum in a transient due to thermal expansion. An empirical factor of $[[\quad]]$ is used to account for the fact that the temperature change considered at the maximum LHGR axial position overestimates the length-averaged temperature change for the whole fuel column.

The plenum gas temperature is calculated separately from the gas temperature in the gap of the fuel column.

Rod perforation is evaluated in the following sequence:

TRACG calculates cladding hoop stress and cladding temperature. A curve in Reference 10, Figure 7.5-5, gives the cladding rupture stress as a function of the cladding temperature. Cladding plastic deformation is assumed to commence at a cladding temperature $[[\quad]]$ below the perforation temperature.

1. Plastic strain is assumed to occur when the cladding hoop stress exceeds the cladding rupture stress corresponding to a cladding temperature $[[\quad]]$ above the current cladding temperature.
2. The cladding strain is calculated by multiplying the strain ratio obtained from Figure 7.5-6 by the strain at rupture. The strain ratio is shown in Reference 10, Figure 7.5-6, as a function of the perforation temperature minus the cladding temperature. It varies from $[[\quad]]$ percent at a delta T of $[[\quad]]$ to 100 percent at a delta T of $[[\quad]]$. The rupture strains were determined from experimental data.

Elastic strain is recovered when a cladding perforation occurs. This has a small impact on the gap size because the irrecoverable plastic component of the total strain is much larger than the elastic strain.

The TRACG gap perforation model is comparable to the model in SAFER, a code previously reviewed and approved by NRC. The cladding rupture stress and plastic strain are based on experimental data and have been reviewed. GENE's response to RAI 79 has demonstrated that the fuel gap models in Sections 7.5.2 and 7.5.3 calculated transient gap responses that agree very well with those calculated by SAFER/GESTR.

The description of the TRACG dynamic gap model will be updated by GENE by incorporating all responses to the RAIs in the approved version of Reference 10, thereby providing a level of detail consistent with a stand-alone document.

3.6.1.7 Neutron Kinetics Model

For LOCA application, TRACG uses core power as input as a table with power as a function of time. The table is generated with their neutronic calculation. A comparison with American Nuclear Society (ANS) 5.1 (1994) is shown and results compare very well after 4 seconds when decay power dominates. The model is conservative as it predicts higher power than the standard for the first 4 seconds when fission power is still continuing. The kinetics model has been assessed through comparisons with SPERT reactivity insertion test data. The staff finds these test data to be acceptable for assessment and sufficient accuracy has been demonstrated to find the TRACG neutron kinetics model acceptable.

3.6.1.8 Numerics

TRACG numerics are a significant improvement over its predecessor TRAC-BD1/MOD1. As a default, TRACG employs fully implicit integration for hydraulic equations. For time-domain stability analyses, TRACG uses an optional explicit integration because the implicit integration may suppress real physical oscillations. The fully implicit integration is accomplished by means of a predictor-corrector iterative technique. The detail of the explicit integration is not described and should be included in the upcoming revised report along with time step control criteria.

TRACG solves the heat conduction equations by implicit integration. The heat transfer coupling between the heat conduction and coolant hydraulics is also treated implicitly via an iterative technique. This implicit coupling represents a significant improvement over commonly used explicit coupling, which may incur an error on the phase shift and amplitude in a thermally induced oscillation.

Once again, the time step control algorithms are not described for heat conduction and need to be included in the revised documentation.

3.6.1.9 Thermodynamic and Material Properties

The thermodynamic properties used in TRACG are calculated from polynomial fits to steam table data for water and from the ideal gas law for the noncondensable gases. The thermodynamic property routines cover a very wide range of pressures ($1.0 \text{ Pa} < P < 45 \text{ MPa}$) and temperatures ([liquid] $273.15 \text{ K} < T_l < 714 \text{ K}$, and [vapor] $273.15 \text{ K} < T_v < 3000 \text{ K}$). Separate liquid and vapor property fits are given along with their fitting constants. The accuracies or uncertainties of these property routines have been mentioned, and it is an improvement from the previous version of TRACG documentation.

The material properties used in TRACG are based on the "GE Material Properties Handbook," which is an extensive library of temperature-dependent properties of nuclear fuel (UO_2 , zircaloy

cladding, zirconium oxide, heater rod insulator, and boron nitride insulator) and structure materials (stainless steel 304 and 316, carbon steel, Inconel 600, and concrete). The accuracies or uncertainties of these material property routines are not stated, and should be clearly stated and referenced in the revised report.

3.6.1.10 Summary

TRACG is a detailed best-estimate BWR transient analysis code, Reference 10. It is based on a two-fluid thermal-hydraulic model for the reactor vessel, primary coolant system and containment, and three-dimensional neutron kinetics model for the reactor core. The modular approach used makes it a general-purpose system code with unnecessary assumptions and approximations minimized as practicable. However, the state of the art does not permit it to eliminate all the important assumptions and approximations necessary at the present time. Assessment of TRACG models has been performed against an adequate data base, and the results have been shown to be sufficiently accurate, generally within the measurement error or standard deviation, to demonstrate that the TRACG models are capable of representing the phenomena anticipated to occur in an ESBWR LOCA event.

3.6.2 ESBWR TRACG Containment Applicability

TRACG will be used for the calculation of the containment pressure and temperature response. The RPV will also be modeled to provide the boundary conditions needed for the containment analysis, and to provide the mass and energy releases into the containment following a LOCA or main steam line break (MSLB). The entire transient will be calculated by TRACG, starting with the postulated LOCA, and including the blowdown, GDCS, and long-term PCCS phases. GENE has taken an approach for qualification and application of TRACG for the ESBWR containment analysis which includes an evaluation of the TRACG models against appropriate test data representative of the ESBWR design. In addition, the approach also includes some elements of a CSAU methodology to define the important phenomena (PIRT), to identify the uncertainties in the TRACG models, and to define the sensitivity of the containment peak pressure to these parameters.

GENE is following a bounding application approach for the containment analysis. Modeling assumptions in the TRACG application bound several key phenomena. [[

]] This conservative TRACG model is used to perform the analysis of the ESBWR containment response. A “nominal” analysis is obtained by setting the other model parameters and plant initial conditions to their expected values. A “bounding” analysis is obtained by setting these other model parameters and plant initial conditions to conservative values to maximize the calculated containment pressure response. A comparison of the bounding and nominal calculations can be used to indicate the margin inherent in the bounding calculation. The bounding calculation will be used to demonstrate margins to the design limits and will be the basis for review of the containment design during the design certification review to demonstrate compliance with GDC 16, 38, and 50.

To ensure a complete PIRT evaluation, the entire spectrum of events was considered by GENE, including events with less limiting conditions than the design basis case with no auxiliary power. The approach used by GENE focused on the design basis cases, in terms of equipment and systems available. This led to the most severe consequences and the greatest challenges to the analytical models in modeling the phenomena. While there are some differences in the assumptions made for the evaluation of different breaks, these were not important in determining the phenomenological progression of the LOCA or the importance of various parameters. The limiting LOCA from the perspective of margin to core uncover is a large liquid line (GDCS line) break. The limiting LOCA from the perspective of containment pressure is the MSLB. Chapter 6 of the Design Certification Document will include the entire matrix of calculations for postulated pipe rupture locations and single failures.

3.6.2.1 Containment Components

The containment is modeled with TRACG as a combination of a three-dimensional vessel component in conjunction with one-dimensional components, such as pipes, tees, and valves. All these components utilize the same conservation equations and constitutive correlations. The following addresses the correlations for wall heat transfer, interfacial heat transfer, wall shear, and interfacial shear.

BWR containments utilizing the pressure suppression principle have similar components. The ESBWR containment is similar in concept to the Mark III and ABWR containments, in that a horizontal vent system is employed to transfer blowdown energy from the drywell to the SP. In addition, the ESBWR design is equipped with a PCCS for long-term decay heat removal.

A schematic of the ESBWR containment and the corresponding TRACG computer code representation can be found in Reference 11.

The TRACG computer code employs all of the physical models needed for analyzing traditional BWR designs (i.e. drywell, pressure suppression system, including vents connecting drywell and wetwell and the VB check valves), and also employs models for the passive containment safety systems (i.e., the PCCS which transfers the drywell energy to the outside atmosphere and designed primarily for the long term containment cooling). In addition, the code is capable of analyzing the behavior of the GDCS which couples the behavior of RPV and containment. In ESBWR the PCCS is totally independent from the GDCS and its pools.

TRACG will be used to perform design basis containment LOCA analysis for the entire transient (i.e., starting with the postulated LOCA and including the blowdown, GDCS, and long-term PCCS phases). In general, the code was developed to perform best-estimate calculations. However, TRACG does not have specific models for multidimensional (3-D) effects like mixing and stratification, thus limiting the code's capability to correctly calculate several key containment phenomena, i.e., the [[

]]. Therefore, to address these phenomena the code is to be used in

a conservative mode by performing "bounding" calculations, i.e., by setting the values of appropriate parameters to maximize the calculated containment pressures and temperatures.

The staff has reviewed the proposed approach and concluded that it satisfies the NRC guidelines specified in Section 6.2.1 of the SRP with regard to calculated wetwell and drywell peak pressure and temperature, and, therefore, is acceptable.

The following contains a brief description of TRACG containment models.

3.6.2.1.1 Drywell

The drywell is composed of an upper drywell, bounded by the drywell head, top slab, containment walls, and the diaphragm floor separating it from the wetwell. The upper drywell constitutes the largest portion of the drywell volume. A break in the main steam line as well as the opening of the DPVs would discharge flow into this region. The annulus region of the drywell comprises the region between the RPV and the inner wall of the wetwell horizontal vent duct system. A break in the GDCS line would be expected to discharge flow into this region. The lower drywell is a separate region that is connected to the drywell annulus by 10 vents of 1.2 m outside diameter (OD). Liquid discharged into the upper drywell or the annulus region (e.g., from a broken GDCS line connected to a GDCS pool) will drain into the lower drywell. A break in the bottom drain line would discharge flow to the lower drywell.

The drywell is modeled as a two-dimensional (axisymmetric) region, with [[]] in the upper drywell and [[]] in the annular and lower drywell regions. This allows natural circulation patterns to develop, if calculated, [[]]. The three-dimensional conservation equations for mass, momentum, and energy are applied in this region.

3.6.2.1.2 Wetwell

The wetwell consists of the suppression pool and the wetwell gas space. The wetwell is bounded by the diaphragm floor on top, containment outer wall, and wetwell inner wall on the sides and the floor of the containment. During blowdown, flow from the SRVs is directed to the SP and quenched via the SRV discharge lines. Flow from the LOCA break and DPVs is directed from the drywell to the SP and quenched via the SP horizontal vent system. Any flow through the passive containment cooling (PCC) vents is also discharged to the SP.

Wetwell Gas Space

The wetwell gas (steam and noncondensibles) space is also represented by multidimensional cells. Typically, [[]] rings and [[]] axial levels are employed in the TRACG model. This would allow for natural circulation in this region. The flow regimes in this region will be the same as in the drywell— single-phase gas, dispersed droplets resulting from entrainment from the suppression pool, and a condensate film on the walls. The models involved in the calculation include turbulent shear between cells, noncondensable distribution, wall friction,

interfacial friction, wall heat transfer, fogging and interfacial heat transfer, and heat transfer at the SP interface. These models are discussed in the next section.

Suppression Pool

The SP is also represented by multidimensional cells. [[]] rings and [[]] axial levels are used to represent the pool. The major phenomena of interest for the SP include steam condensation with or without noncondensable presence, temperature distribution, thermal stratification, and pool two-phase level.

3.6.2.1.3 GDCS Pools

Three separate GDCS pools are located in the upper containment and are isolated from the drywell. During the GDCS phase of the post-LOCA transient, the GDCS pools discharge into the RPV downcomer, following the opening of squib valves and check valves in the four divisionally separated GDCS lines. In the ESBWR configuration, the GDCS pools do not receive condensate from the PCC units.

Following an initiating event, the GDCS is activated by rapid opening of the squib valves allowing water flow into the RPV. Typically, the GDCS pools are about 50 percent drained down in about an hour, and will still be partially filled at the end of 72 hours following a DBA.

The GDCS pools are also modeled as part of the containment model. In practice, two pools are represented, with one accounting for the volume of two of the three pools. The main phenomenon of interest for the GDCS pool is the pool level and the associated inventory of water in the pool. The two-phase level model is also applicable here. Heat transfer at the pool surface is modeled analogously to that for the SP.

3.6.2.1.4 Passive Containment Cooling Pools

The four PCC pools are located outside (above) the containment. Each contains a PCC unit. The four pools are interconnected with each other and with the IC pools.

The pools are represented as part of the 3-D TRACG region, partitioned into the IC and PCC pools. The pools are allowed to communicate with each other at the bottom and the top. [[]]. The pools are modeled with [[]] rings each and with [[]] axial levels. Heat transfer occurs from the PCC headers and tubes to the water in the pools. Pool side heat transfer is calculated either by a [[]] for boiling heat transfer or by single phase convection to liquid [[]] for subcooled conditions.

3.6.2.1.5 Passive Containment Cooling Units

The ESBWR has four PCC heat exchanger units. Each is comprised of two-module drum and tube heat exchangers using horizontal upper and lower drums connected with a multiplicity of vertical tubes (336 tubes per module). Two identical modules are coupled to form one PCC heat exchanger unit. The PCC units are represented by one-dimensional components simulating the inlet piping, headers, condenser tubes, condensate discharge lines, and vent lines. One-dimensional forms of the mass, momentum, and energy equations are applicable. Heat is transferred through the walls of the tubes and headers to the respective pools. Heat transfer inside the tubes is calculated using the [[]].

The PCCS can operate in two distinct modes—a condensation mode and a pressure differential mode. In the condensation mode, the steam is condensed in the vertical tubes and the condensate is drained from the lower drum to the individual unit's drain tank. In the pressure differential mode, the flow through the PCC heat exchangers is caused by a drywell-wetwell pressure difference. Since the PCC vent line outlet is about 0.9 m higher than the outlet of the upper horizontal drywell/wetwell LOCA vents, the flow path through the PCCS is the preferred path for most of the long-term, post-accident conditions. In any case, noncondensibles and uncondensed steam are vented to the suppression pool.

3.6.2.1.6 Horizontal Vent System

The ESBWR has 30 horizontal vents between the drywell and the SP. There are 10 vertical flow channels each containing three horizontal vents attached to a vertical vent pipe. The top row of horizontal vents is approximately 0.9 m below the bottom of the PCC vents. The remaining two rows of vents are each vertically separated by 1.37 m.

The horizontal vents are represented by [[]]. The vent component is shown in more detail in Figure 9.6 in Reference 11.

3.6.2.1.7 GDCS Equalizing Lines

Four GDCS equalizing lines (one per division) connect the SP to the RPV downcomer. During the long-term cooling phase of the post-LOCA transient, the squib valves in these lines will open if the level in the downcomer drops to 1 m above the top of the active fuel and a time delay of 30 minutes has elapsed.

The equalizing lines are represented by a [[]]. The correlations used for wall friction and singular losses are the same as used for the horizontal vents.

3.6.2.1.8 Vacuum Breakers

The ESBWR has three VBs connecting the upper drywell to the wetwell gas space. The VBs will open when the pressure in the wetwell is higher than that of the drywell by a specified value.

The VBs are represented by one-dimensional VALVE components. VBs are lumped together as one component. The VBs are triggered open at a set negative pressure differential between the drywell and wetwell. They will close at a lower value of the pressure differential. The VBs transport flow from the wetwell gas space to the drywell at conditions corresponding to the cell

in the wetwell gas space to which they are connected. The correlations used for the singular losses are the same as for the horizontal vents.

3.6.2.1.9 TRACG Physical Models

Heat Transfer Modes

In the drywell, the important modes of wall heat transfer include forced and free convection to vapor and condensation heat transfer. Inside the PCCS tubes the predominant mode is wall condensation heat transfer. Under conditions where noncondensibles severely degrade steam condensation, forced convection from the vapor to the wall will become the mode of heat transfer. In the wetwell, the dominant mode is interfacial heat transfer at the pool interface.

Table 3.6.1 summarizes TRACG heat transfer modes for containment. The equations and figures quoted below refer to Reference 9.

Table 3.6.1
TRACG Heat Transfer Modes

Heat Transfer Mode	Correlation in TRACG Model Description [Reference 9]	DW	WW	PCC
condensation on vertical/horizontal surfaces	[[]]	x	x	
condensation in vertical tubes	[[]]			x
HT from PCC to outside pool	subcooled/nucleate boiling - [[1-phase convection for $T_w < T_{sat}$, [[]]			x x
interfacial HT at suppression pool surface ¹	[[]]		x	
single phase HT to wall	[[]]	x	x	

¹ Note: This interfacial heat transfer model may be replaced with a more appropriate model for design certification analyses. (See Section 3.6.2.3, "Phenomena Identification and Ranking," Item WW4: Free Surface Condensation/Evaporation, and Section 4.0 "Confirmatory Items," Item 16.)

For forced convection, TRACG uses the Dittus-Boelter correlation (Equation 6.6-3), based on the cell velocities and properties. The hydraulic diameter of the cell in the direction of the wall is used in the correlation. The vapor properties are calculated at the cell fluid temperature.

For free convection, the McAdams correlation (Equation 6.6-22) is used. Again, the cell temperature is used for the calculation of vapor properties and the cell hydraulic diameter for the calculation of the Grashof number. (The heat transfer coefficient is independent of the hydraulic diameter when correlations of the form $h \sim Gr^{1/3}$ are used.)

TRACG evaluates both the free and forced convection correlations and uses the greater of the two calculated values, whether the surface is horizontal or vertical.

For the condensation mode, a Nusselt condensation correlation can be used with multiplicative factors for shear enhancement and degradation by noncondensibles. The Nusselt correlation is expressed in Equations 6.6-66 and 6.6-67. In these equations, the liquid film Reynolds number is calculated based on the condensate flow rate per unit perimeter of surface and the liquid viscosity. However, the recommended (default) TRACG method is the [[]]. As a lower bound, when the noncondensable fraction is below about [[]], the [[]] correlation is available. [[]].

For interfacial heat transfer at the pool interface, the interfacial heat transfer coefficients on the vapor and liquid sides of the interface are defined by Equation 6.5-28. The [[]], is used to calculate degradation of heat transfer at the pool surface due to noncondensable gases.

The staff reviewed the applicability of the wall heat transfer correlations and found them to be acceptable for modeling of the ESBWR containment behavior for the following reasons. Except for the [[]] correlation, the employed heat transfer models are widely used and accepted in the scientific and engineering practices. The [[]] correlation was developed specifically for PCCS-like conditions based on limited, small scale experiments. As applied in the TRACG methodology, the [[]] correlation was successfully tested against SBWR-specific experiments performed at the PANTHERS and PANDA test facilities. The comparison with the test data was favorable, at least on a global parameters level. Therefore, the staff finds the heat transfer models to be acceptable.

Also, the staff reviewed the applicability of the [[]] correlation to the ESBWR interfacial heat transfer at the pool interface. The staff acknowledges that interfacial heat transfer in general is a complex phenomenon and the available physical models are subject to substantial uncertainties. Since the sensitivity study performed by GENE indicates that this phenomenon has a relatively small effect on the peak containment pressure, the staff finds the TRACG interfacial heat transfer at the pool interface to be acceptable. This interfacial heat transfer model may be replaced with a more appropriate model for design certification analyses. (See Section 3.6.2.3, "Phenomena Identification and Ranking," Item WW4: Free Surface Condensation/Evaporation, and Section 4.0 "Confirmatory Items," Item 16.)

Vent Clearing Model

The rising drywell pressure forces the steam and nondensifiable gas mixture to flow through the vertical flow channels into the horizontal vent piping, pushing the water through the horizontal vents. As the water level drops in the vertical section to "uncover" a horizontal vent row, the vents in each row will be opened to allow flow of steam and noncondensable gas to the suppression pool. This phenomenon is referred to as "vent clearing." Vent clearing terminates the initial pressure rise in the drywell, as the pressure is relieved by the vent discharge to the SP. The vents can clear during the early blowdown. As the blowdown flow rate decreases, the water level in the vertical pipes will rise to cover each row of vents. Eventually, the top row is also covered and flow will persist only through the PCC vents. Following vent clearing, the wetwell gas space pressurizes as the noncondensibles from the drywell are purged into that volume. The drywell pressure is maintained higher than the wetwell by an amount corresponding to the PCC vent submergence.

In the prediction of vent clearing and the associated drywell and wetwell pressure histories, the following phenomena are important:

Level Tracking in the Vertical Vent Pipes

The one-dimensional component level tracking model described in Reference 10, Section 6.4 is employed in the vertical pipe that is connected to the three horizontal vents.

Vent Flow Regime

The flow regime in the vents is single-phase liquid, until the vent begins to uncover when it transitions rapidly to bubbly flow. The flow to the vent is "donor celled" at the upstream conditions in the vertical pipe. TRACG calculates a transition from stratified to dispersed flow based on the instability of the interface (Reference 10, Equation 5.1-23).

Pressure Drop Correlations

The single-phase friction factor is obtained from Reference 10, Equation 6.2-2. The Reynolds number is calculated based on the axial velocity in the cell and the hydraulic diameter of the cell. The pressure drop in the vent is actually dominated by the inlet and exit form loss coefficients. A two-phase multiplier will be applied for wall friction as shown in Reference 10, Equation 6.2-5. For singular losses, Reference 10, Equations 6.2-7 and 6.2-8 are applicable.

Vent Back Pressure

As the vent discharges vapor into the suppression pool, it will tend to move the liquid in the pool above the vent upwards as it expands. The inertia of this liquid tends to create a back-pressure effect, reducing the discharge flow, and affecting the drywell pressure after vent clearing. This effect is accounted for in the TRACG momentum equation. The liquid mass in the inner ring

immediately above the discharge location accelerates upwards as the vapor expands into the pool.

Model Assessment

The vent clearing model in TRACG has been assessed by comparison against data from PSTF. Reference 10, Figure 7.11-5 shows a schematic of the facility. In the 5703 series tests, the drywell was connected by a set of three full-scale Mark III horizontal vents to an eight degree simulation of the Mark III suppression pool. A rupture disk in the blowdown pipe simulated the break of a main steam line, and a venturi downstream of the rupture disk set the size of the simulated break. The blowdown flow, the vent flow and the drywell and wetwell pressure were monitored.

Reference 10, Figure 7.11-6 shows a comparison of the measured and predicted drywell pressures for Test 5703-1. Figure 7.11-7 shows a comparison of the measured and calculated vent flow rates. Figure 7.11-6 shows that TRACG follows the drywell pressure rate accurately until the time of vent clearing at 0.8 seconds. TRACG also calculates the time of vent clearing correctly, as seen from Figure 7.11-7. Following the onset of vent clearing, TRACG undercalculates the vent flow, and the drywell pressure increases to a higher value than seen in the data. The discrepancy is due to large vapor bubbles rapidly transiting through the top part of the vent at the inception of vent uncovering. This flow regime is not captured by TRACG. A higher calculated two-phase inertial pressure drop in this transient phase delays the increase in the vent flow, and introduces a lag in the calculated transient response. Subsequent to this period, the transient is captured adequately by TRACG.

The staff did not review details of the TRACG vent clearing model. Instead, the staff reviewed the provided comparison between the TRACG calculation and the PSTF test data and finds the comparison to be consistent with the staff's previous evaluations of the BWR pool dynamic analyses, and therefore, to be acceptable.

Break flow

Critical flow through the break is calculated using the model evaluated in Section 3.6.1.4 of this document. For the reasons set forth in that section, the staff finds this model to be acceptable.

Noncondensable Distribution

TRACG has mass continuity equations for multiple species of noncondensibles in addition to steam (Reference 10, Equation 3.1-14). A noncondensable species is treated as a perfect gas and its properties are specified in terms of the gas constant, R and the specific heat C_p , (Reference 10, Section 6.6.1 1). The noncondensable gas (or mixture of gases) has the same temperature and velocity as the steam in a given cell. The partial pressure of the noncondensable is calculated based on the temperature and mass of the gas in a cell (Ideal Gas Law). Dalton's law (Reference 10, Equation 3.1-17) relates the partial pressures of steam and

noncondensibles to the total pressure. Note that the steam need not be at saturation conditions corresponding to its partial pressure.

The TRACG model for molecular diffusion of noncondensibles driven by concentration gradients is not used. Noncondensibles are transported by bulk convection. Diffusion effects will be small for nitrogen and air. Transport by diffusion could be more significant for hydrogen. Buoyancy effects are not treated at a local level (i.e., steam and noncondensibles have the same velocity in a cell). However, buoyancy effects will be accounted for on a global level. For example, if a light noncondensibile is injected into a cell, a natural circulation pattern will develop between adjacent rings, and lighter fluid will rise to the upper regions.

The distribution of noncondensibles calculated by TRACG was assessed through comparisons against data from the GIRAFFE and PANDA facilities. Based on these comparisons, GE recognized limitations in TRACG's capability to adequately predict mixing and distribution of noncondensibile gases. A bounding analysis approach is proposed for the ESBWR analysis. The staff agrees with GENE's conclusions and, since it is conservative, accepts the proposed bounding approach.

Wall Friction Correlations

The flow regime in the drywell is mostly single-phase gas. In some cells, a dispersed droplet high void fraction regime may exist. This corresponds to cells where liquid from the break or from the GDCS pool with a broken line is falling to the lower regions of the drywell. In some cells, a liquid film can form on the wall because of condensation. The single-phase friction factor is obtained from Equation 6.2-2, Reference 10. The Reynolds number is calculated based on the axial velocity in the cell adjacent to the wall and the hydraulic diameter of the cell in the direction of the wall. In case a two-phase flow regime is present, a two-phase multiplier will be applied as shown in Equation 6.2-5, Reference 10.

Similarly, the flow regime at the inlet to the PCC is single-phase vapor and/or gas mixture. Due to condensation, a liquid film forms inside the vertical tubes. The exit conditions consist of a draining liquid film and a gas mixture that is rich in noncondensibles. The single-phase friction factor is obtained from Equation 6.2-2, Reference 10. The Reynolds number is calculated based on the axial velocity in the cell and the hydraulic diameter of the cell. In the condensing region, a two-phase multiplier will be applied as shown in Equation 6.2-5, Reference 10.

The staff reviewed the employed model and finds it to be acceptable, since expected flow regimes are either single- or two-phase.

Turbulent Shear Between Cells

The TRACG model for turbulent shear between cells at cell boundaries is not being used since the nodalization employed ensures the presence of a wall surface in every cell and such nodalization ensures that no flowing gas is in contact with another stream of gas. All flows in the drywell are driven by buoyancy and wall shear.

The staff reviewed the employed model and finds it to be acceptable.

Interfacial Shear Correlations

For the droplet flow regime, the models described in Section 6.1.5, Reference 10, will be employed to calculate the interfacial shear between vapor and droplets. For cells with wall liquid films, the annular flow correlations in Section 6.1.4, Reference 10, are used.

The staff reviewed the employed model and, since the model includes all expected two-phase flow regimes, finds it to be acceptable.

Interfacial Shear Correlations

For cells with wall liquid films, the annular flow correlations in Section 6.1.4, Reference 10, are used.

The staff reviewed the employed model and finds the correlations used to be appropriate for the expected flow regimes and, therefore, to be acceptable.

Fogging of Drywell Vapor

Heat transfer from the vapor in a cell will result in cooling of the vapor. If the temperature drops below the saturation temperature of the steam corresponding to its partial pressure, condensation will occur. Generally, in this situation a cold wall will be present in the cell. A liquid film will form on the surface because of condensation. This will typically be the dominant form of condensation in the cell. However, if the bulk temperature drops below the saturation temperature, a small amount of liquid droplets will be formed (fogging) by condensation of steam on the airborne impurities. In this situation, a droplet flow regime will exist. Interfacial heat transfer between droplets and vapor will be calculated as per Section 6.5.5, Reference 10. Interfacial shear between the droplets and steam is calculated using the models in Section 6.1.5, Reference 10.

In general, heat transfer from the vapor is more likely to lead to condensation on the walls. Fogging is more likely to occur as a result of adiabatic expansion of steam from pressures higher than 30 bar.

The staff reviewed the employed model for fogging in the drywell and finds it to be acceptable because the pressure in the drywell is expected to remain well below 30 bar, and the effects of fogging on heat transfer in the drywell is not significant.

Condensation of Vapor Bubbles

In the presence of noncondensibles, the bubbles will include steam and noncondensibles. The partial pressure of steam and noncondensibles will be calculated as stated earlier. The interfacial heat transfer from the liquid to the vapor is calculated according to Equations 6.5-8, and 6.5-9, Reference 10. There is no degradation in heat transfer due to the presence of noncondensibles. Humboldt Bay, Reference 21, and Bodega Bay, Reference 22, large-scale data show complete condensation of the vapor in the suppression pool. All of the liquid and vapor entering the pool from the vent system remained in the pool.

The staff reviewed the employed model and finds it to be acceptable because a sensitivity study performed by GENE indicates that this phenomenon has a relatively small effect on the peak containment pressure. This interfacial heat transfer model may be replaced with a more appropriate model for design certification analyses. (See Section 3.6.2.3, "Phenomena Identification and Ranking," Item WW4: Free Surface Condensation/Evaporation, and Section 4.0 "Confirmatory Items," Item 16.)

Pool Temperature Distribution

[[

]]. Figure 7.11-3, Reference 10, shows the results from a number of large-scale tests. The measured temperature at the top of the pool has been compared with calculations using the empirical model described above. All data are predicted either well or conservatively.

The limitations of TRACG to adequately predict pool temperature distribution based on a first principle approach is recognized by GENE. The staff agrees with this assessment. The staff reviewed the proposed empirical model and, since it is conservative, finds it to be acceptable.

Pool Level

The two-phase level model described in Section 6.4, Reference 10, is used to calculate the pool level. The liquid and vapor side interfacial heat transfer coefficients are calculated with Equation 6.5-28, Reference 10. [[

]].

The staff reviewed the employed model and finds the correlation used appropriate for the expected thermodynamic conditions. Further, the correlation is acceptable because a sensitivity study performed by GENE indicates that this phenomenon has a relatively small effect on the peak containment pressure. This interfacial heat transfer model may be replaced with a more appropriate model for design certification analyses. (See Section 3.6.2.3,

“Phenomena Identification and Ranking,” Item WW4: Free Surface Condensation/Evaporation, and Section 4.0 “Confirmatory Items,” Item 16.).

3.6.2.2 Large Main Steam Line Break Description

The important features of the transient resulting from a large break in the main steam line are described for each phase of the accident.

3.6.2.2.1 Blowdown Period

This period is characterized by a rapid depressurization of the RPV through the break, SRVs and DPVs. The steam blowdown from the break and DPVs pressurizes the drywell, forcing a mixture of steam and noncondensable gases through, and then clearing, the main containment vents and the PCCS vents. The steam is condensed in the SP and the noncondensable gas collects in the wetwell gas space above the SP.

For the MSLB, the blowdown flow quickly increases the drywell pressure to the scram setpoint, and a control rod scram occurs. The high velocities in the steam line initiate closure of the main steam line isolation valves (MSIVs) and the reactor isolates in 3 to 5 seconds. This trip also opens the IC drain valves, but no credit is taken in the design basis analysis for heat removal by the ICS. High drywell pressure isolates several other systems, including the containment atmosphere control system purge and vent, the fuel and auxiliary pool cooling system, the high and low conductivity sumps, the fission product sampling system, and the reactor building heating, ventilating, and air conditioning (HVAC) exhaust.

Loss of feedwater and flow from the break cause the RPV water level to drop. Without external makeup, the Level 1 (L1) trip will be reached in about 6 minutes. (During this period, the ICS, if available, would be removing energy and reducing pressure and break flow.) After a 10-second delay to confirm the L1 condition, the ADS logic starts a timed sequential opening of the SRVs, DPVs and the GDCS injection valves. The SRVs open in several stages to stagger SRV line-clearing loads in the suppression pool and to minimize the RPV level swell. Blowdown through the break, the SRVs, and the DPVs causes a level swell in the RPV. The two-phase level in the RPV downcomer decreases at the end of the blowdown period, when GDCS injection begins.

In the containment, the steam entering the drywell increases its pressure, opening the main containment vents and sweeping most of the drywell noncondensable gas through the main vents, through the SP, and into the wetwell gas space. (Depending on the location of the break, a substantial portion of the noncondensibles in the lower drywell region may remain in that region and bleed out slowly later in the transient). During the blowdown phase of the transient, the majority of the blowdown energy is transferred into the SP by condensation of the steam flowing through the main vents. The increase in the drywell pressure causes flow through the PCCS, which also absorbs part of the blowdown energy. Based on GENE’s response to staff RAI 314.2, about 15 percent of the blowdown energy is absorbed by the PCCS with most of the energy being absorbed in the SP. The ADS, activated by the measured

RPV downcomer level, opens the SRVs and the DPVs, and augments the steam flow to the SP and drywell, respectively. The blowdown period of the accident lasts about 10 minutes.

3.6.2.2.2 GDCS Period

This period begins when the pressure difference between the RPV and the wetwell is small enough to enable flow from the GDCS pools to enter the RPV. This is the period during which the GDCS pools drain their inventory. Depending on the break, the pools are drained in between 1 and 6 hours. The GDCS flow fills the RPV to the elevation of the DPVs (below the main steam line) break and then the excess GDCS flow spills over into the drywell. The GDCS period is characterized by condensation of steam in the RPV and drywell, depressurization of the RPV and drywell, and the possible openings of the vacuum breakers, which returns noncondensable gas from the wetwell gas space to the drywell.

Quenching of voids in the core by the GDCS flow reduces the steam outflow from the RPV to the drywell. Once the GDCS flow begins, the drywell pressure begins to decrease. The decrease in drywell pressure stops the steam flow through the PCCS and main vents. This pressure decrease may be sufficient to open the VBs between the drywell and the wetwell gas space. Draining of the GDCS pools also helps to reduce the containment pressure as more wetwell volume becomes available for the noncondensibles in the wetwell gas space. Once GDCS flow begins to spill from the RPV into the drywell, the drywell pressure drops further and additional VBs may open. If the VBs open, some of the noncondensable gas in the wetwell gas space will return to the drywell through the VBs. The GDCS period of the transient continues until the water level in the GDCS pools equalizes with the collapsed level in the downcomer of the RPV and the decay heat is able to overcome the subcooling of the GDCS inventory in the RPV. Then, the drywell pressure rises and flow is reestablished through the PCCS. The PCCS heat removal capacity, even while recycling noncondensable gas back to the wetwell, is sufficient to condense the steam generated by decay heat without reopening the main vents. This period of the accident is expected to last for less than 1 hour.

3.6.2.2.3 Long-Term Cooling Phase

During this period, the noncondensable gas that reentered the drywell through the VBs is returned to the wetwell. Condensate from the PCCS is recycled back into the RPV through the PCCS drain tank in the drywell. The most important part of the LOCA transient for the RPV response is the blowdown period and the early part of the GDCS period when the RPV is reflooded and inventory restored. For some breaks (e.g., bottom drain line break (BDLB)), the equalizing line from the SP to the RPV may open during the long-term cooling period to provide the RPV an additional source of makeup water if the water level in the downcomer falls to 1 meter above the elevation of the TAF. For the containment, the blowdown phase determines the initial pressurization. During the GDCS phase, the pressure levels off and decreases as the GDCS flow to the RPV first shuts off steaming from the RPV and later spills over into the drywell, condensing steam in the drywell. At the end of the GDCS phase, noncondensibles that returned to the drywell because of VB openings are returned to the wetwell gas space, and the PCCS assumes the decay heat load.

After the drywell pressure transient initiated by the GDCS flow is over, the drywell pressure reaches equilibrium slightly above the wetwell gas space pressure. The MSLB is the limiting break in terms of containment pressure and temperature, as most of the noncondensibles are swept out from the drywell into the wetwell in the initial blowdown phase. This part of the containment transient is similar to that for the GDLB. However, unlike the GDLB, the steam generated by the decay heat is condensed in the PCCS and all of it is returned to the RPV via the PCCS drain tanks. Thus, there is no long-term drop in the downcomer and chimney water levels due to boiloff. A larger amount of water inventory is retained inside the RPV and a smaller amount in the lower drywell.

3.6.2.3 Phenomena Identification and Ranking

The critical safety parameters for the containment/LOCA analyses are the peak pressures and temperatures in the drywell and wetwell of the containment. These safety parameters are the criteria used to judge the performance of safety systems (the PCCS) and the margins in the design (to the allowable design pressure and temperature).

The short-term drywell pressure response is governed by energy deposition from the break flow and the DPV discharge flow. Energy removal from the drywell is through the main vent flow, the PCCS flow, and from condensation on walls and internal structures. The pressure difference necessary for clearing of the main vents controls the initial pressure increase in the drywell. Energy deposition in the wetwell is through the main vent flow, and flow through the SRV quenchers and PCCS vent lines. Thermal stratification of the SP is a key factor in determining how this energy is distributed within the SP; it sets the SP surface temperature and, therefore, the temperature and steam partial pressure in the wetwell gas space.

Another key parameter controlling the short-term wetwell pressure response is the extent to which the noncondensibles (nitrogen) initially in the drywell are purged to the wetwell during the initial blowdown. The design of the containment should also account for the hydrodynamic loads due to SP swell, SRV line air clearing, condensation oscillations, and chugging. TRACG is not used in the design process for this purpose. Empirical models that are based on extensive test data will be employed for the design certification review.

The long-term containment response is primarily controlled by the heat removal by the PCCS. The ability of the PCCS to purge noncondensibles and its performance in the presence of noncondensibles are key issues. The rates of drywell and wetwell energy addition and removal become progressively smaller in the long-term transient. The energy deposition in the wetwell is due to the PCCS vent flow and any steam leakage from the drywell that bypasses the PCCS. Energy removal from the wetwell is through heat transfer in the gas space (at the pool interface and walls) and condensation on the wetwell walls.

The PCCS performance may be affected by the noncondensibile distributions in the drywell. Overcooling of the drywell by the PCCS or by cold water spillover from the RPV can result in the drywell pressure falling below the wetwell pressure. Cold water could be added by flow from a broken GDCS line or spillover from the break after the GDCS fills the RPV to the break

or DPV elevation. This will cause the VBs to open, bringing noncondensibles back to the drywell.

Model biases and uncertainties for the containment/LOCA application of TRACG were assessed by GENE, as described below, for the key high-ranked phenomena. These assessments were typically performed as comparisons between separate effects test data and TRACG calculations performed with the "best estimate" modeling use of the code. The biases and uncertainties indicated by the data comparisons are used to establish ranges for TRACG parameters and correlations. These ranges are implemented through special inputs designated as "PIRT multipliers."

BR1: Break Flow

The determining phenomenon for this PIRT parameter is the critical flow. [[

]]. The bias and standard deviation were developed by GENE from the combined data set. [[

]].

MV1: Main Vent Flow

MV3: Main Vent Clearing

The determining phenomenon for the main vent flow is the irreversible pressure loss (mainly at the vent entrance). Vent clearing is controlled by the inertia of the water initially in the vent line. In Reference 16, the short-term peak drywell pressure was shown to be always conservatively overpredicted by TRACG, and variations of the vent line loss coefficient and inertia did not have a significant effect on the long-term drywell pressure. In response to staff RAI 301, GENE stated that the SBWR and ESBWR vent designs are identical and the SBWR studies are applicable to the qualification of TRACG for the ESBWR. [[

]].

DW1: Flashing/Evaporation in Drywell

The basic phenomena associated with this PIRT parameter are flashing of the liquid discharged through the break and evaporation of the liquid accumulated on the drywell floor. The controlling model in TRACG for this phenomenon is the interfacial heat transfer between the liquid and gas phases. Past GENE experience with TRACG has shown very little sensitivity to this parameter [[]]. In response to staff RAI 300, GENE clarified that the past experience was based on SBWR studies, Reference 19.

SQ1: SRV Flow

The determining phenomenon for the SRV flow is the critical flow, and the uncertainty as discussed for BR1 is used for this PIRT parameter.

DW2: Drywell Heat Sources and Sinks

The basic phenomena for this PIRT parameter are condensation and wall/structure heat transfer, which is controlled by conduction and free convection. TRACG uses the [] for the calculation of the condensation on the walls. Degradation due to the presence of noncondensibles is modeled as a correction factor based on the ratio of the partial pressure of the noncondensibles to total pressure. This model was developed for condensation in tubes. Since the uncertainties in DW2 are for condensation on flat surfaces, and the database used is basically for tube configurations, the uncertainties need to be modified for the ESBWR type geometries. In response to staff RAI 300, GENE clarified that the database used was based on the SBWR studies, Reference 19. A GENE comparison of the normalized average heat transfer coefficient predicted by TRACG with three commonly used models for flat plates showed that the TRACG model agreed well with the Dukler model (for laminar and low end turbulent flow conditions). For film Reynolds numbers larger than 20,000, TRACG predictions fell between the predictions from the Seban and the Colburn models. GENE noted that at such high Reynolds numbers, the heat transfer is conduction controlled and the condensation heat transfer coefficient has a very small effect on the overall heat transfer rate. The TRACG calculations fall between the predictions from the two flat plate condensation models, however the distribution and the deviations for these two models are not known. GENE decided to increase the maximum standard deviation for the tube data by [] to account for the spread of the flat plate correlations. The free convection correlation used in TRACG compares with data for $GrPr > 4.1 \times 10^4$ within []. However, the data for turbulent convection at identical conditions can vary by as much as []. This means that, unless the correlation is based on a wide range of data, there could be as much as [] uncertainty in the model. Therefore, GENE allows the free convection heat transfer coefficient to vary [] of the nominal value with a uniform distribution. Because the free convection model in TRACG compares favorably with data for $GrPr > 4.1 \times 10^4$ within [], widening the variation to [] based on turbulent convection data is conservative. Limiting the lower value to [] adequately covers the uncertainty, and addresses the non-realistic zero heat transfer if the lower value was set to [].

DW3: 3-D Effects in Drywell

The basic phenomena associated with this PIRT parameter are noncondensable gas stratification and buoyancy/natural circulation. As discussed in Section 3.6.2.4 of this report, a bounding modeling approach is used for the calculations in all cases. In this approach, []

]].

DW4: Condensation on Reactor Outflow

This PIRT parameter represents the condensation of drywell steam due to the overflow of the subcooled GDCS liquid to the drywell from the RPV. The main effect of steam condensation due to GDCS flow is in the RPV, and steam condensation in the containment from the reactor outflow is small. There are no separate effects or integral tests to define this uncertainty. GENE performed bounding calculations by varying the PIRT multiplier on the interfacial heat transfer coefficient (PIRT91) by [[]]. The TRACG runs were performed for the SBWR base case that was used for the uncertainty calculations. PIRT multiplier PIRT91 was set to [[]] in the drywell nodes containing the broken steam line and also the nodes adjacent to it. GENE found the effect of this change on the thermodynamic conditions in the drywell and the wetwell was negligible. [[]].

WW1: Condensation/Evaporation of Main Vent Discharge

WW2: Condensation/Evaporation of SRV Discharge

The wetwell condensation/evaporation PIRT parameters are controlled by the interfacial heat transfer in the SP. GENE noted that the TRACG model for condensation in the SP does not include any degradation due to the presence of noncondensibles. A large body of experimental data generated by GENE to evaluate the performance of the pressure suppression pool have shown that all the steam discharged into the pool through the main vents will be condensed. No steam channeling was observed based on the measured wetwell gas space pressure. These tests include experiments as early as those performed for the Humboldt Bay reactor, Reference 22, and Bodega Bay reactor, Reference 23. Mark II (4T), Reference 24, pressure suppression confirmatory tests were also performed by GENE. TRACG sensitivity studies have also shown complete condensation of steam within the pool even with substantial changes in the magnitude of the interfacial heat transfer. Therefore, GENE concluded that the total condensation below the pool surface is insensitive to variation in the interfacial heat transfer [[]].

WW3: Condensation/Evaporation of PCCS Vent Discharge

This wetwell condensation/evaporation PIRT parameter is controlled by the interfacial heat transfer in the SP, as discussed above for WW1 and WW2. However, the PCCS vent submergence in the SP is less than that for either the main vents or the SRV quenchers. In response to RAI 314.1, GENE evaluated the adequacy of vent submergence to preclude steam being added to the wetwell air space. Any steam not condensed by the PCCS that enters the SP should be condensed within the SP. Based on the TRACG calculations, GENE determined that a small amount of steam entering the PCCS during the blowdown period would not be

condensed in the PCCS and would enter the SP. After clearing out the noncondensibles above the steam line break location in the first few seconds, the flow through the PCCS is essentially all steam until 10 minutes into the transient. The amount of steam entering the PCCS, and the PCCS performance was found to be within the test data base from the PANTHERS tests. GENE referenced a paper, "Experimental Investigation of Condensation and Mixing During Venting of Steam/Non-Condensable Gas Mixture into a Pressure Suppression Pool," by C. De Walsche and F. de Cachard, ICONE-8565, Proceedings of ICONE 8, 8th International Conference on Nuclear Engineering, April 2–6, 2000, Baltimore, MD, USA, to address the adequacy of the vent submergence to preclude steam release to the wetwell air space. This investigation covered the conditions expected in the ESBWR, and the test data showed that the steam was fully condensed in all the tests, even with shallow submergences, until the pool temperature got to a few degrees below saturation. At typical subcooling, the steam was condensed at a distance of 10 to 15 cm ($L/D = 3$ to 4) above the vent discharge. GENE provided a simple argument that condensation will be complete for a pipe of a different size at the same L/D or less when the mass flux is the same. Also, for the time frame of interest, the main vents are open. The mixing in the SP will be far greater than that for a PCCS vent discharging into a quiescent pool. This will help with the condensation of the steam, resulting in a more efficient process. Based on available test data, GENE concluded that any steam entering the SP through the PCCS vent, based on the design presented for this review, will be condensed within the SP during the blowdown period of the accident.

The actual design configuration of the PCCS vent system, especially the vent submergence, may influence the amount of steam condensed in the SP. Therefore, during the design certification review, the staff will confirm that steam entering the SP through the PCCS vent, as designed, will perform as expected to condense steam entering the SP.

WW4 : Free Surface Condensation/Evaporation

The interfacial heat transfer at the free surface controls this PIRT parameter phenomenon. To evaluate the sensitivity of the containment response to the variation of the free surface interfacial heat transfer, the results of one of the PANDA containment tests were used by GENE. Variation of the PIRT7 multiplier, which affects the liquid side interfacial heat transfer [[]], did not affect the TRACG predictions. GENE therefore concluded that the free surface condensation is insensitive to the liquid side interfacial heat transfer. The steam in the wetwell gas space is superheated and has to be cooled to the saturation temperature before condensation can occur. Since no condensation is occurring, variation of the liquid side interfacial heat transfer coefficient is not expected to affect the overall heat transfer to the wetwell gas space.

The PIRT multiplier should affect the vapor side heat transfer. GENE studied this by varying the vapor side interfacial heat transfer and comparing the predicted wetwell gas space temperature to the results of PANDA Test M3, Reference 16. The objective was to find the appropriate multiplier on the interfacial heat transfer coefficient (PIRT7), which would result in prediction of the PANDA results. The TRACG interfacial heat transfer when increased by a factor of [[]], predicts the correct heat transfer between the pool and wetwell

gas space. GENE concluded that this was probably due to a larger than calculated surface area, either from a wavy interface or from entrained droplets. Increasing PIRT7 beyond [] did not affect the predicted wetwell gas space temperature. Since a value of PIRT7 equal to [] resulted in the best agreement with the data, it is used as the nominal TRACG value [].

The staff could not identify the correlation form used for the interfacial heat transfer at the free surface. In response to staff RAI 306.1, GENE stated that the correlation is for free natural convection in air above a horizontal surface and came from Reference 25, Table 7-2, and is given as $h = 0.22(\Delta T)^{1/3}$ in British units (This equation is taken from Reference 18 and is generally used for free convection above a heated plate or below a cooled plate.) This correlation was then modified by GENE to simulate natural free convection in a medium other than air by []

[]. In the current version of TRACG, there is a conversion error in translating this equation into SI units. The leading coefficient was converted to SI as 1.027, when it should have been 1.52. TRACG assumed [], at about [], resulting in TRACG using the equation form $h = []$, in SI units, for the interfacial heat transfer at the free surface.

GENE stated that in the fourth edition of Holman, Table 7-2, the coefficient has been reduced slightly with the equation in SI units being $h = 1.43(\Delta T)^{1/3}$. [], then the TRACG should be using the equation form $h = []$, in SI units. GENE concluded that the error in the equation as used is less than 0.2 percent, based on the revised equation and a different value for the thermal conductivity of air. The staff accepts this approach and notes that GENE will be replacing this model with an appropriate model for design certification. The correction will be made in the next revision of Reference 10.

To account for noncondensibles, the interfacial heat transfer rate is multiplied by what GENE refers to as the []. In response to staff RAI 306.2, GENE stated that the precise origin of the tabulated values that are referred to as the [] factors is not known. GENE believes that these values were obtained by merging the separate results from []. The tabulated values in the code are used to degrade the condensation heat transfer at the free surface between the mixture and vapor regions when a water level is predicted in a TRACG cell. The [] form shows the same trend as either the [], Reference 27, or the [] degradation forms as the air mass fraction becomes smaller. However the [] form gives less degradation than either the [] or the [] forms. Some difference is expected since [] is based on a flat surface, while [] and [] are based on flow inside tubes. The degradation becomes less important as the pressure is increased. For general TRACG applications, the higher [] curve corresponds to higher pressures and temperatures, and GENE concluded that this form was appropriate for the ESBWR calculations. The [] is intended for use as a best estimate (unbiased) correlation for stratified

mixture-vapor surfaces corresponding to a water level. GENE used the same uncertainty factors as developed for the [[]] for this PIRT parameter.

A sensitivity study was performed by GENE varying the PIRT multiplier on the vapor side interfacial heat transfer at the surface from [[]]. The effect of this variation was to change the peak containment pressure by [[]]. The use of the current interfacial heat transfer model in the containment/LOCA calculation does not have an appreciable effect on the calculated peak containment pressure. Based on the low sensitivities to significant changes in the interfacial heat transfer coefficient at the vapor-liquid interface, GENE concluded, and the staff agrees, that the current model is adequate for the analysis of the ESBWR containment. However, GENE has committed to replace this model with an appropriate correlation for design certification.

WW5: Heat Sources/Sinks

This PIRT parameter phenomenon is controlled by condensation and wall/structure heat transfer. The uncertainties are the same as the values established for DW2.

WW6: 3-D Effects in Suppression Pool

The basic phenomenon associated with this PIRT parameter is the stratification in the SP. Temperature stratification in the pool is important, since it will affect the heat transfer to and from the wetwell gas space, which will then affect the containment temperature and pressure response. SP stratification data from large-scale tests have shown that the condensed steam from the main vent discharge heats that portion of the SP above the vent. Based on TRACG sensitivity studies (discussed in Section 3.6.2.4), a bounding model was developed by GENE [[

]].

WW7: 3-D Effects in Wetwell Gas Space

TRACG predictions of the PANDA test with leakage flow (PANDA Test M6/8) (NEDC-32725P) showed that without [[]], the wetwell gas space remained [[]], unlike the test data. The wetwell cell receiving leakage flow from the drywell remained [[]]] than the other cells, which remained [[]]. GENE needed to [[]]] to reproduce the measured temperature response (Section 3.6.2.4 of this report). A similar method has been used to [[]]] in the ESBWR wetwell gas space model. This was accomplished by [[]]]. This approach produces much [[]]] and is used for conservatism in modeling the 3-D effects in the wetwell gas space for design basis calculations.

PC1: Mass Flow into PCCS

The basic phenomenon controlling the mass flow into the PCCS is the pressure drop in the PCCS inlet line, as indicated by the term k/A^2 . As part of the TRACG qualification effort, the measured PCCS overall pressure drops from the PANTHERS tests have been compared by GENE to the predictions by TRACG, Reference 16. The PANTHERS facility is a full-scale representation of the SBWR PCCS with close simulation of the inlet and vent lines. Using the test results, the absolute error, bias, and standard deviation for k/A^2 was determined for use in TRACG ESBWR calculations. Since the ESBWR PCCS inlet line is identical to the SBWR PCCS inlet line, the staff finds using the SBWR data for the variation in k/A^2 in the analyses to be acceptable.

PC2: Condensation on the PCCS Primary Side

Condensation in the PCCS tubes is modeled with the [[]] in TRACG, and accounts for degradation in the condensation due to the presence of noncondensibles, as discussed under DW2. This model has been compared with a wide range of steam and steam air data. However, for the more limited range of conditions encountered in the ESBWR, the best source of comparisons are the full scale PANTHERS data. [[

]].

PC3: PCCS Secondary Side Heat Transfer

The PCCS secondary side heat transfer is controlled by the nucleate pool boiling phenomenon, which is modeled by the [[]], Reference 28, in TRACG. Comparisons with prototypical PANTHERS data, Reference 16, have shown good agreement between the measured and predicted heat transfer coefficients. Uncertainties in the wall conduction are also included in this PIRT parameter. The PANTHERS tests were carried out with clean tubes and did not include the effect of crud formation that may occur with continued PCCS operation. The nucleate boiling heat transfer coefficients are large and the heat transfer across the PCCS wall is mainly controlled by conduction. Therefore, uncertainties in wall thickness or crud formation will control the heat transfer. The maximum thickness of the crud was calculated by GENE for the design basis fouling factor and was introduced into the model through an increased PCCS tube wall thickness. Based on a design basis fouling factor of [[]], an equivalent inconel thickness of [[]]

]] was calculated to represent the thermal resistance due to crud. TRACG calculations for the ESBWR will be made with a bounding input assumption that the wall thickness is equivalent to the design limit for crud formation.

PC5: Parallel PCCS Unit Effects

Variations in performance of one of the PCCS due to variations in mass flow rates could result from differences in the PCCS inlet line friction. Since the inlet line resistance of each PCCS

was allowed to vary independently, the uncertainties in this parameter are covered by the uncertainties specified for PC1, above.

PC8: Purging of Noncondensibles

Uncertainties in purging of noncondensibles through the PCCS are covered by the bounding modeling approach developed for the drywell 3-D effects (DW3).

DWB1: Wetwell-to-Drywell Leakage

The major paths for leakage between the drywell and wetwell are the possible leakage through the VBs and the electrical penetrations. The design limit of $A/\%k = 1 \text{ cm}^2$ (0.155 in²) will be used as the uncertainty range for this PIRT parameter. Testing of the VBs has shown that the leakage from an area corresponding to $A/\%k = 1 \text{ cm}^2$ (0.155 in²) is conservative. The effective flow area corresponding to the maximum acceptable leakage rate for the VBs is 0.02 cm² (0.0031 in²). The test data, Reference 29, even after considerable cycling and aging, show that the leakage is much smaller than the amount that would be obtained from a 0.02 cm² (0.0031 in²) flow path (0.06 cm², or 0.0093 in², for three VBs). Therefore, a 1 cm² (0.155 in²) leakage area is a bounding limit for the leakage path. It is more than 16 times the maximum design leakage through the VBs.

VB1: Vacuum Breaker Mass Flow Rate

For this PIRT parameter, the VB loss coefficient was calculated from the results of the full flow VB tests, Reference 29. Two sets of tests performed with a 120 mm disc stroke were used for this purpose. The first test was performed with air at 293 K (76.73 °F) and 98.8 kPa (14.33 psi), and the second test at a temperature of 303 K (85.73 °F) and 98.9 kPa (14.34 psi). The measured pressure drop and volumetric flow rate were used to calculate the values of k/A^2 for all the tested differential pressures to develop an average value for k/A^2 and a standard deviation. The uncertainties in the valve opening and closing pressures were determined by GENE from the curves provided in Reference 29 and are [[]] for the opening pressure, and [[]] for the closing pressure, with a uniform distribution.

RPV2: RPV Steam Generation

The basic phenomena affecting RPV2 include decay heat and mixing of GDCS flow as it enters the RPV. TRACG calculates the decay heat with a nominal curve of energy release as a function of time, which approximates the American National Standards Institute (ANSI)/ANS-5.1-1979 standard entitled, "American National Standard for Decay Heat Power in Light Water Reactors." In this standard, values are provided for decay heat power from fission products from fissioning of the major fissionable nuclides present in light-water reactors (LWRs), (i.e., U²³⁵ and Pu²³⁹ thermal and U²³⁸ fast) and methods are prescribed for evaluating the total fission product decay heat power from the data given for these specific fuel nuclides. The decay heat curve becomes a function of the fuel design, depletion environment, and power

history. The variations in decay heat due to the above effects are small, and a generic curve is defined by GENE to cover all locations with little loss in accuracy. The parameters used to generate this generic curve for LOCA analysis have been chosen to be representative of the ESBWR core being analyzed. The details of the derivation as well as the calculation of the uncertainties are described in Reference 30. The magnitude of the uncertainty used for decay heat is a function of time after the accident and has a one-sigma value of approximately [\[5\]](#) percent.

DPV1: DPV Mass Flow

The determining phenomenon for the DPV mass flow is the critical flow and the uncertainty as specified for BR is used for this PIRT parameter.

3.6.2.4 Phenomena Treated with a Bounding Approach

Some phenomena identified by GENE in the PIRT process as being important to the ESBWR Containment/LOCA response are not calculated with TRACG “best estimate” models. These phenomena include the distribution of noncondensable gases in the drywell, the temperature distribution in the wetwell gas space, and the thermal stratification of the SP. Sensitivity studies were performed by GENE to quantify the potential effect of each of these phenomena and to bound their effects on the peak calculated containment pressure.

3.6.2.4.1 Suppression Pool Stratification

The SP stratification model used in TRACG [\[](#)

[\]](#). This modeling results in behavior consistent with observations in several small-scale tests (References 31, and 32). GENE has also shown this approach to be a conservative model for determining the pool surface temperature based on full-scale and scaled pressure suppression condensation tests simulating the RPV blowdown for a LOCA with energy addition to the SP from the main horizontal vents (Reference 16). Without this [\[](#) [\]](#) model in TRACG, the SP becomes [\[](#) [\]](#) and the three-dimensional cells used to model the pool [\[](#) [\]](#) at approximately 1 hour after the start of the LOCA.

The SP model uses [\[](#) [\]](#) axial levels with [\[](#) [\]](#) radial rings in each level and is modeled as a TRACG VSSL (vessel) component. The VSSL component is also used to model the ESBWR drywell, wetwell, and RPV. The top most level represents the [\[](#) [\]](#). The next lower level includes [\[](#) [\]](#). The model for the [\[](#) [\]](#) (see WW4 in Section 3.6.2.3) is used at this location. The next level down includes [\[](#) [\]](#). The remaining [\[](#) [\]](#) levels include the [\[](#) [\]](#). To generalize and automate SP stratification, [\[](#)

]]. In response to staff RAI 321, GENE also described the effects of the SRV quenchers on how the SP stratification model functions. The quenchers at the end of the SRV lines are located in the [[]]. Initially, there is flow through all three of the horizontal main vents for the large steam line break. While there is flow through all vents, the TRACG model allows the flow [[]]. As the blowdown flow decreases, the level in the main vent rises, sequentially closing off the horizontal rows of vents. [[]]

]].

As discussed in GENE's response to staff RAI 321, in general, there will also be flow through the SRV quenchers during a LOCA. The same logic is used to treat the flow from the SRVs. Because the SRVs discharge into the lowest level, [[]]

]] as long as there is flow through the SRVs. This source of flow and energy into the SP results in good mixing within the entire SP. When the SRV flow ceases, the [[]]

]]. Typically, SRV flow will continue after the bottom two rows of horizontal vents have closed. [[]]

]].

To illustrate this [[]] model, GENE provided the results of the LOCA transient for the SBWR with and without the [[]] model to show the SP temperature predictions for the first 5000 seconds. For the case without the model, within the first hour, the [[]]. The calculation using the [[]] model shows the temperatures at different pool levels rising and then becoming constant [[]]

]]. After the top-most horizontal vent closes at around 1000 seconds, [[]]. The effect of this model is to force the temperature in the upper layers of the SP to be about [[]] higher than if the SP were well mixed.

The SP temperature predictions using this stratification model have been compared by GENE to the SP temperature measurements from the PSTF, Reference 16. These comparisons show that the predicted temperatures near the SP surface bound the measured temperatures. With this stratification model, the ESBWR calculation for the liquid temperatures in the cells that contain the pool surface, which are in contact with the wetwell gas space, are bounded. This

ensures that the wetwell gas space pressure, and therefore the containment pressure, will not be under predicted.

3.6.2.4.2 Wetwell Gas Space Stratification

Wetwell gas space stratification was identified by GENE in the PIRT as a phenomenon potentially important for the containment response. Sensitivity studies were performed by GENE to investigate the effects of wetwell gas space stratification. TRACG modeling features to address the wetwell gas space stratification were developed by GENE and are used for the bounding modeling approach.

The wetwell gas space is the region of the wetwell above the SP surface. It has a total volume of about 4500 m³ (151,853 ft³). The wetwell gas space is bounded on top by the diaphragm floor, which separates the wetwell and drywell, on the inside by the vent wall between the wetwell and drywell, and on the outside by the wall between the wetwell and the outer containment wall. The wetwell gas space is reasonably open, with a few side-wall gratings and pipes. In the wetwell ceiling, structural members, which are part of the diaphragm floor, run radially across the wetwell between the inner and outer walls. They extend down from the ceiling approximately 1 meter. While they should not inhibit natural circulation caused by temperature differences between the inner and outer walls, they could enhance stratification from any leakage flow from the VBs that are located in the diaphragm floor. The energy balance on the wetwell gas space, particularly during the long-term phase of the LOCA, is an important part of modeling the ESBWR containment, since it directly affects the containment response. If there is a net heating of the gas space and its pressure increases, the pressure throughout the containment is increased. If there is a net cooling of the gas space, its pressure is reduced, which lowers the containment pressure.

In the ESBWR Containment/LOCA model, the wetwell gas space is modeled with [[]] axial levels and [[]] radial rings, for a total of [[]] cells. (These are the same [[]] levels as discussed in Section 3.6.2.4.1, above.) The cells in the [[]] are in contact with the suppression pool. The inside cells contact the vent wall and the outside cells contact the outer containment wall. The upper cell on the inside, near the vent wall, receives drywell-to-wetwell flow, used to model leakage through the VBs. [[

]]. The basis for choosing this relatively simple arrangement was experience gained by GENE from PANDA post-test analyses. This showed that the [[]] wetwell gas space model provided the best prediction of the wetwell vapor temperatures for most of the PANDA tests.

Double-sided heat slabs are attached to cells in all levels of the wetwell gas space and SP to represent the vent wall and the outer containment wall. Due to the limited ability of TRACG to model condensation on horizontal surfaces, that part of the diaphragm floor which is not covered on the drywell side by the GDCS pools has been included with the inner (vent wall) heat slab. In response to staff RAIs 298 and 307.1, GENE acceptably addressed the treatment of the diaphragm floor and heat transfer to horizontal surfaces as discussed below.

Most of the heat slabs in the ESBWR containment wall (volume boundaries) are vertical surfaces. Non-wall heat structures inside the drywell and wetwell are conservatively ignored. The horizontal heat slabs are the drywell and SP basemats, the diaphragm floor, and the drywell top slab. The two basemats are covered with water and will not see any direct condensation, and are conservatively not modeled in the calculations. The diaphragm floor in the wetwell gas space is not expected to be a condensing surface and is also conservatively not modeled. The remaining two horizontal surfaces in the drywell are the diaphragm floor (not part of the GDCS pools) and the drywell top slab. The drywell top slab is conservatively not modeled. The diaphragm floor, which is not part of the GDCS pools, transfers energy from the drywell to the wetwell gas space during the transient. To model this heat conduction, the diaphragm floor is modeled as part of a vertical structure. The vertical wall between the drywell and wetwell includes the diaphragm floor area and assumes the wall thickness is the same as that for the diaphragm floor. GENE expected this simplification in the modeling to have a small impact on the containment response, as the heat slabs have a small impact on both the short-term and long-term drywell pressure. A sensitivity study was performed by GENE to study the impact of this vertical heat slab modeling, in response to staff RAI 298. In this study, the area of the vertical heat slab between the drywell and wetwell were increased by [[]]. The impact on the calculated long-term containment pressure was a change of [[]].

In the TRACG documentation, it is stated that the [[]] correlation, Reference 33, is available as an option for a lower bound for condensation. Use of this correlation would be consistent with guidance provided in the SRP. As set forth below, in response to staff RAI 307.2, GENE addressed the application of the [[]] correlation and the overall impact of wall heat structures on the containment pressure response.

The [[]] correlation is not used in the base case calculations. However, for licencing analyses, the [[]] correlation will be used if the Uchida correlation rate is less than that from the [[]]. Results of the sensitivity study performed by GENE show that the impact of using this option on the long-term drywell pressure is small. The vertical heat slabs have a small impact on both the short-term and long-term drywell pressure. Sensitivity studies were performed by GENE by changing the surface areas of the vertical heat slabs in the drywell-wetwell wall and the wetwell outer wall. The impact on the long-term drywell pressure was [[]] for a 25 percent increase in the heat slab areas in the drywell-wetwell wall. The impact on the long-term drywell pressure was [[]] for a 25 percent decrease in the heat slab areas in the wetwell outer wall, and [] for essentially no heat slabs in the wetwell outer wall. The impact of the condensation model on the peak calculated drywell pressure is small.

GENE referenced sample results for the SBWR to illustrate the effects of the wetwell gas space stratification model. GENE expects the trends to be similar for the ESBWR due to the similarity of the hardware configurations. Without the model to [[]] stratification in the wetwell gas space, temperatures predicted by the TRACG SBWR model showed only a few degrees of stratification at 72 hours, the end of the long-term transient. The cells in the upper level were about [[]] above those in the lower level. All of the wetwell cells were

initially heated by compression as the noncondensable gas was transferred from the drywell. This was followed by some initial cooling from the walls and then a general heating trend was seen in the calculation. Cells in the lower level remained near the SP temperature while the upper level cells heated up. Results from PANDA Test M6/8, where a conservative leakage flow (compared to the GENE design requirement) was tested, showed stratification of the upper region of the wetwell gas space. Based on these test results, a bounding model was developed by GENE for use in TRACG to account for the effect of this temperature stratification in the wetwell gas space.

[[]]. The lower cells still remain closely coupled to the SP temperature. The upper cells are cooled in the early portion of the transient, but the effect is less than seen without this model and the cell receiving leakage flow heats up significantly by the end of the transient. The other cell is cooled by heat transfer to the outer wall. This model produced conservative results when compared to data from PANDA and the model is expected to be conservative for ESBWR.

3.6.2.4.5 Drywell Stratification

The stratification and holdup of noncondensable gases in the drywell during the blowdown phase of the LOCA and their later release can affect the performance of the PCCS. If the performance of the PCCS, during the long-term cooling phase of the LOCA, is degraded due to the presence of noncondensable gases which were not purged during the blowdown, then the steam which is not condensed in the PCCS will be vented to the SP. This raises the temperature of the SP and increases the containment pressure.

To maximize the effect of noncondensable [[]] during the blowdown phase of the LOCA, [[

]]. The [[]] volume included the volume of the lower drywell, the vents connecting the upper and lower drywells, the region between the RPV and shield wall, and the drywell head. GENE also stated that the region over the GDCS pools, which is not part of the drywell (as it was in the SBWR design), was included in the [[]] volume. In response to staff RAI 164.1, GENE stated that the original statement was incorrect and the region over the GDCS pools is not included in the [[]] volume. [[

]].

To [[]] noncondensibles and control their [[

]]. After 1 hour, [[

]]. This loss coefficient is representative of the loss that would be expected through the restriction area connecting the upper and lower drywell in the ESBWR.

Calculations performed by GENE for the SBWR have shown that there is little effect due to [[]] for this particular event, a large steam line break. [[]]. Another sensitivity of interest is the effect of the [[]] of drywell cells on the rate of release of noncondensibles during the long-term phase of the transient. Calculations were performed by GENE for the drywell noncondensibile gas mass during the first 20 hours of the event, first with a [[]] and then with a [[]] had a small effect on the bleed-down rate of the drywell noncondensibles.

The sensitivity studies performed by GENE showed that rearrangement of the drywell and removal of all dead-ended components results in a significant initial holdup of the drywell noncondensibles for the steam line break. However, the overall effect on the final drywell pressure after 72 hours was on the order of [[]]. Also, the loss coefficient used to represent the drywell vents, when varied over a wide range, had very little effect on the final containment pressures and temperatures, on the order of [[]].

The more significant factor in determining the containment pressure response is the location of the break discharge into the drywell. The discharge location for the steam line break was progressively lowered from the upper most cell in the drywell (the base case) to the lowest level in the drywell. Based on these GENE sensitivity studies, the break located in the lower drywell clears all the noncondensibles quickly. An MSLB located near the top of the drywell results in a slower transport of the noncondensibles from the lower drywell. This results in a longer time over which the performance of the PCCS is degraded by noncondensibles. The maximum pressure was obtained for the break location at the top of the drywell, resulting in a pressure prediction about [[]] higher than for a break in the lower drywell. This is the location to be used for containment/LOCA design basis calculations.

3.6.2.5 Plant Parameters and Ranges for Application

Specific inputs for containment/LOCA calculations will be specified with internal GENE procedures, which are used by GENE to control the application of engineering computer programs for licencing analyses. The specific code input will be developed in connection with the design certification application and the development of the application-specific procedure. GENE provided a limited general discussion of how input is treated with respect to quantifying the impact on the calculated results. As such, it serves as a basis for the staff's understanding of the expected development of the application-specific procedures for design certification.

The TRACG code inputs can be divided into four broad categories—geometry inputs, model selection inputs, initial condition inputs, and plant parameters inputs. For each type of input, it

is necessary to specify the value for the input. If the calculated result is sensitive to the input value, then it is also necessary to quantify the uncertainty in the input.

The geometry inputs are used to specify lengths, areas, and volumes. Uncertainties in these quantities are due to measurement uncertainties and manufacturing tolerances. These uncertainties usually have a much smaller impact on the results than do other uncertainties associated with the modeling simplifications. When this is not the case, the specific uncertainties can usually be quantified in a straightforward manner.

Geometries are also used to develop spatial nodalization. Spatial nodalization includes modeling simplifications such as the lumping together of individual elements into a single model component. For example, several similar main vent pipes may be lumped together and simulated as one pipe. An assessment of these kinds of simplifications, along with the sensitivities to spatial nodalization, is included in the GENE qualification reports (Reference 34 and Reference 16). With respect to the model used for the containment/LOCA calculations, only GENE SBWR- and ESBWR-specific separate and integral test comparisons have been used to qualify the modeling (nodalization).

Model selection inputs are used to select the features of the model to be used for the intended application. Once established, these inputs are fully specified in the procedure for the application and will not be changed.

GENE has made a distinction between initial conditions and plant parameters. Initial conditions are considered to be those key plant inputs that determine the overall steady-state nuclear and hydraulic conditions prior to the transient. These are inputs that are essential to determining that the steady-state condition of the plant has been established. Plant parameters are reserved for such things as protection system setpoints and valve capacities that influence the characteristics of the transient response but which do not (when properly prescribed) have an impact on steady-state operation. The staff accepts these distinctions for the purpose of the analysis of the ESBWR design. GENE did not identify any plant parameters as important for this TRACG evaluation study.

3.6.2.5.1 Plant Initial Conditions Used for Calculations

The plant operating conditions represent initial conditions for the TRACG calculations and have an important effect on the calculated response of the containment. The range of allowable initial conditions is governed by plant operating guidelines and, for containment response calculations, it is assumed that the plant will be operated within these guidelines. In a typical calculation, initial conditions in the containment are assumed to be at steady-state, and at limiting pressures and temperatures. The RPV is assumed to be operating at maximum power, and, for a given feedwater flow and temperature, the RPV steam flow, the initial temperatures and pressures, and vessel internal flows are selected to obtain steady state conditions. Initial RPV power is set at 100 percent of rated power for the base case calculation. Experience with similar BWR containment systems has shown that rated power produces the most limiting containment response. The only exception is a break from hot standby, which is typically

included in a containment response evaluation. For this accident, it is assumed that the plant was at full power operation, is scrammed and isolated, and the SP is heated by SRV operation to the maximum pool temperature limit before the break occurs. This break can, for some plants, be limiting because of the high initial pool temperature.

The following parameters were used for the base case and bounding case calculations performed by GENE in support of the TRACG application review.

Reactor Power Level—[[]]. The analyses performed at the design certification stage will be performed consistent with the power level and appropriate measurement uncertainty.

RPV Level—[[]].

RPV Pressure—[[]].

PCCS Pool Level—The initial PCCS pool level was determined from the minimum water inventory above the top of the condenser tubes. Since the IC, PCCS, and other pools on that level of the containment building are connected, the initial PCCS pool level is the minimum allowed for plant operation and is, therefore, a conservative basis for this parameter. [[]].

PCCS/IC Pool Temperature—[[]]. GENE considers this a reasonable value for the pools that are outside the containment.

Wetwell Gas Space Relative Humidity—[[]]. GENE considers this to be a reasonable value for the relative humidity in this closed volume exposed to the SP.

Drywell Relative Humidity—[[]].

Drywell Pressure—[[

]].

Drywell and Wetwell Temperatures—[[

]].

Suppression Pool and GDCS Pool Temperatures—[[

]].

Suppression Pool and GDCS Pool Levels—[[

]].

3.6.2.5.2 Results for ESBWR Main Steam Line Break LOCA

The MSLB causes the fastest short term pressurization of the ESBWR drywell. It results in minimum drain-down of the GDCS pools because of the elevation of the break, and hence a smaller wetwell gas space volume in the long term. The steam line break discharging at the top of the drywell also results in a slower clearing out of the noncondensibles in the lower drywell degrading the PCCS for a longer time. All these factors lead to the highest containment pressure for the MSLB.

3.6.2.5.3 Baseline Results for Containment Analysis

The RPV and containment were initialized at their base case conditions. Four PCCSs are available with a total rated capacity of 54 MW. A crud thickness assumed on the tube walls corresponded to the design basis fouling factor of [[

]]. No credit was assumed for the ICs. A leakage path was assumed between the drywell and wetwell with an equivalent area of 1 cm² (0.155 in²).

Apart from the conservative modeling assumptions common to all TRACG containment analysis [[

]], the other models were set at their mean values as determined by GENE for the uncertainties in the high-ranked PIRT parameters.

Following the postulated LOCA, the drywell pressure increased rapidly leading to clearing of the PCCS and main vents. The initial pressure rise turns over when the GDCS initiates at about 600 seconds. Vacuum breaker openings occur as the steam production drops off as a result of GDCS injection. Subsequently, decay heat overcomes the subcooling of the GDCS water and steaming resumes. The drywell pressure levels off and remains well below the design pressure of 60 psia (413.69 kPa). The peak drywell pressure for this case was []. It took about [] for the noncondensibles to be cleared from the bottom of the drywell. At the end of 72 hours, the PCCS pool level has dropped to about halfway down the tubes. However, this is still sufficient for effective heat transfer. The level in the GDCS pools reaches an equilibrium with the RPV downcomer level, which is at the elevation of the steam line. After the first [], the PCCSs are able to remove the decay heat. When the PCCS heat removal exceeded the decay heat generation, there is a drop in the drywell pressure to a value below the wetwell pressure. This leads to a temporary cessation of steam flow to the PCCS. The VBs then open and some noncondensibles are returned to the drywell, and the PCCS heat removal increases as the steam flow from the drywell resumes. Initially, all elevations in the SP heat from the main vent and SRV discharge. After the main vents and SRVs close, only the upper levels are impacted by the PCCS vent discharge. For the first [], the decay heat exceeds the PCCS heat removal capacity and the SP surface temperature increases until it levels off at about []. The pool surface temperature directly affects the wetwell pressure through the partial pressure of the steam. There is an early peak in SP temperature to [] from the adiabatic compression of the drywell gas into the wetwell gas space. Afterward, the gas in contact with the wetwell and SP walls cools down. The cell receiving the leakage flow from the drywell locally heats up higher than the rest of the wetwell as a result of the wetwell gas stratification model. However, all temperatures remain below the wetwell temperature design limit of []. The temperature initially peaks to [] as the drywell is pressurized from the steam discharge from the break. This temperature is below the short term temperature limit of []. In the long term, the temperature remains below [].

3.6.2.5.4 Bounding Results for Containment Analysis

The initial conditions used for this analysis were set to their bounding case values. Four PCCSs were available with a total rated capacity of 54 MW. No credit was assumed for the ICs. A leakage path was assumed between the drywell and wetwell with an equivalent area of 1 cm² (0.155 in²). In addition to the conservative modeling assumptions common to all TRACG containment analysis [], other models were ranged in the conservative direction to maximize the calculated containment pressure, as determined by GENE for the uncertainties in the high ranked PIRT parameters.

The drywell pressure for this calculation peaked at []. For the bounding case [], it took longer for the PCCS to assume the full decay heat load. The SP surface temperature also reached a slightly higher value of about [].

The peak drywell pressure for the bounding case was below the design limit of 60 psia (413.69 kPa). The margin to the design limit for the pressure increase (based on absolute pressure) is [[]] percent. The base case peaked at [[]], a margin of [[]] percent. Both of these cases assumed a design basis fouling factor on the PCCS tubes corresponding to end-of-life conditions. For the base case without this fouling factor, the peak drywell pressure was calculated to be [[]] percent margin.

The wetwell gas space temperature results were similar to the base case. The early peak in temperature to [[]] was due to adiabatic compression of the drywell gas into the wetwell gas space. Afterward, the gas in contact with the wetwell and SP walls cools down. [[

]] all temperatures remain below the wetwell temperature design limit of 250 °F (394.3 K). The drywell temperature initially peaked to [[]] as the drywell was pressurized from the steam discharge from the break. This temperature is below the short term temperature limit of 340 °F (444.3 K). In the long term, the temperature is about [[]].

3.6.2.6 Summary of Containment/LOCA Application Methodology

The Commission's regulations in 10 CFR 52.47(b)(2)(i) provide that:

Certification of a standard design which ... utilizes simplified, inherent, passive, or other innovative means to accomplish its safety functions will be granted only if

(A)(1) The performance of each safety feature of the design has been demonstrated through either analysis, appropriate test programs, experience, or a combination thereof;

(2) Interdependent effects among the safety features of the design have been found acceptable by analysis, appropriate test programs, experience, or a combination thereof; [and]

(3) Sufficient data exist on the safety features of the design to assess the analytical tools used for safety analyses over a sufficient range of normal operating conditions, transient conditions, and specified accident sequences, including equilibrium core conditions[.]

The ESBWR uses the PCCS to maintain the containment pressure and temperature below their respective design limits during DBA LOCAs, including MSLBs. In support of design certification, GENE has performed both separate and integral tests of the PCCS to characterize its performance over the ranges of conditions expected to occur in the ESBWR during these accidents.

Analytical comparisons of the PCCS test data performed by GENE using existing TRACG correlations [[

]] have shown that these correlations are adequate to model the PCCS performance during these DBAs. The calculations show that TRACG tends to predict comparable performance as seen in the tests, only with a slightly higher pressure. This is a conservative property of TRACG for containment performances analyses, i.e., the test data show that the PCCS will perform slightly better than predicted by TRACG.

During the review, the staff determined that the interfacial heat transfer correlation used in TRACG to model the liquid to gas heat transfer for the SP to wetwell interface was not adequate. However, GENE performed sensitivity studies varying the interfacial heat transfer rate over a wide range and found that there was very little sensitivity in the calculated peak pressure to the interfacial heat transfer. GENE will replace this model with an appropriate model for design certification. (See Section 3.6.2.3, "Phenomena Identification and Ranking," Item WW4: Free Surface Condensation/Evaporation, and Section 4.0 "Confirmatory Items," Item 16.)

To support design certification, GENE has stated that it will use a bounding application approach for the containment analysis that will encompass the uncertainties associated with several key phenomena. [[

]]. This conservative approach will be used to account for limitations in TRACG to handle these phenomena, as demonstrated through comparison of TRACG calculations performed by GENE, with and without the models for these phenomena, to applicable test data. The resulting design basis calculations will therefore contain conservatism consistent with the guidance in SRP Section 6.2.1, "Containment Functional Design," and SRP Section 6.2.1.C, "Pressure-Suppression Type BWR Containments." GENE has also stated that it will include drywell to wetwell bypass leakage in the design basis calculations, also consistent with SRP 6.2.1.C.

The bounding application model will also include a conservative treatment of heat transfer to containment structures. Most horizontal surfaces are neglected. Nonstructural surfaces, such as piping and grating, are also neglected. Sensitivity studies performed by GENE showed that the overall importance of the heat structure was low in determining the peak pressure response. The major heat removal process is the transfer of the blowdown energy to the SP. After about [[], the PCCS is able to remove the decay heat for the duration of the accident and maintain the SP temperature within acceptable limits. GENE states that the resulting design basis calculations will therefore contain additional conservatism consistent with the guidance in SPR Section 6.2.1, "Containment Functional Design," and SRP Section 6.2.1.C, "Pressure-Suppression Type BWR Containments."

With respect to the model used for the containment/LOCA calculations, only GENE SBWR- and ESBWR-specific separate and integral test comparisons have been used to qualify the modeling (nodalization) and containment performance-related mass and heat transfer

correlations. While there is no compelling reason to believe the models have not been adequately validated for specific use for the ESBWR, the staff believes that additional confirmatory validation studies should be performed by GENE based on widely accepted containment tests.

During the staff's earlier review of the SBWR work that GENE relies on for the ESBWR, Reference 50, the staff noted that GENE had not evaluated more traditional integral containment tests such as the Marviken tests, the Carolinas Virginia Tube Reactor test 3 without sprays, and the Battelle- Frankfurt Model Containment tests C-13 and C-15, for MSLBs. In response to staff RAI 317.1, GENE agreed to perform assessments of TRACG to model containment performance against integral test data that is publicly available for International Standard Problems where the test facilities and tests are well defined. The tests to be analyzed will be specified later, and the analysis will be completed during the design certification review.

The staff also requested that GENE provide a plan and schedule to assess the ability of TRACG to model containment performance against additional separate effects tests. Separate effects tests that should be considered include the Wisconsin Flat Plate condensation tests, (References 36, 37, and 38). In response to staff RAI 317.2, GE agreed to perform assessments of TRACG to model containment performance against separate effects test data that are publicly available for International Standard Problems where the test facilities and tests are well defined. The tests to be analyzed will be specified later, and the analysis will be completed during the design certification review.

Based on the foregoing, the staff has determined that the TRACG computer program, in combination with the bounding modeling approach developed by GENE to address potential weaknesses in TRACG and to ensure a conservative peak containment pressure calculation, is adequate for ESBWR containment performance analyses in support of design certification after the above noted code improvements are made. As set forth above, the base case and bounding calculations performed by GENE for this review demonstrate that TRACG is acceptable for use in design certification of the ESBWR design.

GENE is consistent with this step in the CSAU approach.

Element 2—Assessment and Ranging of Parameters

3.7 Step 7—Establish Assessment Matrix

The Test and Analysis Program Description (TAPD) provides an integrated plan to address the experimental and analytical work needed for analyzing ESBWR performance for normal operations, transients, DBAs, stability, and ATWS conditions in support of ESBWR design certification. A major product of all these activities is the assessed TRACG code for ESBWR analysis. The preapplication review focuses on the review of the TRACG code for LOCA and containment analysis only.

Experimental data from a number of separate effects tests with generic applications (for operating plants as well as ESBWR), integral systems tests and component tests performed for SBWR and ESBWR, and BWR plant operation were used to assess the TRACG code for ESBWR LOCA analysis.

3.7.1 Testing Program

The TAPD provides an integrated plan to address the experimental and analytical work needed for analyzing ESBWR performance for normal operations, transients, DBAs, stability, and ATWS conditions in support of ESBWR design certification. A major product of all these activities is the “qualified” TRACG code for the ESBWR analysis. As stated earlier, this preapplication review focuses on LOCA applicability of TRACG to the ESBWR design. As a result, test data and TRACG qualification for operational transients, ATWS, and stability are excluded. An overview of the interactions between the TAPD and other activities is shown in Figure 3.7.1.1.

Experimental data from a number of basic and separate effects tests with generic applications to operating BWRs and the ESBWR, and full-size component tests and integral systems tests performed specifically for the SBWR and ESBWR, and BWR plant operation have been used to qualify the TRACG code for the ESBWR LOCA analyses. The following is a summary of the test data (excluding the basic tests) used to qualify the TRACG code initially for the SBWR, and now for the ESBWR LOCA applications. The facilities described were designed and scaled based on the SBWR design. The facilities have been reviewed by the staff for applicability to the ESBWR design. The staff conclusions regarding applicability are based on review of the test objectives, test descriptions, and phenomena represented. The staff conclusions are presented in the form of assessment of the strengths, weaknesses, and evaluation of each of the facilities. This assessment references the SBWR design as well as the ESBWR design since the facilities were originally designed relative to the SBWR. The ESBWR/SBWR relationship has been previously discussed in Section 3.0 of this report.

3.7.1.1 Full-Size Component Tests

3.7.1.1.1 PANTHERS/PCC Tests

A full-size PCCS condenser for the SBWR was tested under this program.

- Test Objectives
 - (1) Demonstrate that the prototype PCC heat exchanger for the SBWR is capable of performing as designed with respect to heat rejection (component performance).
 - (2) Provide a sufficient database to confirm the adequacy of TRACG to predict the quasi-steady heat rejection performance of a prototype PCC heat exchanger over a range of air (simulant for nitrogen in the SBWR containment) flow rates,

steam flow rates, operating pressures, and superheat conditions that span and bound the SBWR (and ESBWR) range.

- (3) Determine and quantify any differences in the effects of noncondensable gas buildup in the PCC heat exchanger tubes between lighter-than-steam and heavier-than-steam gases (concept demonstration).

- Test Description

A full-size PCC condenser of the SBWR consists of two identical modules, and each module consists of a top header, a number of vertical condenser tubes, and a bottom header. The PANTHERS/PCC tests provided data for a full-size, two-module PCCS condenser submerged in a pool of water. Although the tests focused on the performance of a PCCS condenser for the SBWR, the data are applicable to a PCCS condenser in the ESBWR, which has the same condenser tube diameter, length, and pitch as the condenser tested in PANTHERS for the SBWR. The only difference is that the PCCS condenser in the ESBWR has about 35 percent more tubes than in the SBWR. As a result, an ESBWR PCC condenser is expected to have a heat removal rate about 35 percent higher than what was measured in the PANTHERS/PCC condenser.

PANTHERS/PCC testing was performed as a joint effort by GENE, Ansaldo, European Nuclear Energy Association, and Ente Nazionale per l'Energia Elettrica at Societa Informazioni Esperienze Termoidrauliche (SIET) in Piacenza, Italy. The test facility consisted of a prototype PCC unit originally designed to represent the SBWR, a steam supply, an air supply, and vent and condensate volumes sufficient to establish PCC thermal-hydraulic performance. The heat exchanger was a prototype unit, built by Ansaldo using prototype procedures and prototype materials. The PCC pool had the appropriate water volume for a prototypical PCC unit.

For the steady-state performance tests, the facility was purged with steam and placed in a condition where steam or an air/steam mixture was sent to the PCC, and the flows of the condensate and vented gases were measured. Once steady-state conditions were established, data were collected for a period of approximately 15 minutes. Ninety-seven steady-state tests were performed, including the steam only tests with either saturated or superheated steam. Test conditions covered the entire range of the PCC inlet flow rates and pressures expected in the SBWR.

Transient tests were conducted by first establishing steady-state conditions and then either varying the water level in the PCC pool or allowing the unit to fill up from an injection of noncondensable gases with the vent line closed off by a blind flange.

- Phenomena

Phenomena investigated are the overall PCC heat removal rate, pool water level effect on the PCC performance, mass flow rate into PCC, condensation inside the tubes with or without the presence of noncondensable gases, pool side heat transfer, parallel PCC tube effects, and parallel PCC modules effects.

Strengths

Full-size component tests have been conducted with the test parameters covering those expected in the SBWR (and in the ESBWR, after a 35 percent increase in the PCC heat removal rate as tested to account for approximately 35 percent increase in the number of condenser tubes) during LOCAs.

Test results demonstrate that a prototype PCC heat exchanger for the ESBWR is capable of performing as designed with respect to heat rejection, and provide a sufficient database to confirm the adequacy of TRACG to predict the quasi-steady heat rejection performance of a prototype heat exchanger over a range of air (as a simulant for nitrogen in the containment) flow rates, steam flow rates, operating pressures, and superheat conditions that cover the expected ranges of values of the parameters for the ESBWR.

Weaknesses

- (1) A large number of the tests were conducted at a pressure higher than the expected containment pressure in the ESBWR during a LOCA, such as an MSLB, a GDLB, or a BDLB. However, there are also lower-pressure data to bracket the expected range of the containment pressure in the ESBWR. The tests could have been better planned to conduct more tests at the expected containment pressures in a LOCA.
- (2) Temperature measurements were made at the inside and outside walls of four condenser tubes. But there were no measurements of the bulk gas temperature inside these tubes. The heat transfer coefficient inside a tube cannot be derived from the test data. There were no measurements for mass flow rate and noncondensable gas concentration at the inlet of a condenser tube where tube wall temperatures were measured. As a result, a correlation between the heat transfer coefficient and the fluid velocity cannot be derived from the test data.
- (3) Documentation of the test results could have been more clearly written.

Evaluation

Since the PCC tested at PANTHERS/PCC is equivalent to a full-size PCCS condenser in the SBWR, no scaling analysis is necessary and the test data provide a global heat removal rate of a full-size condenser in the SBWR. The PANTHERS/PCC data have confirmed that a PCCS condenser in the SBWR is capable of a heat removal rate of 10 MW (or higher depending on

the inlet conditions) as designed. For the ESBWR, the heat removal rate of a PCCS condenser is expected to be around 13.5 MW (with 35 percent more condenser tubes than the one tested at PANTHERS/PCC).

However, the PANTHERS/PCC tests were not designed to provide local thermal-hydraulic parameters, such as the heat transfer coefficient, mass flow rate, and noncondensable gas concentration, inside a condenser tube.

In conclusion, the PANTHERS/PCC test data cover a broad range of the SBWR and ESBWR parameters including inlet pressure, total mass flow rate, and total noncondensable gas concentration to confirm the PCC heat removal rate under various LOCA conditions. The PANTHERS/PCC data are acceptable as a valid database to qualify the TRACG code for the global heat removal rate of a PCCS condenser under the expected LOCA conditions in the ESBWR.

3.7.1.1.2 PANTHERS/IC Tests

An IC unit consists of two identical modules, each module consisting of a top header, a number of vertical condenser tubes, and a bottom header. The PANTHERS/IC tests provide data for one full-size module (half) of the IC condenser submerged in a pool of water. Note that an IC in the ESBWR is identical to the IC in the SBWR which was tested in the PANTHERS/IC tests.

- Test Objectives

- (1) Demonstrate that the prototype IC heat exchanger is capable of performing as designed with respect to heat rejection.
- (2) Provide a sufficient database to confirm the adequacy of TRACG to predict the quasi-steady heat rejection performance of a prototype IC heat exchanger over a range of operating pressures that span and bound the ESBWR range.
- (3) Demonstrate the startup of the IC unit under anticipated transient conditions.
- (4) Demonstrate the capability of the IC design to vent noncondensable gases and to resume condensation following venting.

- Test Description

PANTHERS/IC testing was performed at SIET in Piacenza, Italy. The facility consisted of a prototype IC module, a steam supply vessel simulating the SBWR reactor vessel, a vent volume, and associated piping and instrumentation sufficient to establish IC thermal-hydraulic performance.

The IC tested was one module of a full-scale, two-module vertical tube heat exchanger designed and built by Ansaldo. Only one module was tested because of the high energy

rejection rate of the IC unit, and inherent limitations of facility and steam supply size. The IC was a prototype unit, built using prototypical procedures and prototypical materials. The SBWR has six modules (three heat exchanger units). The IC was installed in a water pool having one half the appropriate volume for one SBWR IC assembly.

For the steady-state tests, the steam supply to the steam vessel was regulated such that the vessel pressure stabilized at the desired value. A constant water level was maintained in the pressure vessel by draining condensate back to the power plant. Data were acquired for a period of approximately 15 minutes. Then the steam supply was increased or decreased to gather data at a different operating pressure, or testing was terminated. In all cases, flow into the IC was natural circulation driven, as is the case for the SBWR.

As with the PCC tests, transient tests were conducted by first establishing steady-state conditions, and then either varying the water level in the IC pool or allowing the unit to fill up from an injection of noncondensable gases. The gases were subsequently purged through vent lines located on both the lower and upper headers.

- Phenomena

Phenomena investigated included the IC heat removal rate, pool water level effect on the IC performance, mass flow rate into the IC, and pool side heat transfer.

Strengths

Full-size component tests were conducted with the test parameters covering those expected in the ESBWR during both normal and accident conditions. Since the IC tested has one of the two identical modules of a full-size IC, a scaling analysis is not necessary and the test data are directly applicable to an IC in the ESBWR (which has twice the heat removal rate compared to the IC tested at PANTHERS/IC).

Weaknesses

- (1) Temperature measurements were made at the inside and outside walls of eight condenser tubes, but there were no measurements of the bulk gas temperature inside these tubes. As a result, the heat transfer coefficient inside the tubes cannot be derived from the test data. There were no measurements of the mass flow rate and noncondensable gas concentration at the inlet of a condenser tube where tube wall temperatures were measured. As a result, a correlation between the heat transfer coefficient and the fluid velocity cannot be derived from the test data.
- (2) There are some concerns regarding the IC structural design and startup for LOCA conditions, which are beyond the scope of this preapplication review. However, they are

raised in the evaluation below as an issue that needs to be addressed in the application for certification of the ESBWR design.

- (3) Documentation of the test results could have been more clearly written.

Evaluation

The IC tested at PANTHERS/IC was one module of a full-scale, two-module IC in the ESBWR, therefore no scaling analysis is necessary. Test results demonstrate that a prototype IC module is capable of performing as designed with respect to heat rejection and provide a database for TRACG qualification regarding the quasi-steady heat removal rate of an IC. The PANTHERS/IC data are acceptable as a valid database to qualify the TRACG code for the IC global heat removal rate.

However, the test results do not sufficiently demonstrate a startup of the IC under anticipated transient and accident conditions. Loud booms were heard during the IC startup testing. Preliminary investigation suggested that it was caused by the fast opening of the IC drain valve and possible interaction between the trapped water and incoming steam flow in the horizontal section of the IC inlet line. This was supported by a follow-up IC startup test in which the IC drain valve opening time was increased to better simulate the plant conditions and the IC inlet line was drained. However, further investigations are needed to conclusively determine the cause of the water hammer and confirm the means to prevent it (e.g., by changing the hardware design of the IC inlet line or the startup procedure). This is an issue to be resolved for the ESBWR design certification.

Furthermore, the PANTHERS-IC testing was terminated when leakages were detected in the IC upper header. As a result, the leakage issue was never resolved, and it is an IC structural integrity issue that needs to be resolved for the ESBWR design certification.

3.7.1.1.3 Depressurization Valve Tests

Full-size DPV tests were conducted at the Wyle Laboratory in the United States.

- Test Objectives

Demonstrate reliable operation of the DPV.

- Phenomena

Mass flow rate in a DPV was not measured because the tests focused on the successful opening of the DPV.

Full-size testing of the DPV was conducted by GENE to demonstrate its operation and reliability. However, the design and testing of the DPV are not part of the ESBWR preapplication review.

3.7.1.1.4 Vacuum Breaker Tests

Full-size VB tests were conducted at a GENE facility in the U.S.

- Test Objectives

Demonstrate reliable operation of the VB.

- Phenomena

Opening pressure and closing pressure of a VB were measured.

GENE has conducted full-size VB tests to demonstrate its operation and reliability. However, technical evaluation of the VB testing program is not part of the ESBWR preapplication review.

3.7.1.2 Integral Systems Tests

Integral systems tests were conducted at three test facilities — GIST, GIRAFFE, and PANDA.

3.7.1.2.1 GIST Tests

- Test Objectives

(1) Demonstrate the technical feasibility of the GDCS concept.

(2) Provide a sufficient database to confirm the adequacy of TRACG to predict GDCS flow initiation times, GDCS flow rates, and RPV water levels.

- Test Description

The Gravity-Driven Integrated Systems Tests (GIST) focused on the GDCS performance for maintaining core cooling in a LOCA and were performed by GENE in San Jose, California, in 1988. The GIST facility was a section-scaled simulation of the 1987 SBWR design configuration, with a 1:1 vertical scale and a 1:508 horizontal area scale of the RPV and containment volumes. Because of the 1:1 vertical scaling, the tests provided real-time response of the 1987 SBWR pressures and temperatures.

The GIST test program included the effects of various plant conditions on GDCS initiation and performance. The GIST facility consisted of four pressure vessels—the RPV, upper Drywell, lower Drywell, and the wetwell. The wetwell included the GDCS fluid. The RPV included internal structures, an electrically heated core, and bypass and chimney regions.

The GIST facility modeled the SBWR plant behavior during the late stage of the RPV blowdown. The tests were started with the RPV at 791 kPa (100 psig) and continued

until the GDCS flow initiated and flooded the RPV. Four types of tests were conducted—MSLB, GDLB, BDLB, and no break scenario (e.g., loss of feedwater). All these tests lasted from 600 to 1210 seconds. Twenty-nine integral systems tests were conducted.

- Phenomena

Integral systems response of the RPV and containment during the late blowdown phase and GDCS injection phase of LOCAs was investigated.

Strengths

Unlike the PANDA M-series and GIRAFFE tests, GIST tests were obtained in a facility that was based on an older SBWR design without a separate GDCS pool. Instead, the elevated SP also served as the GDCS coolant source. In this aspect, the GIST design is closer to the ESBWR.

Three kinds of LOCAs were tested in GIST — the MSLB, GDLB, and BDLB. Sensitivity studies have shown that these breaks can be expected to bracket other LOCAs in terms of break sizes, locations, and coolant flow. Nineteen LOCA tests were conducted, which included eight MSLB tests, four GDLB tests, and seven BDLB tests. For the same kind of LOCA (e.g., MSLB), initial test conditions were varied among the reactor vessel water level, SP level, and the number of GDCS injection lines operational. The figure of merit, the critical safety parameter, for the GIST tests was the minimum downcomer water level.

The tests have demonstrated technical feasibility of depressurizing the RPV to sufficiently low pressures below the static head of an elevated pool of water in the containment, enabling coolant injection to the core.

Weaknesses

There were two phenomenon distortions caused by design limitations. First, GIST used two vertical pipes as the replacement for the annular downcomer of the reactor vessel between the lower plenum and the upper plenum above the core. Asymmetrical behavior was observed during part of the tests that revealed a two-phase or frothy mixture in one downcomer pipe and phase separation (low-void water in the bottom with steam above) in another downcomer pipe. This kind of asymmetry is not expected to occur in the annular vessel downcomer of the ESBWR since it does not have the separation as with the test facility's separate downcomer pipes. Second, a single standpipe was installed above the upper plenum of the RPV, where periodic percolation was found to exist during part of the tests, which led to periodic variations in the RPV pressure. However, these distortions are not expected to invalidate the overall integral systems behavior observed in the GIST tests.

Evaluation

The GIST tests have demonstrated technical feasibility of the GDCS concept, which involves RPV depressurization to allow coolant injection to the vessel from an elevated pool of water in the containment. Despite the phenomenological distortions described above, the overall GDCS performance providing coolant to a depressurized RPV remains valid as shown in the GIST tests for a broad spectrum of LOCAs. The GIST data are acceptable as a valid database to qualify the TRACG code for the late blowdown and early GDCS injection phase of the LOCAs, including the MSLB, GDLB, and BDLB.

3.7.1.2.2 GIRAFFE Helium Tests

- Test Objectives

- (1) Demonstrate the operation of a passive containment cooling system with the presence of a lighter-than-steam noncondensable gas, including demonstrating the process of purging noncondensable gases from the PCC.
- (2) Provide a database to confirm the adequacy of TRACG to predict SBWR containment system performance in the presence of a lighter-than-steam noncondensable gas, including potential systems interaction effects.
- (3) Provide a tie-back test, which includes the appropriate quality assurance documentation, to repeat a previous GIRAFFE test.

- Test Description

GIRAFFE/helium tests were performed as a joint effort by GE and Toshiba in Kawasaki City, Japan. The GIRAFFE facility is a large-scale, integral system test facility designed to exhibit post-LOCA thermal-hydraulic behavior similar to the SBWR systems that are important to long-term containment cooling following a LOCA.

The global volume scaling of the facility is approximately 1:400, with a nominal height scaling of 1:1. The SBWR components simulated in the facility are the RPV, PCCS, GDCS, drywell, wetwell, and the connecting piping and valves. Five separate vessels represent the SBWR RPV, drywell, wetwell, GDCS pools, and the PCCS pool. The facility was equipped with one PCC, approximately scaled to represent the three SBWR PCCS condensers. Electric heaters provided a variable power source to simulate the core decay heat and the stored energy in the reactor structures.

For the helium series tests, once the test initial conditions were established, all control (except for the decay of RPV power and helium injection, if called for) was terminated, and the GIRAFFE containment was allowed to function without operator intervention (except that the VB was operated manually to simulate automatic operation in SBWR

and minor wetwell microheater power adjustments were made to compensate for facility heat losses).

- Phenomena

Integral systems response of the RPV and containment during the long-term cooling phase of LOCAs was investigated.

Strengths

Four tests were conducted to demonstrate the PCCS operation with the presence of a lighter-than-steam noncondensable gas (using helium as a substitute for hydrogen gas) and a heavier-than-steam noncondensable gas (nitrogen). Test H1 was the base case test with the initial test conditions based on TRACG calculations for the SBWR during the long-term cooling phase at 1 hour after the break initiation (RPV initial pressure at 295 kPa or 42.8 psia). Test H2 was a repeat of Test H1 but with helium to replace nitrogen in the drywell. Test H3 was a variation of Test H1 by replacing some steam in the drywell with helium. Test H4 was similar to Test H1 but with a constant helium injection into the drywell.

In addition, two other MSLB tests, Tests T1 and T2, were conducted with nitrogen as the only noncondensable gas in the containment. The initial nitrogen concentrations were much higher than those in helium tests, but the tests were initiated at lower RPV and containment pressures.

Weaknesses

- (1) Heat loss was a concern in the GIRAFFE facility, which was tall and thin. Electric microheaters were installed to wrap around the metal walls of the drywell, wetwell, and GDCS pool, which were covered with an insulation material. Microheater power for each component was determined during the shakedown tests to compensate for the heat loss. Since the microheater power could not fully compensate for the heat loss, the RPV electric heater power was raised above the scaled decay heat to further compensate for the heat loss in the facility with microheaters on. But this provision could not eliminate the local heat loss in the lower drywell, for which the heat loss was found to be significant. The heat loss could introduce some local distortions in the test data.
- (2) There were only two noncondensable gas sampling locations in the drywell — one at the top of the drywell and the other at the very bottom of the drywell located in the lower drywell where the local heat loss was significant. The heat loss at the bottom sampling location could somewhat distort the noncondensable gas behavior in the drywell. This problem was compounded with the scarcity of the noncondensable sampling locations. For the wetwell gas space, there was only one noncondensable gas sampling location. However, unlike the lower drywell, the wetwell wall heat loss was found to be insignificant. The scarcity of the noncondensable gas sampling locations and the heat

loss problem at the lower drywell tended to reduce the quality of the containment noncondensable gas distribution data.

- (3) All the GIRAFFE helium tests (including tests T1 and T2) focused on the long-term cooling phase of the MSLB and did not include the late blowdown phase and GDCS phase. One of the tests should have been selected as a typical MSLB test to cover the late blowdown phase, GDCS phase, and the long-term cooling phase, which is within the capability of the GIRAFFE facility. The lack of a typical MSLB test starting at the late blowdown phase was a weakness of this test program.

Evaluation

The GIRAFFE helium tests have demonstrated the PCCS performance to maintain containment cooling during the long-term cooling phase of the MSLB, which is the most critical LOCA to challenge the containment. The impact on the PCCS performance has been investigated for both heavier-than-steam (nitrogen gas) and lighter-than-steam (helium gas) noncondensable gases present in the containment under various test conditions.

Because of the heat loss at the lower drywell, noncondensable gas distribution in the drywell is distorted by having a much higher noncondensable concentration (due to local steam condensation) than expected in the lower drywell. Furthermore, since there were only two noncondensable sampling locations in the drywell and only one in the wetwell gas space, extra efforts are needed to interpret the data and use the data to qualify the TRACG code regarding the noncondensable gas distributions in the containment. Nevertheless, there were many measurements on pressures, temperatures, and water levels that are sufficient to explain the containment response with the presence of the heavier-than-steam and lighter-than-steam noncondensable gases.

The GIRAFFE helium tests were based on the SBWR design, which is very similar to the ESBWR design in terms of the RPV and containment phenomena expected in a LOCA. Furthermore, there aren't any new phenomena introduced as a result of the design changes from the SBWR to the ESBWR. In view of the above, the staff concludes that the GIRAFFE helium tests provide a valid database to qualify the TRACG code for the long-term cooling phase of a LOCA involving both lighter-than-steam and heavier-than-steam noncondensable gases, although a careful examination of all the data was necessary.

3.7.1.2.3 GIRAFFE Systems Interactions Tests

- Test Objectives

Provide a database to confirm the adequacy of TRACG to predict the SBWR ECCS performance during the late blowdown phase and GDCS injection phase of a LOCA, with specific focus on potential systems interaction effects.

- Test Description

A series of four transient systems tests was conducted to provide an integral systems database for potential systems interaction effects in the late blowdown phase and GDCS injection phase. All four tests involved liquid breaks—three GDLBs and one BDLB. Tests were performed with and without the ICS and PCCS in operation, and with two different single failures.

The post-LOCA thermal-hydraulic behavior (especially the RPV pressure transient and water level transient), the GDCS injection characteristics, and possible systems interactions were investigated in the tests. The test facility modeled the whole containment system of the SBWR. The SBWR components modeled in the facility were the RPV, ICS, GDCS, PCCS, drywell, wetwell, and the connecting piping and valves. Major portions of the SBWR containment (drywell, wetwell, and GDCS pool, as well as IC pool and PCCS pool) were modeled using separate vessels.

The PCC unit was the same as that used for the GIRAFFE Helium Tests and consisted of a steam box, heat transfer tubes, and a water box. The PCC had three heat transfer tubes corresponding to the scaled volume. The heat transfer tubes were full height, and the internal tube flow area was almost the same as the scaled SBWR flow area. One scaled IC was mounted above the drywell vessel. The IC had three tubes, two of which were plugged in order to reduce the heat transfer surface of the unit. This single condenser represented two IC condensers found in the SBWR.

Testing followed a methodology very similar to that used in the PANDA tests and GIRAFFE helium tests. Once the initial conditions for a given test were established, all controls (except for the decay of RPV power) were terminated. The GIRAFFE RPV and containment were allowed to function without operator intervention, mirroring the Standard Safety Analysis Report (SSAR) assumptions for the SBWR. The GDCS pool-to-drywell flow was manually terminated at 1 hour in the GDCS break cases to avoid an inappropriate emptying of the pool. This was necessary since a single pool in GIRAFFE simulated the three SBWR pools, only one of which would have pool-to-drywell flow.

Manually stopping GDCS flow to the drywell in GIRAFFE simulated the end of draining for that one pool in the SBWR and maintained the simulation of flow from the remaining pools to the RPV.

- Phenomena

Integral systems responses of the RPV and containment in the late blowdown phase and GDCS injection phase of the GDLB and BDLB were measured. By comparing two similar GDLB tests with and without the PCCS and ICS operation, interactions between the PCCS/ICS and GDCS were assessed. Phenomena associated with the integral systems tests were investigated.

Strengths

Four integral systems tests were conducted to assess the GDCS performance in maintaining a covered core with and without the operation of the ICS and PCCS. Two kinds of LOCAs were investigated with break locations below the main steam line elevation—GDLB and BDLB. Test GS1 was for a GDLB without the operation of the PCCS and ICS assuming a DPV failure (failed to open upon demand). Test GS2 was similar to Test GS1 but with the operation of the PCCS and ICS. Test GS3 was a BDLB with the operation of the PCCS and ICS assuming a DPV failure. Test GS4 was a GDLB with the operation of the PCCS and ICS assuming a valve failure on a GDCS injection line. These tests complemented the GIRAFFE helium tests for which only the MSLB was investigated. Potential interactions between the GDCS operation and the PCCS/ICS operation were assessed.

Weaknesses

- (1) The GIRAFFE heat loss problem, discussed in the GIRAFFE helium tests, was also present in the GIRAFFE systems interaction tests. Although electric microheaters were used around the drywell, wetwell, and GDCS pool, and the RPV heater power was increased beyond the scaled decay heat to compensate for the heat loss, the heat loss problem could not be fully eliminated. For instance, the local heat loss in the lower drywell was found to be significant. The heat loss could introduce some distortions in the test data.
- (2) GIRAFFE/systems interactions tests lasted only two hours, which were not long enough to lead to the potential opening of the equalizing lines to provide SP water to the RPV. As a result, the equalizing line mass flow, which is a high-ranked phenomenon in the LOCA/Containment PIRT, was not observed in the test data.

Evaluation

In all four tests conducted, the GDCS injection ran smoothly without noticeable flow oscillations. It performed well to keep the core covered and maintain core cooling. Comparing Tests GS1 and GS2, the PCCS/ICS operation had no adverse impact on GDCS performance and led to a lower containment pressure as expected. Operation of the ICS significantly reduced the steam flow available to the PCCS except for the initial 200 to 300 seconds.

The GIRAFFE helium tests were based on the SBWR design, which is very similar to the ESBWR design in terms of the RPV and containment phenomena expected in a LOCA. Furthermore, there aren't any new phenomena introduced as a result of the design changes from the SBWR to the ESBWR. Accordingly, the staff concludes the GIRAFFE systems interactions tests provide a valid database to qualify the TRACG code for the late blowdown phase and GDCS injection phase of a LOCA.

3.7.1.2.4 PANDA M-Series Tests

- Test Objectives

- (1) Provide a sufficient database to confirm the capability of TRACG to predict SBWR containment system performance, including potential systems interaction effects.
- (2) Demonstrate startup and long-term operation of a passive containment cooling system.

- Test Description

PANDA M-series tests were performed as a joint effort by GENE and the Paul Scherrer Institute (PSI) in Wuerenlingen, Switzerland. The test facility was a large-scale integrated containment structure which was a 1/25 volumetric, full-height, scaled model of the SBWR containment. It was a modular facility with separate pressure vessels representing the RPV, drywell, wetwell, and GDCS pool. The facility was equipped with three scaled PCC heat exchangers and one IC unit (scaled from two SBWR IC units), each with a separate pool of water. Electrical heaters were used in the RPV to simulate decay heat and the thermal capacitance of the RPV walls and internals in the SBWR. The test facility also had interconnecting piping arrangements needed to conduct the MSLB tests. The tests were started at an equivalent condition from about 1040 seconds (transition from the GDCS injection phase to the long-term cooling phase) to about 3600 seconds (beginning of the long-term cooling phase) after the initiation of the MSLB in the SBWR. The duration of a test was up to 20 hours.

When the initial conditions for a given test were established, all controls were terminated except for automatic control of the wetwell-to-drywell VB position and the electric heater simulation of the RPV structure stored energy release and core decay heat power. The PANDA containment was then allowed to function without operator intervention, consistent with the SSAR assumptions for the SBWR. The only exceptions to the procedure described above were for tests M3A and M3B, which included operator action to maintain PCC pool level, and test M6/8 during which the operator established a drywell-to-wetwell flow path (bypass leakage) and later valved the IC unit out of service.

- Phenomena

Integral systems response of the RPV, drywell, and wetwell was investigated for the late GDCS injection phase and long-term cooling phase of a MSLB LOCA. PCCS performance for maintaining containment cooling was assessed.

Strengths

PANDA was a “large” test facility at a scale of 1/25 of the SBWR. It had all the necessary components to conduct the integral systems tests to investigate the long-term cooling phase of a DBA, namely the MSLB accident that is most challenging to the containment.

The PANDA M-series tests consisted of 10 integral systems tests for the MSLB that covered a broad spectrum of test conditions expected in the SBWR. Except for test M9, these tests focused on the long-term cooling phase of the MSLB (occurring at about 1 hour after break initiation). Test M9 included both the late GDCS injection phase (with the initial test conditions based on 1040 seconds after the break initiation in the SBWR) and the long-term cooling phase of a LOCA. These tests have demonstrated successful operation of the PCCS for maintaining adequate containment cooling under various MSLB conditions in a large test facility.

Weaknesses

- (1) PANDA M-series tests were designed to focus on the MSLB accident that is the most challenging LOCA to the containment. There was no lower drywell in PANDA, and consequently the GDLB and the BDLB could not be tested. Potential opening of the GDCS equalizing lines (expected to occur during the long-term cooling phase of the BDLB) to provide SP water to the RPV could not be investigated.
- (2) The volume of the GDCS pool was much smaller than the scaled volume, and consequently there was an insufficient amount of water to cover the entire spectrum of the GDCS injection phase. As a result, the long-term cooling phase and only a portion of the GDCS injection phase of the MSLB LOCA were investigated in the PANDA tests.
- (3) Large oscillations occurred in the main steam line mass flow rates, when the water level in the RPV was high (close to the top of the chimney). The flow oscillations were greatly reduced if the initial RPV water level was at a low level (several meters below the top of the chimney). The flow oscillations might have been caused by design distortions in PANDA (e.g., lack of core inlet orifices, fuel assemblies, steam separators, dryers, and multiple fuel assemblies in the RPV), although they did not prevent the PCCS from maintaining containment cooling.

Evaluation

The PANDA test facility had all the necessary components to conduct the integral systems tests for a design-basis LOCA such as the MSLB. The M-series tests covered a broad spectrum of the test parameters expected in the SBWR (which are similar to the ESBWR test parameters) to investigate the long-term cooling phase of a LOCA. The PCCS performed well, and maintained adequate containment cooling in the MSLB test. Drywell air was purged to the wetwell via the PCCS. There was a smooth transition from the GDCS injection phase to the long-term cooling phase. The VB openings in a test did not significantly affect the global drywell and pressure response, in comparison to a similar test without the VB openings.

Although the PANDA M-series data are for the MSLB test conditions, the containment phenomena in the long-term cooling phase of other LOCAs, such as the GDLB and BDLB, are generally similar to those of the MSLB (with an exception to be discussed below). This is because before the start of the long-term cooling phase (with variations in the starting time that is LOCA-dependent), the RPV has depressurized from the ADS actuation and the GDCS injection has become insignificant. However, there is one exception. As stated in the “Weaknesses” above, the potential opening of the GDCS equalizing lines (expected to occur during the long-term cooling phase of the BDLB) to provide SP water to the RPV cannot be investigated in PANDA. Nevertheless, the physical process (as well as code modeling) for the SP injection to the RPV is similar to that for the GDCS injection to the RPV (in PANDA test M9). The lack of the PANDA data on the SP injection to the RPV is a deficiency in the test data, but not a critical one.

As stated earlier, the PANDA M-series tests were based on the SBWR design, which is very similar to the ESBWR design in terms of the RPV and containment phenomena expected in a LOCA. Furthermore, no new phenomena were introduced as a result of the design changes from the SBWR to the ESBWR. Equally important, the phenomena observed in the PANDA M-series tests are generally understood and seem to be reasonable. For instance, the addition of relatively cold water at room temperature to the PCC pools temporarily enhances the overall PCC heat removal rate and can lead to VB opening. But this does not significantly affect the overall behavior of the drywell and wetwell pressures.

In conclusion, the PANDA M-series tests provide a valid database to qualify the TRACG code for the long-term cooling phase of a LOCA relevant to the ESBWR LOCA analyses.

3.7.1.2.5 PANDA P-Series Confirmatory Tests

- Test Objectives

- (1) Reinforce the existing database to confirm the adequacy of TRACG to predict the ESBWR containment performance, including potential systems interaction effects.
- (2) Confirm the performance of the ESBWR containment configuration with the GDCS gas space connected to the wetwell gas space.

- Test Description

PANDA is a large-scale integral test facility originally designed to model the long-term cooling phase of a LOCA for the SBWR. It has all the major components, including the RPV, drywell, wetwell, and a GDCS pool. The RPV was equipped with electrical heaters and heater controls to simulate decay heat and the release of RPV stored energy. The facility included all three scaled PCC heat exchangers and one IC unit and their associated water pools. Other components represented in PANDA include VBs

between the drywell and the wetwell, and the equalizing lines between the SP and the RPV.

The RPV was represented by a single vessel in PANDA, while the drywell and wetwell were represented by two pairs of vessels, connected by large pipes. This double-vessel arrangement permitted investigation of spatial distribution effects within the containment volumes. The water in the RPV was heated by a bank of controlled electrical heaters that could be programmed to match the decay heat curve. Main steam lines conveyed boiloff steam from the RPV to the two drywell vessels. The PCC and IC inlet lines were connected to the drywell and RPV, respectively. Drain lines from the lower headers of the PCC and IC units returned condensate to the RPV. Vent lines from the lower headers of the PCCs and the upper and lower headers of the IC were at prototypical submergences in the SP. VBs were located in the lines connecting the drywell and wetwell gas spaces. PANDA had the capability to valve out one of the main steam lines, the IC and individual PCCs. It also had the capability to inject noncondensable gas (air or helium) into the drywell over a prescribed time period during the post-LOCA transient tests.

In the original PANDA/SBWR configuration (for the PANDA M-series tests), the GDCS gas space was connected to the drywell. A major modification of PANDA for the ESBWR was to connect the GDCS gas space to the wetwell gas space. This ESBWR design feature provided a larger volume for the noncondensable gases that are purged from the drywell to the wetwell during the blowdown phase and therefore reduced the containment pressure. In its original configuration for the SBWR, PANDA was a 1/25 volume scaled, full-height representation of the SBWR primary system and containment. As configured for the P-series tests for the ESBWR, the PANDA facility is a full-height representation of the ESBWR containment at a nominal volumetric scale of 1:45. The piping interconnecting the PANDA vessels was scaled (primarily with the use of orifice plates) to produce the same pressure loss as the corresponding ESBWR piping. The three PANDA PCC units were approximately equivalent to the four ESBWR PCC units, and the one PANDA IC unit was about 10 percent underscaled relative to the four ESBWR IC units.

- Phenomena

Integral systems response of the RPV, drywell, and wetwell was investigated for the late GDCS injection phase and the long-term cooling phase of the MSLB. PCCS performance for maintaining containment cooling was assessed.

Strengths

The PANDA P-series tests were based on the ESBWR design, in which the GDCS pool is isolated from the drywell and its gas space is connected to the wetwell gas space instead of the drywell, as in the SBWR, and the PCCS drain lines were connected to the RPV instead of the GDCS pool, as in the SBWR. This was a minor deviation from the ESBWR design, in which a

PCCS drain line is connected to a condensate drain tank that is connected to the RPV. The P-series tests consisted of eight integral systems tests for the MSLB (which is the most challenging LOCA to the containment) to investigate the containment response and phenomena during the long-term cooling phase under various initial and boundary conditions. PCCS performance was successfully demonstrated to maintain containment cooling. Various containment phenomena were investigated. The changes noted made the PANDA-P tests consistent with the ESBWR design with minor deviations.

Weaknesses

- (1) Like the PANDA M-series tests, the PANDA P-series tests were conducted in the same facility except with modifications necessary to conform to the ESBWR design as stated earlier. There was no lower drywell, and other LOCAs with a lower break location such as the GDLB and the BDLB could not be tested. Potential openings of the GDCS equalizing lines (expected to occur during the long-term cooling phase of the BDLB) to provide SP water to the RPV were not investigated.
- (2) Unlike the ESBWR, the two vertical main vent pipes between the PANDA drywell and wetwell were exposed to the wetwell gas space. There was drywell gas condensation inside the main vent pipes surrounded by the relatively colder wetwell gas. As a result, the wetwell gas temperature increased. This is a non-prototypical phenomenon not expected in the ESBWR, because all of the vertical main vent pipes in the ESBWR are located inside an annular concrete wall between the drywell and wetwell and are not exposed to the wetwell gas. Because of this non-prototypical condensation, PANDA test operators had to isolate the main vent pipes (by closing valves) from the drywell at 11 hours after initiation of the P1 test. The main vent gas condensation in the P1 test was nonprototypical and caused by a design distortion in PANDA.
- (3) The PCC pools in PANDA were much smaller than the scaled volume. For tests longer than about 35,000 seconds (9.7 hours), the PCC condenser tubes were uncovered unless water was added to the pool from an outside source.

Evaluation

The PANDA facility has all the necessary components to conduct the integral systems tests for a design-basis LOCA such as the MSLB. The P-series tests covered a broad spectrum of the test conditions expected in the ESBWR to investigate the long-term cooling phase of a LOCA. The PCCS performed well, and maintained adequate containment cooling in the MSLB tested. The transition was smooth from the late GDCS injection phase to the long-term cooling phase. Injection of a noncondensable gas (using either air as a simulant of nitrogen or helium as a simulant of hydrogen) to the drywell degraded the PCC performance. Depending on the amount of the noncondensable gas injected, it seems that the PCCS was capable of purging it from the drywell to the wetwell.

At a low decay heat equivalent to several hours into the MSLB, the test data suggest that the PCCS is capable of maintaining containment cooling even when the PCC condenser tubes are substantially uncovered.

Although the PANDA P-series data are for the MSLB application, the containment phenomena in the long-term cooling phase of other LOCAs, such as the GDLB and BDLB, are generally similar to those of the MSLB (with an exception discussed below). This is because prior to the start of the long-term cooling phase, the RPV has depressurized from the ADS actuation. However, there is one exception. As stated in the "Weaknesses" above, the potential opening of the GDCS equalizing lines (expected to occur during the long-term cooling phase of the BDLB) to provide SP water to the RPV could not be investigated in PANDA. Nevertheless, the physical process (as well as code modeling) for the SP injection to the RPV is similar to that for the GDCS injection to the RPV (in PANDA test P2). This is a potential question to be reviewed at the design certification stage since it is a long term cooling item.

As stated in the "Weaknesses" above, some of the data have revealed distortions, e.g., temperature rise in the wetwell gas space due to nonprototypical heating from the gas flow in the vertical main vent pipe until it was valved out. However, these distortions are not expected to change the overall containment behavior. The phenomena observed in the PANDA P-series tests are generally understood and seem to be reasonable. For example, when a VB opened, some of the wetwell noncondensable gas flowed to the drywell and degraded the PCC performance. As a result, the drywell pressure first rose and eventually leveled off when the pressure difference between the drywell and the wetwell was sufficient to overcome the PCC vent submergence and vent pipe flow resistance. As expected, main vents cleared (to vent the drywell gas directly into the wetwell) when there was insufficient heat removal in the PCCS as a result of either the absence of one PCC unit (out of a total of three) or noncondensable gas injection to the drywell during a test.

Comparing the counterpart tests between the PANDA P-series and M-series, it reveals that the drywell and wetwell pressures in a P-series test were several psi lower than in a similar M-series test. This favorable comparison supports the statement that the design change made for the ESBWR (by connecting the GDCS pool gas space to the wetwell instead of connecting it to the drywell as in the SBWR) is a design improvement, because the wetwell gas space increases as the GDCS pools drain to the RPV. The larger the wetwell gas space, the smaller the wetwell pressure rise from the same amount of noncondensable gas that fills the containment during the normal operation.

In conclusion, based on the above, the PANDA P-series tests provide a valid database to confirm the qualification of the TRACG code for the long-term cooling phase of a LOCA relevant to the ESBWR LOCA analyses.

Summary of the ESBWR Component and Integral Systems Testing Programs

The full-size component test data from the PANTHERS/PCC and PANTHERS/IC test programs cover the range of the operational conditions expected in the design-basis LOCAs in the

ESBWR. These data are deemed to be adequate for validating the TRACG code regarding the PCCS and ICS performance in the ESBWR (with the understanding that a PCCS condenser in the ESBWR has approximately 35 percent more heat removal capability compared to the PANTHERS/PCC condenser and an ICS condenser has twice the heat removal capability as the single-module PANTHERS/IC condenser).

The integral systems test data from the GIST, GIRAFFE helium, GIRAFFE systems interactions, PANDA M-series, and PANDA P-series testing programs as a whole cover a range of the late blowdown phase, GDSCS phase, and long-term cooling phase of the accidents. Strengths and weaknesses of the individual testing program are identified and evaluated. The staff understands the phenomena revealed in the data and concludes that the weaknesses (including some phenomenon distortions) in general do not invalidate the overall reactor vessel and containment response in a LOCA. The combined data from the GIST, GIRAFFE, and PANDA integral systems tests cover the LOCA phenomena and processes defined in the PIRTs for the late blowdown phase, GDSCS phase, and long-term cooling phase.

It should be pointed out that each integral systems test provides a set of “valuable” data on the time-dependent, thermal-hydraulic response of its RPV, drywell, and wetwell with the operation of the GDSCS, PCCS, or ICS in a LOCA. In order for the TRACG code to properly simulate the test, the code must have technically-sound conservation equations including the constitutive package and numerics. As a result, the data of an integral systems test are useful for assessing a code against the test for the specific test configuration and initial and boundary conditions. However, to link the integral systems test data to the ESBWR response in a LOCA, an adequate scaling analysis is needed to demonstrate the applicability of the test data to the ESBWR response. Otherwise, a satisfactory TRACG simulation of the integral systems test data should not be used as an indication of a satisfactory TRACG simulation of the ESBWR LOCA response. Review of the GENE scaling analysis is found in Section 3.10 of this report.

Comparing the similar PANDA M-series and P-series tests reveals that a design change introduced in the ESBWR by connecting the gas space of the GDSCS pools to the wetwell (instead of the drywell as in the SBWR) seems to be an improvement, because it leads to a lower containment pressure.

Scaling analyses performed by GENE have shown that the test facilities were scaled properly for their intended purpose. All the test facilities meet the top-down scaling criteria. However, the power-to-volume scaling approach introduces scaling distortions related to structural heating/cooling, aspect ratio, and geometrical complexity. These distortions were identified and evaluated by GENE. GENE concluded that they did not exclude the essential phenomena expected to occur in the ESBWR design and that the experimental results are appropriate for TRACG qualification.

The distortions, as identified by GENE, were due to heat transfer from RPV structures, heat transfer to and from the drywell and wetwell structures, and drywell 3-D effects, including drywell mixing, noncondensable gas stratification, and buoyancy/natural circulation. GENE has developed bounding models to address these 3-D effects such that TRACG is able to

adequately predict these effects . GENE concluded that the data from the GIRAFFE and the PANDA facilities can be used for scale-up to the ESBWR through the TRACG code. Based on this evaluation, GENE also concluded that the TRACG model used for the containment/LOCA evaluation is conservatively biased.

The staff has reviewed and evaluated the test programs performed initially in support of the GENE SBWR design and finds the testing to be applicable to the ESBWR design, based on the PIRT and scaling analysis found in Section 3.10 of this report. Based on the design description for the ESBWR provided in Reference 15, the staff concludes that no further testing in support of the thermal hydraulic behavior of the design is necessary. Should significant changes be made to the design as described in Reference 15, the staff will reevaluate that conclusion.

3.7.2 Staff Calculations

The use of a single code for both the reactor coolant system performance and containment performance triggered the thought that an independent calculation with a containment-specific code would provide a check on this dual use approach. The staff decided to initiate model development and use of the CONTAIN code as a means of performing an independent confirmatory calculation for comparison with the TRACG results.

In addition, the staff decided to also perform confirmatory calculations using its own audit code, TRACE. Through each of these confirmatory analyses it would be possible for the staff to determine whether or not the TRACG results were reasonably representative of the ESBWR response. The staff did not perform a full assessment of its own codes against all of the assessment cases used in the TRACG assessment. Sufficient assessment has been performed, however, to ascertain the performance characteristics of the staff supported codes.

3.7.2.1 Staff Independent Analyses and TRACG ESBWR Input Model Review

3.7.2.1.1 Confirmatory Analysis Scope and Review Approach

The GENE ESBWR design, although developed from the ABWR and operating BWR technology, has several unique features developed during the smaller SBWR design effort—the use of a long chimney on top of the core to enhance in-vessel natural circulation, the venturi type nozzle at the GDCS injection line, the ADS using DPVs, ECCS injection from the GDCS pools, and containment cooling by the PCCS system. These new features pose challenges to the modeling capabilities of the TRACG code, which is used to model containment phenomenon as well as the reactor coolant system behavior . As a part of the review process, the staff performed a series of independent analyses to evaluate the TRACG code's capability to model these new features.

The ESBWR PIRT and TAPD, Reference 12, have identified many important physical phenomenon. The staff developed a confirmatory analysis matrix to examine the following list of major code modeling features, which are important to analyze the system response of this reactor during a LOCA event.

- in-vessel chimney two-phase flow
- critical flow through the break during blow-down
- mass and energy discharge from the reactor pressure vessel to the containment
- mass and energy transfer in wetwell pool.

Based on the examination of separate effect models, the GDLB LOCA and the MSLB LOCA case were examined using both TRACG and NRC independent audit codes TRACE/CONTAIN. Table 3.7.2.1 lists the calculation matrix and a brief description of the purposes. The staff performed 11 sets of calculations.

Table 3.7.2.1 Confirmatory Calculation Matrix

#	Case Descriptions	Computer Code Used By Staff	Comparison With	Examined TRACG Features
1	Ontario Hydro Steady State Test	TRACG	Ontario Hydro Test Data	Two-phase flow in the chimney partition. Void fraction distribution.
2	Critical Flow Model Examination	TRACG	Edwards Pipe Test Data	Critical flow through the break.
3	Kinetic Energy Deposition Verification	TRACG	Hand Calculation	Energy conservation through the break into the containment.
4	Suppression Pool Energy Deposition	TRACG	PSTF Test	Mass & energy transfer from drywell to wetwell.
5	Gravity Preservation	TRACG	Hand Calculation	Gravity head calculation.
6	Main Steam Line LOCA With Full Feed Water	TRACG	GENE Bounding Calculation	Examine the peak containment pressure and temperature.
7	Main Steam Line LOCA Base Case	TRACG	GENE Base Case Calculation	Staff independent analysis verifying GENE's calculation.
8	GDCS Line LOCA Base Case	TRACG	GENE Base Case Calculation	Staff independent analysis verifying GENE's calculation.
9	Main Steam Line LOCA Base Case	TRACG, CONTAIN TRACE/CONTAIN	GENE Base Case Calculation	Evaluate short term containment pressure and temperature responses, long term PCCS cooling.

10	GDCS Line LOCA Base Case	TRACE/ CONTAIN	GENE Base Case Calculation	Evaluate short term ECCS performance and long term cooling.
11	Bottom Drain Line LOCA Base Case	TRACG	GENE Base Case Calculation	Evaluate long term chimney collapsed water level and core heatup

3.7.2.1.2 Separate Effect Model Evaluation

Two-Phase Flow In Chimney Partition

The ESBWR uses chimney partition plates to divide the space in the chimney region into many small square flow channels. Each chimney partition has up to 16 fuel bundles including the corresponding bypass area to provide the inlet flow. The void fraction distribution in the chimney partition has a strong influence on the core flow as the core flow depends on the net gravity driving head between the downcomer and chimney/core regions. In order to examine the void distribution in the chimney region, Ontario Hydro Technologies in Canada performed 61 cm diameter vertical tube two-phase flow tests, references 11 and 16. The tests covered the pressure range between 2.8 MPa and 6.4 MPa, the temperature range between 230 EC and 280 EC and the void fraction range between 80 percent and 50 percent. The Multi-beam Gamma Ray Attenuation Technique was used to measure the void fraction radial distribution. The test results showed that the void fraction radial distribution was relatively flat and the average void fractions calculated from the axial pressure drop data were found to be in good agreement with those obtained using the Gamma Densitometer.

For the low pressure and low mass flux flow condition, data from Wilson's and Bartolomei's experiments were used to benchmark the TRACG code, Reference 16. In Wilson's test, steam was bubbled through saturated water in a vertical pressure vessel 0.48 m in diameter and 3.66 m high. The Bartolomei tests were performed in a thick-walled vertical pressure vessel, 1.22 m in diameter and about 5 m tall. Water was heated by high pressure hot water coils inside the vessel. The test covers the pressure range up to 4.6 MPa, with the vapor flux between 0.04–0.1 m/s and the void fraction varying from 12 percent to 20 percent.

GENE performed TRACG calculations to verify the code's capability to calculate the axial void fraction and pressure drop for all three tests. The staff examined the TRACG input model for the Ontario Hydro Test facility and independently ran the TRACG code. Figure 3.7.2.1, in Section 8 of this report, shows the calculated void fraction versus test data. The TRACG calculated void fraction closely followed the transient void fraction measured during the test. Therefore, the staff concluded that TRACG has demonstrated its capability to accurately calculate the void fraction and the pressure drop. Accordingly, the uniform radial void fraction distribution in the chimney partition is a reasonable assumption to model the two-phase flow in that region.

Critical Flow Model Verification

The choked flow rate through the break determines the pressurization rate of the containment and the two-phase water level in the chimney. The accuracy of the model significantly affects the outcome of the LOCA evaluation and the containment peak pressure and temperature analyses. TRACG uses the equilibrium critical flow model based on a semi-empirical approximation of the choking criteria derived from the general one-dimensional, two-phase fluid field equations. From the input, a user can turn on the choke option at any given cell face. GENE has validated the model using several tests and experimental data.

The Edwards Pipe blowdown test has been used as a standard for evaluating critical flow models for rapid depressurization. The test section for this experiment consisted of a 4.096 m long horizontal pipe, with an inner diameter of 0.073 m, filled with liquid, heated, and pressurized to 7.0 MPa. The saturation pressure corresponding to the initial liquid temperature was about 2.4 MPa. At time zero, a glass plate covering the end of the pipe was broken, and the pipe depressurized through the open end of the pipe in approximately 0.6 seconds. As this test covers the choked flow for subcooled liquid and saturated two-phase mixture, it was selected as the confirmatory case to evaluate the TRACG critical flow model.

A TRACG model consisting of a FILL component, a 20-cell horizontal PIPE component, and a BREAK component were used to simulate the test. The results show the critical flow model was turned on at the outlet cell face of the PIPE component during the blowdown. Figure 3.7.2.2, in Section 8 of this report, shows the comparison between the measured void fraction and the TRACG results. Good agreement between these two sets was observed. The measured pipe internal pressure and the TRACG results are shown in a similar trend. This confirmatory analysis case verifies not only the capability to calculate the choked flow, but also the interfacial heat transfer and other physical models.

Therefore, this case further demonstrates that TRACG has the capability to accurately calculate the critical (choked) flow through a break.

Kinetic Energy Deposition

Historically, the TRAC series of codes eliminated the kinetic energy term from the energy equations through algebraic manipulations involving the momentum equation. In that form, the flow work in the energy equation was of a nonconserving form, and energy balance errors could occur. This simplified approach has been identified as one obstacle when the TRAC series of codes are used to model the interaction between the RPV and the containment during the blowdown phase. With this deficiency, a computer code may significantly underestimate the energy discharge into the containment during a LOCA, thus resulting in nonconservative containment peak pressure and temperature predictions.

TRACG avoids this problem by retaining the kinetic energy term in the energy equations for both the vapor and liquid phases. The internal energy and the kinetic energy are lumped in both time and spacial derivatives. Therefore, the kinetic energy of the break flow transported

into the containment during the blowdown period should be preserved. In order to verify the proper implementation of the kinetic energy convection in TRACG code, a simple test problem was developed. As shown in Figure 3.7.2.4, in Section 8 of this report, a straight horizontal PIPE component with a flow area of 0.5 m^2 and a length of 0.6 meter is modeled. An orifice with a flow area of $1.0\text{E-}3 \text{ m}^2$ is located in the middle of the pipe. Two BREAK components set up the pressure boundary conditions at 5 MPa and the entire pipe is filled with saturated stagnant water. Then, the pressure of one of the BREAK components ramps down to atmospheric pressure within 50 seconds. The choked flow through the orifice is stabilized around 80 seconds. The vapor and liquid flowing through the orifice reach the speed of sound. After passing through the orifice, both vapor and liquid slow down and the kinetic energy is converted into fluid internal energy.

If the code properly conserves the energy and accurately models the kinetic energy conversion, the inlet and outlet total enthalpy and work should be identical. This TRACG case was run to 100 seconds and all the system variables are stabilized. A hand calculation was performed to verify the change of total enthalpy plus pressure-volume work across cell face #2 and #6 based on TRACG output at 100 seconds. The results show that the change is less than 0.1 percent. Therefore, this proves that TRACG has overcome the deficiency of the TRAC series of codes of not conserving energy, and has the capability to accurately calculate the energy discharge from the RPV to the containment, which is essential to model the ESBWR containment pressurization during a LOCA.

Suppression Pool Mass and Energy Transfer

One of the major containment phenomena is SP steam condensation. TRACG was developed primarily for modeling vessel internal flow and heat transfer. It was not intended to be used for containment analysis. In order to model suppression pool mass and energy transfer, a special modeling approach was used. As shown in Figure 3.3-1 of Reference 11[[

]].

During the MSLB LOCA, as the blowdown flow decreases, the level in the main vent rises, sequentially closing off the horizontal rows of vents. When the flow stops in each of the lower two rows of horizontal vents, the fluid in that level of the pool is [[

]]. This modeling approach has been developed largely based on the PSTF test documented in Reference 16. Therefore, the PSTF full-scale vent test case

(5803 series) was selected as the basis to examine TRACG's capability to model the SP condensation.

The TRACG model consists of a VESSEL component, combined with several one-dimensional components. The VESSEL component was used for both the drywell and wetwell, with the top level used to represent the drywell volume. The geometry of the PSTF 8-degree section of the suppression pool was preserved in TRACG modeling using a sector of the outer two rings of the VESSEL component. The TRACG result is shown in Figure 3.7.2.8a in Section 8 of this report. The temperature of Volume 5 of the VESSEL model is compared with the measured test data. It is confirmed that TRACG overpredicts the measured temperature profile by approximately 5 °C. Thus, the result confirms that the PSTF assessment was reasonably done and the nodalization developed through the PSTF assessment is applicable to the ESBWR configuration.

Gravity Head Preservation

The ESBWR TRACG GDCS line LOCA model used a 3-D VESSEL component to model both the RPV and the containment. As shown in Figure 2.7-1 of Reference 11, the VESSEL component is divided into $[[\quad]]$ radial rings and $[[\quad]]$ axial levels. The bottom $[[\quad]]$ levels model the reactor vessel and vessel internals, while levels $[[\quad]]$ model the containment, including the drywell, GDCS pools, SP, and PCCS drain tanks. Within the 3-D vessel component, all containment volumes have an arbitrary higher elevation than their real elevations. As the gravity driving head is the dominant force to inject the GDCS pool water into the RPV, it becomes a concern whether the gravity head has been correctly calculated using this modeling approach. A further evaluation of the TRACG code concluded that if two cells within a 3-D VESSEL component only interact with each other through another 1-D component, then the actual elevation difference between two cells must be reflected by the gravity terms defined by the connecting 1-D component.

In order to verify this code feature, a TRACG test problem was set up to examine the flow through a "U" tube with two pools connecting with each end of the PIPE component. As shown in Figure 3.7.2.5, in Section 8 of this report, a 3-D VESSEL component has two pools. One is located at level 2 and ring 1; another is located at level 4 and ring 4. Both pools have the same initial water level and cell center pressure. The top of level 3 is assumed sealed with a zero axial flow area. The two pools are connected by a 5 cell "U" tube. The split of the 3-D vessel component into two volumes with two identical pools should have zero flow rate through the connecting TRACG 1-D PIPE component. The TRACG calculation results show that the flow through the 1-D PIPE is very close to zero. The two pools have the same actual elevations with respect to the "U" tube PIPE component, although they appear to be at different elevations within the 3-D VESSEL component. Therefore, the ESBWR ECCS model preserves the gravity head and the actual elevations with the 1-D component solver.

In addition, this test problem demonstrates that the TRACG code can correctly pass the 3-D cell pressure to the connecting 1-D component cell for a given 1-D connection relative elevation with respect to the 3-D cell bottom cell face.

3.7.2.1.3 Integral Effect Evaluation Using TRACG

GENE submitted two TRACG base input decks for the staff to review, the GDCS LOCA ECCS evaluation model and the MSLB LOCA containment evaluation model. The GDCS line LOCA ECCS model evaluates the effectiveness of the gravity-driven injection and calculates the PCT, minimum water level above the core, and the containment responses. The MSLB LOCA containment model predicts the containment peak pressure and temperature. The staff ran both cases with TRACG04 independently and examined the input and the output of the analysis.

GDCS Line Break LOCA

The GDLB scenario is a double-ended guillotine break of a GDCS drain line. There are three GDCS pools in the ESBWR containment, supplying four divisions of GDCS to the vessel. Each drain divides into two branches before entering into the pressure vessel. Each branch has a check valve followed by a squib-operated injection valve, and finally a nozzle in the vessel wall to limit the blowdown flow in case of a break. The GDCS break is assumed to occur in one branch, between the squib-operated valve and the nozzle entering the vessel. GENE has demonstrated that the GDCS line LOCA is the most limiting case to challenge the ECCS system driven by gravity and the pressure difference between the wetwell and the reactor pressure vessel.

In order to model the in-vessel fluid flow and the distribution in detail, GENE developed a specific TRACG model to evaluate the effectiveness of the ECCS injection. As shown in Figure 2.7-1 of Reference 17, a 2-D TRACG VESSEL component is used to model both the RPV and the containment. The first [] levels model the reactor vessel, while levels [] model the containment. The radial nodalization is primarily determined based on in-vessel component physical structures. There are a total of [] rings with the [] inner rings for the reactor core region and []. [] TRACG CHAN components are used to model the core with the hot channel located in the first ring, which has a bundle power peaking factor of 1.4791. The radial direction flow area [] are set to zero to model the lumped 1-D two-phase flow through the chimney partitions. Above the upper plenum, []. The main steam lines, DPVs, SRVs, and main steam isolation valves are modeled using typical TRACG PIPE, TEE, and VALVE components.

The containment is modeled with the same radial nodalization which is determined by the reactor vessel radial dimensions. Therefore, the TRACG VESSEL cell volume fractions and flow area fractions are set to significantly greater than 1.0 to preserve the total fluid volume in each containment level. The axial elevations from level [] reflect the physical geometry boundary. []

[]

[]. The GDCS pools are modeled by

[]. The PCC and IC heat exchanger are

modeled by PIPE and TEE components. The vertical PIPE, with constant external heat transfer coefficients and outside temperatures, represents the heat exchanger tube bundles.

The staff examined the TRACG input model and independently performed the GDLB LOCA calculation. The results were found identical to what were documented in Reference 11. Several code features and modeling practices are evaluated in detail and documented below.

Core Power Model

Although the TRACG code has the capability to model the core power history during a LOCA using its 3-D kinetics model, only the power versus time table with a fixed axial power distribution was used for both ECCS LOCA and containment LOCA analysis. GENE indicated in response to RAI 4 and RAI 325 that GENE has calculated the core power history considering both decay heat and fission power after the scram signal. GENE used its NRC-approved method, SAFER-GESTR, Reference 30, to calculate decay heat with the following improvements:

- decay heat from fission products were updated to conform with the ANSI/ANS-5.1-1994 standard, Reference 39, which the staff previously approved in Reference 3
- the fuel cycle parameters were conservative, bounding values rather than nominal values
- two-sigma data uncertainty from the standard was used
- new, more conservative evaluations of miscellaneous actinides and structural activation products were used.

Even though the method to generate the decay heat table is acceptable, the base GDCS LOCA model assumes the scram at time zero, when the break occurs, without considering the lag between the high drywell pressure signal and the scram. In response to the staff's concern, GENE estimated a scram delay of [[]] and performed a sensitivity study assuming full power operation during the delay of the scram. The analysis shows that the Level 1 trip occurs at about [[]] earlier than the baseline case. The resulting minimum static collapsed water level in the shroud only dropped [[]] during the first 2000 seconds into the LOCA.

In addition, the staff found that the base case did not include a 2 percent power measurement uncertainty which was later included in GENE sensitivity cases.

Therefore, the staff concluded that the TRACG code has the capability of modeling the core power history for ESBWR LOCA evaluation. During the design certification review stage, the ECCS baseline model should justify the scram delay time and the power measurement uncertainty. In addition, the quick closure of the MSIVs while control rods are being inserted

may increase the total core power due to void collapse. At the design certification stage, GENE should evaluate the effects of void collapse for GDLB and BDLB LOCA cases.

Minimum Water Level Inside The Chimney Partition

TRACG models the chimney region with [[]]. The localized void fraction in different chimney partitions is smeared away. This averaging assumption is employed by the TRACG 3-D VESSEL two-phase level tracking algorithm to calculate the two-phase water level location in the chimney during the GDCS LOCA transient. For those chimney partitions above high power bundles, it is expected that the void fraction in the chimney is different from the averaged value and the baseline model may predict nonconservative minimum water level above the core.

In response to the staff's concern, GENE performed additional parametric analysis to examine the effect of the bundle power distribution on the minimum chimney water level. GENE set the radial power peaking factor of [[]] fuel bundles [[]]. The other radial peaking factors were [[]] for [[]] bundles feeding the chimney region [[]] for the [[]] feeding the chimney region [[]]. The results demonstrated that the minimum static head calculated by the baseline model is greater than that calculated in the parametric study. The base model overestimated the minimum static head [[]], which is [[]] percent of the margin in the static head. In addition to the impact on the minimum static head, GENE observed enhanced two-phase flow through the hot channel due to additional two-phase driving head in the chimney partition, the so-called "drafting" effect.

Independently from GENE, the staff performed a TRACG run using a different but conservative approach to analyze the two-phase flow in the chimney partition above the hot channel. Instead of lumping all the fuel bundles in ring 1 into one channel component with the maximum radial power peaking factor, a PIPE component representing 1/4 of a regular chimney partition is connected with the hot channel and the upper plenum. It was conservatively assumed that the bypass flow does not join the channel outlet flow. The results showed a reduction of the minimum chimney static head and the "drafting" effect.

In conclusion, the staff believes that TRACG code and the baseline GDCS LOCA model are able to predict the average static water head in the chimney partition. Nodalization studies will be necessary at design certification to calculate the minimum water level in the chimney partition.

Hot Channel High Void Fraction Flashing

Based on the GDLB LOCA analysis, GENE states that the ESBWR core would never be uncovered during a LOCA since the two-phase water level is always above the top of active fuel region, and no core heatup, no dryout, and no boiling transition would occur. Staff independent analysis identified that the hot channel, which was modeled by CHAN0011, experienced high

void fraction flow for a period of 30 seconds starting from 400 seconds into the LOCA event. The maximum channel inlet and outlet void fractions were [[] and [[]] respectively, while the void fraction in the heated region was about [[]]. Figure 3.7.2.6, in the figures section of this report, shows the hot channel outlet void fraction during the transient. The staff was concerned with the possibility that the ESBWR core experiences boiling transition, and that film boiling may cause core heatup. Consequently, the staff requested additional analyses from GENE to identify the maximum duration for which the hot channel experiences high void fraction flashing and the minimum thermal margin.

In response to the staff's request, GENE analyzed three additional LOCA cases, MSLB LOCA, GDCS LOCA, and BDLB LOCA, with conservative assumptions of 102 percent of rated power prior to the break and delayed scram time. As opposed to the baseline model, the TRACG input models defined all the fuel bundles inside ring 1 as the hot channel.

The staff agrees with GENE that a hot channel "drafting" effect does exist. However, defining all of the fuel bundles in ring one as the hot channel would overestimate the effect and the results may tend to be nonconservative. The staff requested further justification. GENE modified TRACG04 and performed the GDCS LOCA base case analysis. The newly calculated minimum thermal margin is shown in Figure 3.7.2.7 in Section 8 of this report. The minimum value of the thermal margin is above 2.0 throughout the transient, demonstrating that film boiling does not occur. Based on these calculations, the staff agrees with GENE that no core heatup is predicted during a LOCA event.

GDCS Pool Over Pressure

According to the ESBWR design, the GDCS pool gas space is connected with the SP gas space through three large-diameter vent pipes. Therefore, the pressure should be equalized during normal operation. However, an examination of the GDCS LOCA baseline calculation revealed that the TRACG code calculated a higher GDCS pool gas space pressure than the SP pressure due to the simplified GDCS pool nodalization. The unrealistic pressure results in a higher initial inventory of air in the GDCS gas space, which causes slightly higher GDCS air space pressure during the GDCS phase of injection. GENE examined the input model and indicated that this is caused by the coarse nodalization of the GDCS pool. For the TRACG code, if there is a water level in the cell that is higher than the cell center, the pressure will be correctly calculated at the cell center, accounting for the static head above the cell center. The cell center pressure will be higher than the pressure in the gas space above the level by that static head. Since in TRACG the gas space pressure above the water level in the cell is the same as the cell center pressure, it is overestimated. The initial noncondensable volume at the top of the GDCS pool is of the order of 80 m³. The error in the initial noncondensable inventory in the GDCS pool is of the order of 10 percent of the total mass in the 80 m³ volume. The wetwell gas space volume is of the order of 4500 m³. Thus, the fractional error in the total noncondensable inventory in the wetwell gas space plus the GDCS pool is negligible.

Therefore, the staff agrees that TRACG acceptably calculates the cell center pressure and the overestimation of the noncondensable mass in the GDCS pool can be resolved using a different

nodalization. The additional amount of noncondensable gas mass is negligible comparing the total amount of initial noncondensable gas mass in the wetwell and GDCS pool air space.

Wetwell and GDCS Pool Connecting Vent Pipe Model

There are three vertical vent pipes connecting GDCS pool gas space with the wetwell gas space. The TRACG GDCS LOCA model lumps two GDCS pools [[]], and the third pool, which has a broken GDCS injection line, is modeled by a separate volume. Two TRACG PIPE components, PIPE42 and PIPE43, are used to model the vent pipes. The staff found that the volume and the flow area of these two PIPE components are identical, however one of them should be twice as large as the other. Considering a very small pressure difference between the GDCS air space and the wetwell, this modeling practice does not affect the results significantly. However, during the design certification stage, correct vent pipe volume should be used.

PCCS Pool Modeling

Instead of explicitly modeling the PCCS and ICS pool on top of the drywell, GENE models the heat transfer between the PCCS tube bundle external surface and the pool with a constant heat transfer coefficient and a constant temperature. Although the initial pool temperature is 316.5 K (110EF), the bundle surface bulk fluid temperature is set to 378 K (220EF). During the blowdown period, which is between 0 and 600 seconds into the transient, the dominant mass and heat transfer is steam condensation inside the SP. The impact of PCC operation on the drywell pressure and the wetwell pressure is negligible. Therefore, GENE believes that it is not important to realistically model the heat transfer between the pool and the PCCS heat exchanger. During GDCS injection, since the noncondensibles have been largely swept into the wetwell and the pressure is strongly affected by the VB operation, PCCS operation also does not significantly affect the course of GDCS injection. After the GDCS injection, the pool temperature gradually increases to the saturation temperature and the assumption of 378 K (220EF) for the fluid temperature is acceptable. [The assumption of a constant heat transfer coefficient is reasonable for the first 2000 seconds while the PCCS heat exchanger is covered.] For transients beyond 2000 seconds, the heat transfer coefficient is subject to change when the condenser tubes are gradually uncovered due to pool boiloff.

Therefore, the staff concludes that the current PCCS pool modeling approach for the first 2000 seconds of ECCS LOCA evaluation is reasonable. During the design certification stage, if the ECCS evaluation model is used beyond 2000 seconds, additional VESSEL levels need to be added on [[]], and the pool needs to be modeled in the same fashion as it is done for the containment/LOCA model.

MSLB LOCA Analysis Using TRACG Code

As described in Section 3.7.2.1.2 of Reference 11, GENE used [[]] component to model the entire ESBWR containment and the RPV for containment LOCA analysis, as shown in Figure 3.7-1 of Reference 11. The reactor vessel was coarsely modeled by [[]]

]] and [[]] levels. [[

]].

The model includes the DPV lines and SRV lines. The drywell to wetwell vents are modeled by several TEE components and VALVE components.

The staff independently ran the TRACG code with the MSLB LOCA model and produced the same results as what was submitted in Reference 11. The following two modeling features are examined in detail.

Heat Structure Modeling

The ESBWR RPV is made of carbon steel with a thickness of approximate 184 mm. Outside the steel vessel there is an air gap of 250 mm, and then the reflective type of thermal shield with a thickness of 90 mm. Further out stands the 160 mm thick vessel shield which is made of low alloy structural steel. In order to model heat conduction through these structures, GENE's MSLB containment/LOCA base deck defined a [[]] thick heat structure around the RPV. The thermal properties are assumed to be uniform across the heat structure. The inner surface of the heat structure is assumed to have an initial temperature equal to the vessel internal fluid temperature. GENE performed a parametric study, replacing the [[]] heat structure with a thickness of [[]], that demonstrated there was a nonphysical heat sink effect. However, the impact on peak drywell pressure was found to be small, with a pressure increase of [[]]. Therefore, the staff agrees that the [[]] heat structure does not significantly alter the peak pressure prediction. However, during the design certification stage, the separation of the vessel shield, the reflective thermal insulation layer, and the air gap from the lumped heat structure is considered necessary.

Feedwater Mass And Energy Discharge

In Section 2.2.1.2 of Reference 11, GENE defines the MSLB LOCA scenario. It was assumed that the feedwater pump is tripped and the feedwater flow is lost after the break. From the perspective of LOCA ECCS performance evaluation, the assumption leads to a conservative PCT evaluation as it reduces the available coolant inventory. For containment analysis, the feedwater carrying the feedwater heater train stored energy significantly increases the mass and energy discharge through the break into the containment. The assumption of the loss of feedwater flow used by GENE for the current design is nonconservative, resulting in underestimation of the maximum containment pressure and temperature. The feedwater flow assumption should be justified at the design certification phase.

In order to examine the impact of the feedwater system mass and energy discharge into the RPV, the staff independently performed a sensitivity study using a bounding assumption for the feedwater mass and energy discharge. Without detailed design information for the feedwater

heater train, the staff assumed that the feedwater injection lasts for 600 seconds and the temperature ramps down linearly from the initial feedwater temperature to the saturation temperature at the containment design pressure limit. The calculation was done using the baseline MSLB LOCA model. The result is shown in Figure 3.7.2.8 in Section 8 of this report. The peak drywell pressure of [[]] occurs about [[]] into the transient and is greater than the bounding value calculated by GENE in Reference 11, [[]]. Consequently, GENE performed additional analyses in response to the staff's concern. GENE assumed that the hot water residing in the feedwater heater system (98,144 kg, 215,917 lb) prior to the LOCA is injected into the RPV [[]]. Using the baseline MSLB model, GENE predicted a [[]] peak drywell pressure increase. The results show the feedwater mass and energy release during the MSLB LOCA increases the peak drywell pressure by about [[]]. There is also a possibility that the wetwell volume is flooded and the noncondensable gas is purged to the drywell. Should significant amounts of noncondensable gas be discharged into the drywell volume, the PCCS performance may be degraded.

Without detailed feedwater heater system design information, both the staff and GENE had to make assumptions about the mass and energy discharge from the feedwater heater system. The bounding containment peak pressure and temperature will be evaluated during the design certification stage after the feedwater heater system design is finalized. If the evaluation indicates that the code application range is exceeded or that a new scenario, such as wetwell flooding, has not been examined during the preapplication stage, the staff may choose to review the TRACG code for its new use.

Bottom Drain Line Break LOCA Analysis Using TRACG Code

The BDLB is one of the three design basis LOCA scenarios defined by GENE. The initial short term scoping analysis performed by GE indicated that the GDLB is the most limiting case in terms of the minimum chimney collapsed water level. Therefore, GENE did not include the BDLB LOCA case in Reference 11. Concerned about the long term ECCS behavior during a BDLB break event, the staff requested an analysis of the BDLB LOCA case up to 72 hours as RAI 183. GENE responded to this RAI and performed the long term BDLB LOCA analysis using the MSLB LOCA model with break location changes. GENE found that the bypass region was uncovered at about 7 hours. The staff therefore requested the TRACG base input model for the BDLB LOCA case for independent verification. After the input model was submitted, the staff independently ran the TRACG code with the BDLB LOCA model and produced the same results as were submitted by GE in response to RAI 183. The following two issues are discussed in detail.

Possible Core Uncovery And Heat Up

The staff's major concerns are potential core uncovery during the long term cooling stage of the BDLB LOCA and the potential for subsequent core heatup. The staff found that the calculated minimum collapsed water level in the chimney is zero around 7 hours into the transient for the base case and confirmed that the water level in the bypass region dropped below the TAF.

However, the in-channel two-phase level did not drop below TAF. As shown in Figure 3.7.2.35 in Section 8 of this report, the top node of the average channel component active fuel region experienced a maximum void fraction of about 65%. Except for the bypass region, the core remains covered.

Although the average channel remains covered during the entire transient and there is no core heatup, the calculated zero minimum chimney water level is not consistent with GENE's determination that the GDCS LOCA case is the most limiting case for ECCS evaluation. In addition, the base case does not differentiate the hot channel from the core average channel. It is unknown whether the hot channel is subject to dryout. Therefore, GENE performed sensitivity studies of collapsed water level versus lower drywell volume. Their calculations indicated that, with a 200 m³ volume reduction in the lower drywell volume, the ECCS system could provide sufficient coolant to flood the drywell to the elevation of 1 meter above TAF. For the GDCS LOCA case, the minimum collapsed water level in the chimney region is 1.84 m throughout the entire 72 hours of the transient. Therefore, GENE has demonstrated that with a revised lower drywell volume, the ECCS will have the capability to prevent core uncover and core heatup for all three design basis LOCA scenarios. More detailed evaluation will be performed by the staff performed during the design certification stage to verify that the core remains covered for the final ESBWR design configuration.

Modeling Application Procedures

For the ECCS performance evaluation during the long term cooling stage, GENE has performed BDLB and GDCS LOCA analyses with both the reference design and with the reduced drywell volume configuration. GENE demonstrated that there was sufficient collapsed water level above the core with the reduced drywell volume for the GDCS and BDLB cases. The BDLB case eventually relied on ECCS injection through the suppression pool equalizing line to maintain the level. It was observed that the collapsed water level is sensitive to the pressure balance between the reactor pressure vessel, drywell and wetwell. However, all the long term phenomenon were analyzed using the CONTAINMENT LOCA model documented in Ref. 11, which was specifically tailored to maximize the containment pressure and temperature. At this point, GENE has not demonstrated that the CONTAINMENT LOCA model and relevant application procedures are applicable to the ECCS long term performance evaluation and no uncertainty analysis has been done to quantify the minimum water level. Therefore, for the design certification, appropriate TRACG application procedures should be developed to conservatively calculate the collapsed water level in the chimney above the hot channel for the three break locations, MSLB, BDLB and GDLB. The procedures and the associated uncertainty analysis methodology should be applicable to both short term and long term LOCA events (up to 72 hours).

3.7.2.2 CONTAIN

Staff predictions of the behavior of the GENE ESBWR containment design following an MSLB were obtained using the CONTAIN computer code. These predictions were compared with the GENE predictions from the TRACG baseline containment analysis presented in Reference 11.

In order to compare the CONTAIN containment thermodynamic predictions with the TRACG containment predictions from GENE, the mass and energy releases obtained from the TRACG code, up until the time cooling water is determined to enter the RPV, were used as input for the CONTAIN containment analysis. It should be noted that the TRACG analysis includes models of the primary system and containment. During this initial period, choked flow is expected to exist at the break location. Consequently, the break flow during this time is not dependent on containment pressure conditions. During this initial time period, the TRACG calculated mass and energy flows through the DPVs and the SRVs were also provided as input into CONTAIN.

After the initial time period when the break mass and energy conditions were input into CONTAIN, the CONTAIN analysis uses an RPV volume to calculate the mass and energy releases to the containment. The thermodynamic conditions for the RPV at the transition time from choked flow were obtained from the TRACG calculations. Consequently, the CONTAIN code could calculate the mass and energy flowrate from the RPV to the containment through the break, the DPVs and the SRVs. Based on their setpoint actuation conditions, the DPVs were determined by TRACG to open during the initial time period when the mass and energy flow is input into CONTAIN. Consequently, the DPVs are assumed to be fully open at the end of the initial time period; however, SRV operation after the initial time period is determined by the pressure dependent valve operating characteristics input into CONTAIN.

Three CONTAIN models were used to analyze the ESBWR containment. One model divides the drywell into five vertical volumes, a second model divides the drywell into ten volumes, and a third model uses a single drywell volume. The results from the three models are presented in order to provide a sensitivity assessment for noncondensable gas redistribution in the ESBWR containment and the resulting effects on drywell-wetwell vacuum breaker operation, and to assess the PCCS heat exchanger long-term heat removal performance.

For the model with one drywell volume, the volume of the drywell is equal to the sum of the volumes of the five drywell volumes. Similarly, for the CONTAIN model with ten drywell volumes, the volumes of the drywell volumes are half of those used in the five volume model .

The initial containment conditions for the three CONTAIN input models are consistent with the conditions specified for the TRACG containment analysis baseline results described in Reference 11. The CONTAIN modeling is also consistent with the TRACG containment model. Specific characteristics of this model are listed below.

- (1) The ten vents between the drywell and suppression pool are modeled as a single volume with one entrance interface and three exit interfaces to the suppression pool at the three horizontal exit elevations.
- (2) Three GDCS pools are modeled. A valve in the GDCS line between each tank and the RPV is opened at 539 seconds after the MSLB. The time at which this valve opens is obtained from the TRACG analysis. Flow from each GDCS tank to the RPV is determined by CONTAIN using flow path junctions.

- (3) The PCCS heat exchangers are available and operational during and after the initial blowdown period. A flow path representing the PCCS gas vent line connects the top of the outlet plenum and the wetwell suppression pool. The CONTAIN model will account for the condensation of steam flowing out of the PCCS gas vent line as a result of contact with the suppression pool. Water condensed in the PCCS heat exchangers is directed to the PCCS outlet plenum volume. A flow path connects the outlet plenum to the drain tank volume. Flow can exist from the drain tank to the RPV volume after the valve between the drain tank and the RPV opens at 519.66 seconds. The time at which this valve opens is obtained from the TRACG analysis. Consistent with the GENE assumptions for the TRACG baseline containment analysis, four PCCS heat exchangers are assumed available. The CONTAIN model has the ability to perform analyses assuming the availability of three or four PCCS heat exchangers.
- (4) Condensation in the interior surface of the PCCS heat exchanger tubes is calculated using the CONTAIN heat and mass transfer model, which accounts for the presence of noncondensable flow in the steam flow. The condensed liquid is added to the outlet plenum using the CONTAIN "filmflow" calculation, which tracks the condensation film thickness on the inner tube surfaces. The outer surfaces of the PCCS tubes are placed in contact with a constant temperature sink, equivalent to the boiling temperature in the cooling pool, with an input boundary condition heat transfer coefficient of 4500 W/(m²-K) to simulate boiling conditions on the PCCS tube exterior. The PCCS heat exchanger model is consistent with the CONTAIN model described in Reference 41 which was developed for use with the GENE SBWR and compared against GIRAFFE test results.

This calculation method does not allow for the determination of the PCCS cooling pool conditions within the CONTAIN calculations. Consequently, the reduction of the water level in the cooling pool was calculated external to the CONTAIN calculations. However, the water level calculation uses the heat removal rates calculated by the CONTAIN code. Specifically, the cooling pool water mass loss was calculated using the following equation, which assumes that all the heat added to the cooling pool by the PCCS heat exchangers will result from pool boiling.

$$\Delta m_{\text{pool boiling}} = Q_{\text{to cooling pool}} / (h_g \text{ (at 373.15 K) } - h_f \text{ (at 316.5 K) })$$

The saturated vapor enthalpy, h_g , is obtained for the saturation conditions of 100 EC at 1 atmosphere which is equivalent to outside atmosphere conditions. The liquid enthalpy, h_f , is determined at the initial water temperature of the PCCS cooling pool.

- (5) The drywell-wetwell VBs are modeled as one lumped pressure dependent flow path. Consistent with the assumptions in the TRACG containment model for the GENE baseline analysis, the current analysis assumes the availability of three VBs; however, the CONTAIN input model can be run assuming the availability of two or three VBs.
- (6) During the initial time period after the MSLB, i.e. before 517 seconds, the break mass and energy are added to the break drywell volume using a source table. The break

mass and energy release is obtained from the TRACG analysis. After the initial time period, the break blowdown is calculated by CONTAIN using a flow path junction from the RPV volume.

- (7) The mass and energy flow from the DPVs during the initial time period before 517 seconds are added to the appropriate drywell volume using a source table. The mass and energy releases are obtained from the TRACG analysis and reflect that code's determination of setpoint conditions and actuation delays. After the initial time period, the mass and energy flow through the DPVs are calculated by CONTAIN using a flow path junction to the RPV volume.
- (8) The SRV flows during the initial time period are obtained from the TRACG analysis. The mass and energy flows are added to the corresponding CONTAIN SRV discharge piping volume modeled in CONTAIN using a source table. After the initial time period, flows through the SRVs are determined by a pressure dependent flow junction modeled in CONTAIN.
- (9) Heat slabs have been added to the CONTAIN input using the surface areas, thicknesses, and material definitions contained in the TRACG model. The outer wall atmospheric boundary temperature and heat transfer coefficient were also obtained from the TRACG model.
- (10) Natural convection is used in the CONTAIN analysis to calculate heat transfer coefficients for all structures in the containment volumes by setting the forced convection velocity equal to zero. Forced convection is allowed, however, inside the PCCS heat exchanger tubing.
- (11) The procedure for calculating RPV vapor formation presented in Reference 41 represents an upper end calculation of long-term containment response. This approach was used because the previous version of the CONTAIN code did not have the ability to calculate boiling conditions such as are present in the RPV. Consequently, after the initial time period, which lasts 517 seconds, vaporization in the RPV is calculated assuming the maximum amount of vaporization due to decay heat addition. The vaporization in the RPV volume is set equal to:

$$m = q_{\text{decay heat}} / (h_g(\text{at } 3 \times 10^5 \text{ Pa}) - h_f(\text{at } 316.5 \text{ K})).$$

The steam enthalpy value is assumed at a typical long-term containment pressure of 3×10^5 Pa. The liquid enthalpy is assumed consistent with the GDCS pool temperature of 316.5 K (110 EF). This mass and energy release rate is added to the RPV volume in a source table. At the same time, liquid mass is removed from the RPV pool at 316.5 K (110 EF) to preserve mass and energy balance. Flows from the RPV to the drywell break volume are calculated for both the break and DPV flow paths. Similarly, flow from the RPV through the SRVs are calculated by CONTAIN using the pressure dependent flow paths.

The analyses using the CONTAIN models with five or ten drywell volumes were run assuming that vapor formation in the RPV starts at 517 seconds as indicated above. The analysis using a single volume drywell was executed assuming a delay in the generation of vapor in the RPV volume. The vapor was assumed to stop being generated between 600 and 1500 seconds; during that time the decay heat is added directly to the water in the RPV. This assumption was made to approximate the delay in vapor flow from the break that was predicted by the GE TRACG model, which contains a detailed two-phase model of the RPV. The delay in vapor generation is believed to be attributed to the cooling effect of the GDCS flow entering the RPV. The delay in vapor generation also provides a greater possibility for drywell-wetwell vacuum breaker operation resulting from steam condensation in the drywell. A single drywell volume also results in a more uniform concentration of noncondensable gas than the multi-volume drywell models. With the multi-volume drywell models, the noncondensable gas is calculated to accumulate in the lowest elevation dead-ended drywell volumes.

- (12) Consistent with the GENE TRACG containment model, the CONTAIN input has included a bypass flow path of $1 \times 10^{-4} \text{ m}^2$ between the drywell and wetwell.
- (13) During the performance of the ESBWR analyses using all three CONTAIN models, numerical solution problems were encountered with the gaseous flow connection between the drywell and the PCCS drain tank. In the ESBWR design, the top of the PCCS drain tank is fully open to the drywell. Unfortunately, because of limitations in the CONTAIN numerical solution, the code would "stall" and stop execution if the full flow area of 2 to 3 m^2 was input. The solution could only be successfully executed if this flow area was set equal to zero or a small value.

3.7.2.2.1 Results

The ESBWR containment analysis for an MSLB, performed by GENE using the TRACG computer code, has been compared to MSLB analyses performed by the staff using the CONTAIN computer code.

Comparison of CONTAIN and TRACG Predictions

This section compares the results of the three CONTAIN analyses to each other and to the results reported by GE using TRACG.

Pressure Predictions - The drywell and wetwell pressures predicted by the CONTAIN five and ten drywell volume models are very close in value, however, these results differ from the one drywell volume CONTAIN analysis results. It is interesting to note that containment pressures for the five and ten drywell volume CONTAIN models are predicted to be lower than the TRACG calculation. In contrast, the containment pressures for the one drywell volume exceed the TRACG results in the short-term, but drop below the TRACG predictions in the long-term. The multi-volume drywell models provide a better model of the temperature variations which can occur in the tall drywell compartment.

The multi-volume approach can also account for noncondensable gas distribution effects in the containment. Concerns regarding noncondensable gas distribution were the primary reason for performing a one-volume drywell analysis. The one-volume drywell model would produce a uniform noncondensable gas distribution in the drywell and could affect the distribution of the noncondensable gas in the drywell and wetwell. In fact, the one-volume drywell model resulted in the transfer of almost all the drywell nitrogen to the wetwell early in the calculations; whereas, in the five and ten drywell volume models, nitrogen accumulated in the wetwell and the lower drywell volumes.

It should be noted that the one-volume drywell analysis with an RPV vaporization delay did predict a drop in drywell pressure below wetwell pressure resulting in drywell-wetwell vacuum breaker operation. However, when a vaporization delay was introduced into the multi-volume drywell models, the drywell pressure did not fall below the wetwell pressure and vacuum breaker operation was not predicted.

All CONTAIN analyses predicted lower long-term pressure than TRACG even though tabular inputs for break, DPV and SRV flows obtained from TRACG were used by CONTAIN for the short-term, 0 to 517 second, period. After the short-term period, the "best estimate" assumptions for mass and energy releases were used to calculate the CONTAIN mass and energy releases. However, the CONTAIN analyses did not employ many of the conservative modeling assumptions used in TRACG, nor was CONTAIN able as accurately model the boiling heat transfer in the RPV liquid region and the PCCS cooling pools as TRACG. The differences between the CONTAIN and TRACG results may be due, in part, to the "forced" models activated to produce a conservative TRACG analysis. [[

]]. The staff finds it difficult to draw conclusions at this time regarding long-term behavior based on comparison of the two codes. The differences in capability are significant and call for different approaches to modeling the ESBWR with TRACE or CONTAIN at the design certification stage. The staff conclusion that the TRACG pressure predictions are conservative is not altered by the CONTAIN predictions due to the lack of CONTAIN's ability to adequately model boiling in the RPV liquid region and in the PCCS cooling pool, and the lack of ability to model suppression pool temperature.

Temperature Predictions - The CONTAIN model with one drywell volume predicts short-term drywell temperatures close to the TRACG predictions. The CONTAIN models with five and ten drywell volumes predict a maximum drywell temperature higher than those predicted by TRACG. Because of mixing flows in the ten drywell volume models, the elevated drywell temperature is predicted to decrease in magnitude while the high drywell temperature for the five drywell volume case remains elevated in the long-term. The temperature prediction for the CONTAIN analysis with a single drywell volume results in an artificially low temperature due to mixing. It should be noted that all the CONTAIN analyses predict lower long-term drywell temperatures than TRACG.

The wetwell in the CONTAIN analysis models was modeled as one volume. The wetwell gas temperatures predicted by the five and ten drywell volume CONTAIN models are very close in value. The wetwell gas temperature predicted by the one drywell volume CONTAIN analysis is lower, but follows the same basic shape. The short-term wetwell gas temperatures for the five and ten drywell volume models are closer to the TRACG predictions. However, all the CONTAIN analyses predict lower long-term wetwell gas temperatures than TRACG.

The wetwell suppression pool temperature predicted by the five and ten drywell volume CONTAIN models are close in value. The one drywell volume CONTAIN analysis predicts lower suppression pool temperatures because CONTAIN assumes that the SP is completely mixed and cannot calculate pool temperature gradients. All the CONTAIN long-term suppression pool temperature predictions are lower than those predicted by TRACG.

The differences between the CONTAIN and TRACG predictions are affected by the previously discussed modeling assumptions used in running TRACG with the staff conclusion stated in the previous discussion of the pressure predictions equally applicable here.

Nitrogen Distribution - The five and ten drywell volume CONTAIN models predict nitrogen accumulation in the lowest drywell volumes where the liquid pool collects. The nitrogen accumulations in the wetwell predicted by these two analyses are also close in value. As expected, the one drywell volume CONTAIN model predicts a larger nitrogen accumulation in the wetwell because a single drywell volume does not allow volume for nitrogen accumulation. Consequently, the single drywell volume model responds to the stop in RPV vaporization in the one drywell volume CONTAIN model with a larger drop in drywell pressure due to condensation resulting in a subsequent vacuum breaker operation. As previously stated, when a vaporization delay was introduced into the multi-volume drywell models, the drywell pressure did not fall below the wetwell pressure and vacuum breaker operation was not predicted.

The TRACG analysis predicts vacuum breaker operation throughout the calculated MSLB transient. This effect is most strongly affected by the previously mentioned modeling assumptions used in running TRACG with the staff conclusion stated in the previous discussion of the pressure predictions equally applicable here.

Flow to the RPV - The five and ten drywell volume CONTAIN analyses predict similar flows from the GDCS to the RPV, as evidenced by the drop in GDCS water level elevation, and which differ from the GDCS flows predicted for the one drywell volume model. All the CONTAIN analyses predict a slower drop in GDCS water level elevation than TRACG, and thus CONTAIN predicts GDCS flow to the RPV at a smaller rate than TRACG.

The flow from the PCCS drain tank to the RPV predicted by the five and ten drywell volume CONTAIN models, as evidenced by the PCCS drain tank elevation change, are about the same. However, the PCCS water level for the one drywell volume CONTAIN model is different, implying a different condensation and heat removal rate in the PCCS heat exchangers.

The differences in GDCS and PCCS flow to the RPV could be affected by the previously mentioned TRACG modeling assumptions.

PCCS Heat Removal - The heat removal via the PCCS heat exchanger predicted by the five and ten drywell volume CONTAIN models are very close. The one drywell volume CONTAIN model predicts that the PCCS will remove more heat in the short-term, but the CONTAIN prediction approaches the values predicted by the multi-volume drywell models in the long-term when the PCCS heat removal approaches the decay heat addition. All the CONTAIN models predict a smaller short-term PCCS heat removal than TRACG. In the long-term, TRACG predicts a slightly larger PCCS heat removal than the CONTAIN models.

The CONTAIN models assume free convection on structural surfaces by specifying a zero surface velocity for all surfaces except the inner PCCS heat exchanger surface. Therefore, a free convective, condensing heat transfer coefficient is used on most containment structural surfaces. The PCCS heat exchanger is allowed to account for forced convection effects to determine a forced convective, condensation heat transfer coefficient. In contrast, the TRACG modeling assumptions include the presence of forced convective flow on heat structure surfaces. Consequently, the TRACG heat structures would be expected to heat up faster than the CONTAIN structures. The larger long-term structural heat removal in CONTAIN could result in a lower calculated PCCS heat load. This could account for the slight differences in long-term PCCS heat removal calculated by the CONTAIN models and TRACG. However, the short-term TRACG calculated PCCS heat removal is larger than that calculated by CONTAIN, implying that the overall heat transfer coefficient predicted in the TRACG for the PCCS heat exchanger is larger than that calculated for CONTAIN PCCS heat exchanger using a forced convection heat transfer coefficient. The difference in PCCS heat removal can be related to differences in the overall heat exchanger heat transfer modeling in CONTAIN and TRACG. The condensing heat transfer correlation used in TRACG for the inner tube surface could be different from the one used in CONTAIN. Additionally, the differences between the CONTAIN and TRACG PCCS heat removal may be affected by the differences in heat transfer modeling between the outer surface of the PCCS heat exchanger tubes and the cooling pool. CONTAIN assumes a constant boiling type heat transfer coefficient of $4500 \text{ W}/(\text{m}^2\text{-K})$ with a constant temperature sink equivalent to the boiling temperature in the cooling pool; in contrast, the TRACG code employs an internal boiling heat transfer model with code calculated cooling pool thermodynamic conditions.

3.7.2.2.2 Overall CONTAIN Conclusions

Overall, based on examination of the behavior of CONTAIN, the staff notes that noncondensable gases take longer to get to the wetwell than predicted by TRACG, resulting in a tendency to predict a higher initial drywell pressure, and a slower pressurization of the wetwell compared with the behavior of TRACG. Between about 600 seconds and 2000 seconds, the CONTAIN and TRACG calculations agree very well.

3.7.2.3 TRACE/CONTAIN

TRACE and CONTAIN were first coupled using the Exterior Component Interface (ECI) logic of TRACE to analyze the LOCA containment response of the Westinghouse AP1000 reactor design, which utilizes either a sockets-based or shared memory-based protocol for handling all interprocess communication. In this coupling scheme, TRACE functions as the master process and spawns CONTAIN as a child process. The time step size and edit frequency are controlled by TRACE and communicated to CONTAIN. The boundary conditions, initial conditions, and output variables communicated between TRACE and CONTAIN are specified by the user in a separate input file which is read by a new interface routine added to CONTAIN. This design gives the user flexibility to choose the precise variables to be communicated based on the need for a particular transient.

Several improvements related to ESBWR modeling were later added to the TRACE/CONTAIN coupling interface logic. The first of these was the ability to handle noncondensable flow to and from the RPV modeled by the TRACE code. The second improvement was the ability to handle bi-directional flow between TRACE and CONTAIN, permitting a two-phase mixture to flow from TRACE to CONTAIN and a single-phase liquid to flow from a CONTAIN pool to TRACE. Additional minor improvements which were made include (1) the ability to specify multiple TRACE mass/enthalpy sources to the same CONTAIN cell, (2) improved types of mass/enthalpy sources (e.g., single-phase liquid, single-phase vapor with or without noncondensibles, and two-phase mixture with or without noncondensibles), (3) the ability to handle flow reversals and provide the correct donoring, (4) the ability to handle the situation where a CONTAIN modeled pool completely drains, (5) functionality to allow the time step to be limited by the CONTAIN user-input maximum time step size, (6) error checking the input, and (7) the ability to utilize any TRACE numerical scheme.

The current time advancement logic utilized in TRACE/CONTAIN is explicit in nature, whereby CONTAIN is advanced first, followed by TRACE. In this scheme, CONTAIN uses the previous time step mass flow and enthalpy to compute new time pressure and temperature boundary conditions which are then passed to TRACE prior to the start of TRACE's time step advancement.

3.7.2.3.1 GDCS Line Break LOCA Analysis Using Coupled TRACE and CONTAIN Codes

In addition to using the TRACG code to perform independent analyses, the staff analyzed the limiting GDCS LOCA case using NRC's independent codes, TRACE and CONTAIN. TRACE is used to model the RPV and relevant piping systems. CONTAIN models the entire ESBWR containment and PCCS system. The analysis was performed by running the TRACE and CONTAIN codes in a coupled mode.

Steady State Model

The steady-state ESBWR TRACE model was developed by converting the GENE ESBWR TRACG input deck into the TRAC-BF1 format. A TRACG input deck modeling only the reactor

vessel was first extracted from the TRACG GDCS LOCA baseline model. A steady state calculation was performed and demonstrated that the control system was fully functional to maintain the downcomer water level. A PERL script was executed to convert the input model into the TRAC-BF1 format. Therefore, NRC's TRACE model is almost identical to the TRACG input model.

The TRACE vessel nodalization for the ESBWR model is shown in Figure 3.7.2.9 in Section 8 of this report. The vessel is divided into [[]] and [[]] radial rings, with dimensions indicated on the figure. The three inner rings in the vessel correspond to the steam generation region, and the fourth outer ring corresponds to the vessel downcomer. The level in the downcomer is maintained by a controller on the feedwater flow, which enters the vessel near the top of level 16. The target value for the downcomer level is set at 20.6916 m above the vessel bottom, or 13.2518 m above the TAF.

[[]] CHAN components [[]] are used to model the reactor core; CHAN [[]]

]]. Each CHAN component is based on a GE-12 fuel bundle and is modeled using [[]] axial cells, [[]] of which correspond to the active fuel region. This model is illustrated in Figure 3.7.2.10 in the figures section of this report. Both the water rods and part length fuel rods are explicitly modeled using the TRACE advanced fuel channel model.

The nominal power for the ESBWR core is 4000 MW, and the TRACE model uses point kinetics with reactivity feedback to calculate the core power. The axial power distribution used for each CHAN component is shown above in Figure 3.7.2.10 in Section 8 of this report. The power component modeled in TRACE also includes a scram table and decay heat data. The scram table is designed to insert all of the negative reactivity ($-0.2175 \Delta k/k$) into the core over a period of 2.8 seconds following receipt of the scram signal.

The chimney region of the ESBWR vessel is separated among the [[]] and spans axial levels [[]]. Levels [[]] comprise the mixing section below the inlet to the separators. The separators are currently modeled using [[]] SEPD components (SEPD 80–82), one for each radial ring. The simple separator model is utilized here, where the liquid carryover and vapor carryunder qualities are both set to zero. The dryer region above the separators is modeled at [[]], with the steam dome comprising [[]]. The inlet to the steam lines is modeled at a position of 1.015 m above the bottom of [[]].

The steam lines themselves are modeled with two trains, one representing one line and one representing three lines, as illustrated in Figure 3.7.2.11 in Section 8 of this report. TEE 83 and 84 connect to the vessel and correspond to the steam inlet, and both include a branch for 1 DPV and 3 DPVs, respectively. Connecting to TEE 83 and 84 are TEE 88 and 89, respectively, both of which include a branch for the SRVs. Connecting to TEE 88 and 89 are

VALVE 94 and 95, respectively, which represent the “in board” MSIV and are followed by the “out board” MSIV modeled by VALVE 85 and 86, respectively. VALVEs 85 and 86 come into a single steam manifold, modeled by TEE 96, which leads to TEE 87, which models the direction of steam flow to the first stage of the turbine or the turbine bypass.

The CONTAIN model used for the TRACE/CONTAIN LOCA analysis was developed based on the model used in the CONTAIN stand-alone analysis described in Section 3.7.2.2 of this report. The nodalization of the model with elevations is shown in Figure 3.7.2.12 in Section 8 of this report. There were 21 cells used to model the ESBWR containment building, five of which were used for the drywell. One cell each was used for the PCCS upper and lower plenum, and six cells were used for the PCCS tubes. The PCCS pool, PCCS drain line, wetwell, and wetwell vent pipes were modeled with one cell each. An additional cell (Cell 10) was used to provide the atmospheric condition for the PCCS pool.

The connections to the TRACE model are highlighted in red in Figure 3.7.2.12 in Section 8 of this report. BREAKs 41-43, which represent the DPV boundaries, are connected to the upper drywell of the CONTAIN model (Cell 2). BREAKs 44 and 45, which represent the SRV boundaries, connect to the SRV discharge pipes modeled by Cell 7 and Cell 8, respectively. BREAKs 66 and 67, which represent the wetwell boundary for the GDCS tanks, are both connected to the wetwell modeled by Cell 6. And lastly, BREAKs 98 and 99, which represent the GDLB, are both connected to the portion of the drywell modeled with Cell 3.

Steady State Results

A few key parameters from the steady-state calculation performed with TRACE were compared against results obtained with TRACG, and also against design values, where available. This comparison, which examined steam dome pressure, feedwater temperature and flow rate, downcomer level and flow rate, core inlet subcooling, and core exit void fraction is shown in Table 3.7.2.2. The steam dome pressure and the downcomer water level match the TRACG results very well since these parameters were target values for the steady-state control system. The feedwater flow, however, was not a target value, but still matched well with both the TRACG result and the design value.

Table 3.7.2.2 Comparison of Steady-State Key Parameters.

Key Parameter	Units	TRACE Value	TRACG Value	Design Value	% Deviation
Steam Dome Pressure	Pa	7.16085e6	7.161418e6	7.171e6	-7.39e-3
Feedwater Temperature	K	488.12	488.1	488.75	0.0
Feedwater Flow	kg/sec	2161.2	2161.0	2160.0	9.25e-3

Downcomer Flow	kg/sec	11530.7	11767.8	11833.3	-2.015
Downcomer Level	m	19.4903	19.4916		-6.67e-3
Core Inlet Subcooling	k	13.51	12.85		5.136
Core Exit Void Fraction		0.7493	0.7594		-1.330

The downcomer flow rate (or core flow rate), the core inlet subcooling, and the core exit void fraction also agree very well between the two codes. Even though the TRACE and TRACG codes use different numerical integration schemes and physics packages, only 1% difference in core exit void fraction is observed. The largest relative difference occurs with the core inlet subcooling, which is only 0.66 K (1.19 EF). The slightly different core inlet subcooling results in about 2% difference in the total core flow rate. The comparison of steady state results confirmed that TRACG is capable of calculating the correct initial conditions for the current ESBWR reference design.

GDCS Line Break Model

The GDCS system contains three tanks, one of which provides flow to two 200 mm lines. The other two tanks each provide flow to one 200 mm line. Each of the four lines branches off into two 150 mm lines, giving eight branches into the reactor vessel. On each of the eight GDCS branches, a squib valve and a check valve are present. A diagram of this system is shown in Figure 3.7.2.13 in Section 8 of this report. As indicated in the figure, the assumed break in the GDCS line occurs between the check valve and the vessel wall on one of the four branches coming from the first GDCS pool. Also noted in the figure, one of the squib valves in one of the four lines from the other two tanks is assumed to fail to open, which will be taken into account in the TRACE model.

The TRACE nodalization for the GDLB LOCA, which is based on the diagram previously discussed, is shown in Figure 3.7.2.12 in Section 8 of this report. The two GDCS tanks that are not associated with the break are lumped into a single tank, which is modeled with TEE 77. This TEE connects to VALVE 78, which represents only three GDCS check valves since one squib valve has an assumed failure. Connected to the top of TEE 77 is a vent line modeled by PIPE 76, which connects to the wetwell boundary modeled by BREAK 67.

The other GDCS tank is modeled by TEE 71, which uses PIPE 70 to connect to the wetwell boundary, modeled by BREAK 66. It should be noted that BREAKs 66 and 67 both receive their boundary conditions from the same wetwell volume. TEE 71 connects to TEE 72, which is used to branch into two GDCS lines. TEE 72 connects to VALVE 73 on one end, which represents one GDCS check valve on the broken line, and VALVE 74 on the other, which represents two intact GDCS check valves. VALVE 73 connects to BREAK 98, which

corresponds to the drywell to which the GDLB will blow down. BREAK 99 is the vessel-side break component and is connected to the vessel via PIPE 75. BREAKs 98 and 99 both dump mass and energy to, and receive pressure/temperature boundary conditions from, the same drywell location.

The initiation of the GDLB comes at time zero of the LOCA transient. One second after the break occurs, the turbine is isolated by closing both in-board MSIVs (VALVEs 94 and 95) and both outboard MSIVs (VALVEs 85 and 86). One second later, the feedwater pumps trip, causing the feedwater pumps to coast down. The reactor receives the confirmed scram signal 6.05 seconds into the event and begins to insert the control rods over a period of 2.8 seconds. The vessel will continue to drain until the L1 setpoint is reached, and the ADS sequence is initiated. All information concerning the sequence of events was taken from References 1 and 15.

The control system used for the ADS sequence controls the flow area of the SRVs (VALVEs 92 and 93) and the trip status of the DPVs (VALVEs 58, 90, and 91) and GDCS valves (VALVEs 73, 74, and 78). The control logic for the ADS sequence is based on the L1 level setpoint. Once the L1 setpoint is hit, the SRVs begin to open in stages following a 10-second delay to confirm the L1 condition. The first stage of the DPVs are then tripped open 45 seconds after receipt of the confirmed L1 condition. One hundred and fifty seconds following the confirmed L1 condition, the GDCS check valves begin to open once the upstream pressure is less than the downstream pressure. The GDCS LOCA analysis proceeds for 2000 seconds, at which point the downcomer level is near the top of the chimney region.

GDCS Line Break Results

The GDLB case was run for 2000 seconds, which encompassed the initial blowdown period and the GDCS period. In order to establish a direct comparison between the TRACG analysis results and TRACE/CONTAIN results, the TRACG power-time table is used to model the total reactor core power in TRACE. It is assumed that the reactor is scrammed at time zero due to high drywell pressure. When the downcomer level drops below the Level 2 (L2) set point, a trip signal isolates the steam lines and opens the isolation condenser drain valves. As in the TRACG analysis, no credit is taken for heat removal by the IC. After L2, the downcomer water level continues to decrease, and, without external makeup, the Level 1 (L1) setpoint is reached. After a 10-second delay to confirm the L1 condition, the ADS logic starts the timed sequential opening of the depressurization and injection valves. Four SRVs open first with the remaining eight SRVs opening in two stages to stagger SRV line clearing loads in the SP and to minimize downcomer level swell. Similarly, the opening of the DPVs is delayed 45 seconds. Ten seconds after the last DPV opens, the GDCS injection valves are opened. In the TRACE model, only one valve component is used to model the functional features of both the squib valve and the check valve on each GDCS injection line. Therefore, the GDCS flow does not begin to refill the vessel and the downcomer until the pressure drop opens the check valve. After the GDCS injection starts, both the downcomer and the chimney collapsed water levels start to recover. When the two-phase water level reaches the break, the GDCS flow spills back into the drywell. It is predicted that the GDCS water flow is sufficient to raise the downcomer

two-phase level above the break until the pools empty, after which the level drains back to the break elevation. Figures 3.7.2.15 to 3.7.2.23 in Section 8 of this report depict the major parameters of the system.

Break Flow

The mass flow rate through the GDLB is shown in Figure 3.7.2.15. Both codes predict the same trend of the mass flow rate. At the beginning of the transient, the mass flow rate increases due to increasing dome pressure. After the ADS opens all of the SRVs and DPVs, the break flow rate drops. From 650 to 950 seconds, both codes calculate very small mass flow through the break due to the pressure equalization between the vessel and the drywell. After 1200 seconds the flow from the GDSC spills through the break, and the calculated mass flow rates by both codes are almost identical.

Vessel Steam Dome Pressure

Figure 3.7.2.16 shows the steam dome pressure calculated by the TRACG and TRACE/CONTAIN codes. Both codes predict the initial pressure rise due to the MSIV closure after the break. The dome pressure rises until the downcomer L1 trip activates the ADS system. Both the TRACE/CONTAIN and the TRACG predictions reach the L1 trip about 310 seconds into the transient. After the ADS activates, both codes predict the rapid depressurization and a nearly identical long term pressure trend.

Collapsed Water Level

The collapsed water levels in the downcomer and the chimney partition are shown in Figures 3.7.2.17 and 3.7.2.18. While there are differences in the downcomer water level calculated by the two codes for the early stage of the GDSC injection due to the different containment wetwell pressure, the trends of the downcomer water level prediction are almost identical. Both codes predict that the minimum water level in the downcomer is lower than the TAF. TRACE/CONTAIN predicts a slightly lower minimum water level in the downcomer. The collapsed water level in the chimney decreases at different times consistent with the ADS opening times. The lowest water level remains 1.95 meters above the TAF. Both codes predict a similar trend of level increase following GDSC injection, indicating that the ECCS is capable of preventing core uncover.

Drywell Pressure

The upper drywell total pressure and the noncondensable partial pressure are shown in Figure 3.7.2.19. Both codes predict that most of the noncondensables in the drywell are purged into the wetwell during the early blowdown. The same trend of pressure stabilization is observed. The total pressure difference between the TRACG and TRACE/CONTAIN results is about 0.75 bar, with the TRACG code predicting a higher pressure at about 670 seconds. The difference appears to be caused by different nodalization schemes used for the two codes.

Wetwell Pressure

Figure 3.7.2.20, indicates that the total pressure in the wetwell increases primarily due to the transfer of noncondensibles through the drywell to wetwell vents. The dominant mass transfer through the wetwell liquid is the noncondensable gases which accumulate in the wetwell air space. The TRACG code predicts higher pressure (by about 0.75 bar) at about 670 seconds.

Drywell and Wetwell Temperature

The difference in these two codes is demonstrated clearly in the calculated drywell and wetwell air space temperature, shown in Figure 3.7.2.21. TRACG predicts a 50 K (90 EF) degree higher wetwell air space temperature than does TRACE/CONTAIN. The major difference may be due to the code internal physics packages, e.g, for calculating interfacial heat transfer and pool water surface condensation. Also contributing to the difference is the nodalization schemes used for the two calculations. While the TRACG nodalization partitions the wetwell air space into [[]] nodes, the TRACE/CONTAIN nodalization represents the wetwell by one node. TRACG calculates different air space temperature in different nodes. Although the temperature distributions in the containment are different, the pressure distributions in different containment compartments is similar.

GDCS Injection Mass Flow Rate

A significant feature of the ESBWR ECCS design is the use of a gravity driven cooling system. Figure 3.7.2.22 shows the total GDCS injection mass flow rate. The magnitude and the trend of the TRACG and TRACE predictions are almost identical, with the exception of a shift in the timing of the injection. This timing difference is caused by the different wetwell pressure, confirming not only that the ESBWR gravity driven ECCS system can be expected to function as intended, but also that the TRACG code is capable of realistically modeling the ECCS performance during the GDCS LOCA.

Core Peak Cladding Temperature

The requirement of limiting the PCT to 2200 EF is clearly stated in 10 CFR 50.46. Figure 3.7.2.23 shows the PCT calculated by both TRACG and TRACE/CONTAIN. The PCT peaks at approximately 590 K (602 EF) in the early stage of the blowdown. After the ADS actuation, the PCT drops to about 420 K (296 EF). Both codes predict almost identical trends and maximum peaks, confirming that the ESBWR ECCS system is capable of maintaining core cooling during the blowdown and GDCS injection periods.

Staff Findings And Conclusions

Through the comparison of the ESBWR GDCS LOCA response as calculated with the TRACG and TRACE/CONTAIN codes, the staff has observed the following—

- (1) The Automatic Depressurization System is important to reduce the system pressure to equalize it with the drywell pressure so that GDCS injection can maintain the in-vessel water level. TRACG is capable of predicting the ADS actuation timing.
- (2) Although the TRACG code may tend to overpredict the temperature and pressure in the containment, it is still be able to predict the physical timing of GDCS injection initiation and the injection mass flow rate.
- (3) The chimney collapsed water level remains above the core with significant margin (1.9 m for the base case). The reactor core remains covered and the PCT remains significantly below the regulatory limit of 2200 EF.
- (4) The two codes, TRACG and TRACE/CONTAIN, using different models, correlations and numerical solution techniques, produce very similar predicted behavior of the ESBWR design for the first 2000 seconds of the GDCS LOCA. The similarity of the comparisons of the major parameters, described above, increases confidence in the capability of the TRACG code to support analytical needs at the design certification phase.
- (5) Although significant differences exist between the TRACE/CONTAIN and TRACG codes in modeling containment behavior during the GDCS LOCA, the similarity of the predicted containment behavior supports the conclusion that the TRACG code is able to predict the first order effects in the containment response and has sufficient accuracy for this application.

3.7.2.3.2 MSLB LOCA Analysis Using Coupled TRACE and CONTAIN Codes

The coupled TRACE and CONTAIN code suite was again selected to analyze the MSLB LOCA. Unlike the specific approach GENE used to maximize the containment pressurization rate and the special treatment of the suppression pool model, the staff used the same containment and reactor vessel model to perform the analysis. The advantage of using a single set of reactor and containment models is that the model is not biased for either ECCS evaluation or containment integrity evaluation. The detailed reactor vessel model can also more accurately predict mass and energy releases through the break and provide a more detailed thermal-hydraulic solution in the vessel.

TRACE/CONTAIN Model Modifications

The MSLB model, and the sequence of events, are similar to those described for the GDCS LOCA case in the previous section. The GDCS line model is the same as that shown in Figure 3.7.2.14, in Section 8 of this report, except that the break between the vessel and one of

the GDCS valves was removed. Specifically, PIPE 75, BREAK 98, and BREAK 99 are not modeled, and VALVE 73 connects directly to the vessel.

As for the steam line modeling, it is the same as that shown in Figure 3.7.2.25, in Section 8 of this report, with the exception that a double-ended break in one steam line is modeled between the vessel and TEE 83. A diagram of the break is shown in Figure 3.7.2.25 in Section 8 of this report. BREAKs 36 and 37 connect to the upper drywell volume of the CONTAIN model. No significant containment model change is made except that the break location was moved to the upper drywell volume.

MSLB LOCA Calculation Results

The sequence of the MSLB LOCA events is very similar to the GDCS LOCA. At the break initiation, the blowdown flow quickly increases the drywell pressure to the scram set point, and a control rod scram occurs. The high velocities in the main steam line initiate the closure of the MSIVs and the reactor is isolated within 3-5 seconds. For the base case, the feedwater system is assumed to be unavailable to make up the coolant loss. The downcomer water level quickly reaches the L1 setpoint and triggers the actuation of the ADS system. Because of quick depressurization through the main steam line as well as the ADS, the reactor vessel pressure drops much faster than it does in the GDCS LOCA, resulting in earlier GDCS injection initiation. In the containment, the steam entering the drywell quickly raises the pressure, opening the main containment vents and sweeping most of the drywell noncondensable gas through the main vents. During the blowdown phase of the transient, the majority of the blowdown energy is transferred into the suppression pool by condensation of the steam flowing through the main vents. This increases the pressure of the wetwell and GDCS pool air space. During the early GDCS injection period, the GDCS flow reaches its peak mass flow rate and the cold water collapses the void in the reactor pressure vessel. Because of a limitation of the CONTAIN model, the MSLB simulation stops at 2000 seconds into the transient. Figures 3.7.2.25 to 3.7.2.34 in Section 8 of this report depict the major parameters of the system.

Vessel Steam Dome Pressure

Figure 3.7.2.26 in Section 8 of this report shows the steam dome pressure calculated by the TRACG and TRACE/CONTAIN codes. Both codes predict the same trend of the depressurization process.

Break Flow

The mass flow rate through the MSLB is shown in Figure 3.7.2.25 in Section 8 of this report. Both TRACG and TRACE/CONTAIN predict the same trend in the mass flow rate. However, between 0 and 600 seconds, TRACE/CONTAIN predicts higher oscillatory break mass flow rate. This is mainly caused by the high entrainment in the vessel steam dome and main steam line, while the upstream steam quality calculated by TRACG is much higher. The integrated

coolant discharge for the two codes does not differ significantly, thus giving confidence in the prediction of both codes.

Drywell Pressure

The upper drywell total pressures calculated by both TRACG and TRACE/CONTAIN are shown in Figure 3.7.2.28 in Section 8 of this report. The peak pressure calculated by TRACG during the first 2000 seconds is much higher than that calculated by TRACE/CONTAIN. However, it is still below the design limit. The difference in the calculations appears to be caused by different nodalization schemes used for the two codes with the result that the TRACE/CONTAIN calculation tends to predict more mixing than TRACG.

Wetwell Pressure

Similar to the drywell pressure prediction, TRACG predicts a higher wetwell pressure peak value. As shown in Figure 3.7.2.29 in Section 8 of this report, the wetwell pressure calculated by TRACG peaks at about 550 seconds. The TRACE/CONTAIN peak value is much lower, demonstrating that TRACG is possibly more conservative in terms of calculating the wetwell pressure load.

Drywell and Wetwell Temperature

As shown in Figure 3.7.2.32 in Section 8 of this report, TRACG again predicts higher drywell and wetwell air space temperatures. This is again due to the different nodalization schemes used with the code input models. The drywell and wetwell temperatures are from the "hottest" cell in the drywell and the wetwell. Using the peak temperature values in the drywell and wetwell, the staff finds that the temperatures are lower than the design limit. Figure 3.7.2.33 in Section 8 of this report shows the wetwell liquid temperature. For the cell down stream of the highest vent in the wetwell, TRACG and TRACE/CONTAIN predict almost identical liquid temperatures.

Collapsed Water Level

The collapsed water level in the chimney partition is shown in Figures 3.7.2.31 in Section 8 of this report. The chimney collapsed water level for TRACE/CONTAIN for the GDCS and MSLB LOCA cases are compared. It is observed that the lowest chimney collapsed water level is similar for both GDCS and MSLB LOCA cases. The level starts to rise after the GDCS injection is initiated. There is significant liquid inventory in the chimney to prevent core uncover.

GDCS Injection Mass Flow Rate

Both codes predict very similar GDCS injection mass flow rates. As shown in Figure 3.7.2.32 in Section 8 of this report, both the trend and the maximum peak values are in good agreement. As does the GDCS LOCA case, the MSLB case demonstrates that TRACG is capable of modeling the early GDCS injection.

Core Peak Cladding Temperature

Unlike the TRACG GDCS LOCA model, the MSLB LOCA model uses [[]] to model the entire reactor core. Without a hot channel component, no peak cladding temperature can be obtained from the TRACG MSLB LOCA calculation for comparison. Therefore, Figure 3.7.2.34 in Section 8 of this report shows only the PCT calculated by TRACE/CONTAIN. It is observed that no heat up occurs, and that the entire core is well cooled.

Staff Findings And Conclusions

Through the comparison of the ESBWR MSLB LOCA responses using the TRACG and TRACE/CONTAIN codes, staff has observed the following—

- (1) During the first 2000 seconds of the MSLB LOCA, TRACG predicts higher drywell and wetwell pressures and temperatures than does TRACE/CONTAIN. The pressures and temperatures are all below the design limits.
- (2) The calculated MSLB chimney collapsed water level is generally much higher than that of the GDCS LOCA case. This confirms GENE's position that the GDCS break is more limiting for ECCS evaluation. Again, the level remains above the core with significant margin. The reactor core remains covered and the PCT remains significantly below the regulatory limit of 2200 EF.
- (3) The two codes, TRACG and TRACE/CONTAIN, using different models, correlations and numerical solution techniques, produce very similar predicted behavior of the ESBWR design for the first 2000 seconds of the MSLB LOCA. The similarity of the comparisons of the major parameters described above, increases confidence in the capability of the TRACG code to support independent analytical needs of the design certification process.
- (4) Significant differences exist between the TRACE/CONTAIN and TRACG codes in modeling the containment behavior during the MSLB LOCA. However, the similarity of the predicted containment behavior supports the conclusion that the TRACG code is able to predict the first order effects in the containment response and has sufficient accuracy for this application.

GENE is consistent with this step in the CSAU approach.

3.8 Step 8—NPP Nodalization Definition

References 1 and 11 discuss the tradeoffs in determining an adequate NPP nodalization. GENE developed guidelines for the ESBWR nodalization in such a manner as to remove, as far as possible, nodalization as a contributor to calculational uncertainty. The nodalization strategy applied by GENE takes into consideration basic geometric considerations, experience with

nodalization used in prior studies for the operating fleet of BWRs, nodalization for the various SBWR test facilities, and qualification studies in Reference 16. In addition, GENE relied on standard nodalization developed in assessment cases against separate and integral effects tests. Nodalization studies were performed in assessing the test data to establish the level of detail necessary to represent the important phenomena. The standard nodalization for modeling the ESBWR design was also used for the SBWR design.

GENE is consistent with this step in the CSAU approach.

3.9 Step 9—Definition of Code and Experimental Accuracy

Simulation of experiments developed from Step 7 using the NPP nodalization from Step 8 provides checks to determine code accuracy. The differences between the code calculated results and the test data provide bias and deviation information. Code scale-up capability can also be evaluated from separate effects data, full-scale component tests data, plant test data, and plant operating data, where available. Overall code capabilities are assessed from integral systems test data and plant operational data. These assessments were performed as part of the SBWR qualification of the TRACG methodology documented in References 11, 13, and 16. The assessments have been extended to the ESBWR based on the similarity of the designs, which results in no new phenomena being expected in the ESBWR.

GENE is consistent with this step in the CSAU approach.

3.10 Step 10—Determination of Effect of Scale

Various physical processes may give different results as components or facilities vary in scale from small to full size. The effect of scale must be included in the quantification of bias and deviation to determine the potential for scale-up effects.

GENE uses the Hierarchical Two-Tier Scaling (H2TS) process. One of the key elements of the H2TS approach is the identification of the important physical phenomena governing a process. Generally, the phenomena will be identified and ranked in importance by a group of experts. The results of this effort are documented in a PIRT. The H2TS approach consists of a “top-down” method, which is a system scaling analysis used to derive scaling groups and establish a scaling hierarchy, and a “bottom-up” method, which focuses on the important processes and introduces similitude to assure that the scaled test data is applicable to the prototype. The H2TS approach is described by Zuber (Reference 49). However, the top-down system scaling does not replace, but rather provides a rational framework for the bottom-up scaling.

Evaluation of GENE Scaling

GENE adopted the H2TS approach for the ESBWR. The LOCA serves as the basic event for the scaling analysis. Since the importance of the governing phenomena changes as the event unfolds, GENE defined four accident phases (shown in Figure 3.10.1 in Section 8 of this report)

which span the accident, namely, late blowdown, GDCS initiation, GDCS phase, and PCCS phase. The early blowdown period is not significant for passive safety system performance and is ignored. The primary test facilities scaled for SBWR and ESBWR testing can simulate decay power levels starting at approximately one hour after the initiation of the accident. Since a key issue is PCCS performance, the scaling is directed at the “late blowdown phase extending into the long-term cooling phase.” The long-term cooling phase is unique to the SBWR and ESBWR containment because of the substitution of passive for active cooling systems.

GENE begins their scaling efforts with a PIRT. The top-down scaling approach complements the PIRT by identifying the important phenomena during each accident phase based on non-dimensionalization of the governing equations. The global momentum and energy conservation equations used are based on the lumped-parameter approach. The bottom-up scaling considers the individual phenomena at a local level.

3.10.1 Top Down Scaling

Methodology Description

The system was divided into several large volumes. The equations of energy and mass balance developed for a generic volume were then applied to each of these volumes at different time periods during the transient. The equations were made non-dimensional and the resulting non-dimensional coefficients were defined as the Pi's to represent the relative importance of the participating phenomena.

Evaluation Metrics

In this section, we define the objectives of a scaling analysis for code assessment and use that definition to evaluate how the GENE ESBWR scaling report demonstrates that the objectives have been accomplished. General and specific comments are made about yet unresolved questions and issues with the content of the aforementioned report.

Criterion

In the Scaling Report, Reference 46, the objective is defined as “to show that the test facilities properly ‘scale’ the important phenomena and processes identified in the ESBWR PIRT and/or provide assurance that the experimental observations from the test programs are sufficiently representative of ESBWR behavior for use in qualifying TRACG for ESBWR design basis calculations.” The staff accepts the objective as stated.

The main objective of integral scaled facilities is to capture not only the component behavior but also their dynamic interactions as a complete system. To a certain extent, the GENE report acknowledges this in the executive summary, where it states that “A comprehensive experimental program was carried out to demonstrate the thermal-hydraulic performance of these passive systems and their components.” While one cannot expect that any of the scaled facilities represent a simulation of the prototype, for completeness, they must at least exhibit the

same kind of interactions between components and subsystems as expected of the prototype. It is up to the scaling analysis, therefore, to determine how relevant these interactions are. System interactions are not explicitly called out in the PIRT as phenomena. They are, however, an integral part of the transient and determine the sequence of events that define the beginning of a phase, the end of a phase, and what process controls the state of the system during that phase.

The Approach

In general, the reactor system is divided into subsystems for which governing equations are developed. The governing equations are made non-dimensional by referring all variables to a set of norms or reference parameters (including a reference time), according to the purpose of the analysis. The intent of this process is to obtain non-dimensional parameters. The non-dimensional coefficients of these equations, the system Π 's, contain information about how the different components of the system interact, and which of these many interactions dominates the transient behavior during a given phase.

During each transient, the system state and its configuration changes as the transient progresses from one phenomenologically distinct phase to the next. In each of these phases there will be a process or a set of competing processes that define the beginning and the end of the phase, and therefore its reference time. The general approach needs to be repeated for each system configuration and each reference time.

It is difficult to prescribe the level of system detail that the top-down scaling should reach. In one extreme, one could assume that the entire reactor system is one comprehensive volume, and conduct the analysis accordingly. The result would be simple and of limited value. Another approach is to go into as much detail as possible, without invoking multi-dimensional effects or the local distribution of a phenomenon. The latter would likely result in a system representation that varies from phase to phase of the transient, as the system configuration varies (valves open and close, tanks empty or fill).

GENE selected an in-between approach and identified the major system volumes as the components, all represented, in principle, by the same equations of energy and mass conservation. It appears that the momentum equations of the connecting lines or paths are neglected as having no dynamic contribution. Furthermore, Reference 46, Section 6.2 cites previous efforts— "results from the SBWR work showed that there are no significant interactions in the SBWR system or the related tests and no new Π numbers resulted." What the SBWR study found is that the lines and connecting paths have very fast response times compared to other simultaneous processes, and that they contribute enough damping so as to suppress oscillations. In the same section (6.2), the last paragraph suggests that the analysis conducted for SBWR was not carried out for ESBWR because they are "similar enough." In both SBWR and ESBWR, the volumes do interact because they are connected. Part of the difference between these two systems is in the connecting paths between volumes.

The statement in Reference 46, Section 6.3 “these equations are applied to the specific regions of the ESBWR” raised the question that interactions were ignored in the GENE approach. Even when there are two or three volumes actively participating and interacting with each other, the volumes are dealt with independently. The volume equations (mass and energy) have terms that represent inflows and outflows. In most cases, these are not external inputs to the reactor system, but result from gradients between connecting volumes and, therefore, are not independent variables. A single volume equation can neither capture nor describe this system behavior, and is insufficient to draw conclusions about that behavior. It is likely that the two or three volumes involved are interdependent and can be represented by a single equation.

However, the equation used by GENE in its analysis is not capable of demonstrating this. In fact, there seems to be no analysis of system interactions at all.

Closeout of Top Down Scaling for the GDCS Transition Phase

In response to staff RAIs, GENE addressed the deficiencies in the top down scaling with a subsequent revision of the GENE scaling analysis using new equations that account for the interactions between volumes. The system Pi's that resulted from the revised analysis were significantly different than the system Pi's from the non-interacting equations. GENE successfully applied the equations to the "GDCS Transition Phase" which is the onset of GDCS injection and the time period when the minimum vessel inventory occurs. They showed that the experiments behave qualitatively the same as their scaling model and the TRACG ESBWR model.

Specific Comments On Application of Top Down Scaling to Long Term Cooling

The proposed representation of the ESBWR system, provided in Figure 3.10.1 in Section 8 of this report, is an approximation for the formulation of the top-down scaling relationships. The ESBWR system encompasses two major energy sinks—the SP and the PCCS pool. The SP is the primary sink in the initial portion of the transient. The PCCS pool takes over in the long-term portion of the transient.

The view of GENE is influenced by the behavior of current generation reactors. In responding to RAI 283, GENE stated, “It is important to understand that in any pressure suppression containment system, the long-term containment pressure is dominated by the wetwell air space response, not by the drywell.” The staff disagrees with this because, in the long term, the wetwell cannot serve as a sink unless one postulates that the containment pressure can increase indefinitely. The functionality of the SP as a sink will decrease as the heat transferred to the PCCS pool becomes the leading process in the long-term portion of the transient. The system interactions between the drywell and wetwell will determine the distribution of the noncondensibles. These processes may be verified by analysis of appropriate long-term tests that were performed in the PANDA facility.

The transition from heat deposition in the wetwell to heat deposition in the PCCS pool is a fundamental element of the ESBWR system. In current reactors, reliance is on active heat

removal from the SP resulting in the functional statement quoted from RAI-283. However, this is not the case for the ESBWR and, therefore, the energy partition between the wetwell and the PCCS pool must be represented in the initial formulation of the top-down scaling. By limiting the representation to a single volume system with only one pool, as shown in Figure 3.10.1 in Section 8 of this report, implicit assumptions on the system behavior are imposed and important terms are removed from the governing equations. A more inclusive representation of the system would consider two equations for the vessel (similar to Reference 46, Equations 3.1-6 and 3.1-7), two equations for the wetwell, and one equation for the pressure in the drywell connected to the PCCS pool saturation condition via appropriate heat transfer through the PCCS. This heat transfer would also be a function of the noncondensable distribution dictated by the wetwell governing equations. Such a system of five governing equations would enable a proper representation of the system interactions that GENE has represented by two equations.

Another approach would be to consider the various portions of the transient with different representations of the system. This would require an *a priori* knowledge of the energy partition in the various sinks. In previous scaling efforts, this approach has been successful because significant knowledge of system behavior was available from integral test programs at different scales. Nonetheless, significant difficulties had to be circumvented to properly transition from short-term transients to their long-term states.

Additionally, one could argue that in the long term, the cumulative effect of the heat removal by the massive containment structures will result in lower pressures. Lower pressures in turn would result in lower density of the noncondensibles. This means that larger volumes would be necessary to completely segregate them or that a more active participation of the noncondensibles in the heat transfer at the PCCS should be incorporated into the analysis. Appropriate tests and analyses will clarify this issue. Therefore, it would be desirable to include the structural contribution to heat removal in the formulation of the top-down scaling as well. This could be accomplished with appropriate terms in the drywell and wetwell pressure equations.

The staff recognizes the deficiencies in the submitted scaling analysis regarding the system interactions, the energy partition between the SP and PCCS pools, and the effect of containment structures. Consequently, the ESBWR responses to various accident scenarios may be subject to additional uncertainties that will be reviewed during the design certification stage.

3.10.2 Bottom-Up Scaling

Methodology Description

Bottom up scaling is used to look at specific processes important to system behavior in more detail. For the ESBWR, the bottom-up scaling process is described in Section 3 of the TAPD Report, Reference 12, and Section 7.6 of the Scaling Report, Reference 46. As noted on page 3-1 of Reference 12, the ESBWR bottom-up process relies heavily on the SBWR study documented in References 47 and 48. The bottom-up process is similar for the SBWR and

ESBWR. There is a significant difference, however, between the bottom-up scaling discussions for the SBWR and ESBWR.

The ESBWR TAPD Report, Reference 12, page 3-3, identifies 46 highly ranked phenomena needing detailed evaluation. A summary of the detailed evaluations is given in Section 3.3 of Reference 12. The bottom-up process for the SBWR is described in Section 3 of Reference 48. For the SBWR, a total of 79 phenomena called for detailed evaluation, as discussed on page 3-2 of Reference 48. For both the SBWR and ESBWR, the evaluations make reference to the relevant test reports and provide the basis for acceptability of the data for TRACG qualification.

Bottom-up scaling of SBWR specific phenomena is described in some detail in Section 3 of Reference 47. The governing equations and similarity variables describing each phenomenon are presented and discussed. For The ESBWR, bottom-up scaling is reduced to consideration of just four processes as discussed in Section 7.6 of Reference 46. Three of these phenomena are dismissed as not being of significant interest. Only PCC and IC behavior are stated to be of significant interest. GENE states that full height testing of PCC and IC behavior has been conducted for the SBWR in PANDA, GIRAFFE, and PANTHERS, and that a detailed data base for low-pressure condensation heat transfer in the presence of noncondensibles is provided by the Massachusetts Institute of Technology and University of California at Berkeley single tube tests. The bottom-up scaling for PCC and IC behavior in the ESBWR is stated to be the same as for the SBWR. This is the only bottom-up scaling item addressed specifically for the ESBWR. While additional highly ranked items are discussed for the SBWR, there is not enough information to determine whether the available data cover the range expected for the prototype.

Evaluation

The non-dimensional coefficients, or Pi groups, identified in the top down scaling are more complex than the more traditional similarity parameters derived in the study of physical phenomena such as the Reynolds number and Prandtl number. Evidence of this complexity is the fact that a characteristic system time is an integral part of these Pi groups, and also that they come in sets of two or more. The Pi groups are derived from the macroscopic analysis of distinct elements of the system that accounts for the way in which the elements interact and exchange mass, energy, or both, with each other and with the environment. These Pi groups are a useful tool to determine what processes or mechanisms dominate the behavior for each particular system. They can also be used to assess if two different systems can be expected to have similar behavior. However, the similarity can only be guaranteed *a priori* if the two systems have identical Pi groups. If the Pi group values are different, further analysis is necessary to assess the similarity between the different systems. The most important part of this further analysis is the verification that the data—and code calculation for the test facility—exhibit the same trends, magnitudes, and variations in non-dimensional space. The other aspect of this analysis is the evaluation of local phenomena to ensure that while the systems are expected to be similar in their macroscopic behavior, the local phenomena (bottom-up) support this expectation by producing the same regime. This invokes the more

traditional non-dimensional groups, such as Reynolds, Prandtl, and Biot numbers, which correspond to the local processes not captured by the top down formulation of the system equations. The GENE scaling report, in its original version, is very weak in this area because it does not produce these analyses. Instead, it relies on an arbitrary range of Pi groups for similarity assessment. During the review process, GENE abandoned the arbitrarily defined range and conducted a rigorous analysis for the GDCS injection period of an ESBWR LOCA.

As a further observation, the systems test facilities are scaled and designed in such a way that little data was obtained regarding multi-dimensional phenomena. Analysis of the system test data is based on a lumped-parameter approach that eliminates multi-dimensional spatial variations. As such, the tests do not provide sufficient data to credit multi-dimensional effects. Since the data are not suitable to qualify TRACG to predict multi-dimensional effects, TRACG is not used to credit multi-dimensional effects in the ESBWR analysis.

3.10.3 Scaling Conclusion

The staff concludes that GENE demonstrated that there are relevant and sufficient data to qualify TRACG in its simulation of the phase for which the scaling analysis was completed. The phase for which this has been done, the GDCS injection phase, is indeed the most important period of the transient. Conservative, bounding analyses have been employed for the remainder of the LOCA events. The rigor of the analyses is not at issue, but rather the completeness of the analysis. As a part of this review, the staff has determined that it is acceptable for GENE to perform a rigorous scaling analysis limited to the most important phase of the LOCA event, and in terms of the most critical variable (core collapsed water level), thereby demonstrating that the scaling analysis tools are correct while the detailed scaling analysis itself may be incomplete. GENE has been fully responsive to the staff concerns regarding the scaling analysis and methodology.

Element 3—Sensitivity and Uncertainty Analysis

3.11 Step 11—Determination of the Effect of Reactor Input Parameters and State

The purpose of this step is to determine the effect that variations in the plant operating parameters have on the uncertainty analysis. Plant process parameters characterize the state of operation and are controllable by the plant operators to a certain degree. The design basis ECCS/LOCA analyses were performed assuming loss of the preferred electric power, and assuming that the non-ECCS vessel inventory control systems, specifically, the feedwater system, the ICS and the control rod drive system are not credited. In addition, the plant initial conditions, which are anticipated from the operating fleet of BWRs and the test programs to have the greatest influence on the minimum core/chimney mixture level, were selected for the evaluation of uncertainties.

GENE is consistent with this step in the CSAU approach.

3.12 Step 12—Performance of NPP Sensitivity Calculations

Sensitivity calculations are performed to evaluate methodology sensitivity to various operating conditions that arise from uncertainties in the reactor state at the initiation of the transient, in addition to sensitivity to plant configuration. Sensitivity studies were performed for the GDLB for the plant conditions found to have the greatest influence on the minimum core/chimney mixture level. The base case was defined to minimize the drywell pressurization. All perturbations were found to be small with the minimum static head occurring at slightly different times in the transient. The bounding calculations were performed using the combination of parameters that resulted in the minimum static head in the chimney.

GENE is consistent with this step in the CSAU approach.

3.13 Step 13—Determination of Combined Bias and Uncertainty

The individual uncertainties resulting from code models of important phenomena, scale effects, and NPP input parameter variations should be combined to obtain an overall bias and uncertainty. The CSAU approach does not prescribe the manner in which the individual biases and uncertainties are to be combined. Regulatory Guide 1.157, Reference 8, suggests that a one-sided upper statistical limit calculated at the 95 percent probability level for the primary safety parameters is preferred. Lack of core heatup in the ESBWR analyses suggests a statistical analysis of the PCT would not be the best metric for acceptable performance. The approach taken by GENE is to perform [[

]]. The staff finds the GENE approach acceptable due to confirmation of the GENE results through staff calculations performed independently.

In addressing the containment analysis application of TRACG, GENE has stated that a rigorous statistical calculation is not performed. [[]].

GENE is consistent with this step in the CSAU approach

3.14 Step 14—Determination of Total Uncertainty

Previous uses of the TRACG methodology have made use of Normal Distribution One-Sided Upper Tolerance Limit statistics to assess the uncertainty in the analyses. Application of the code to the ESBWR advanced passive system design relies on a very different approach to uncertainty since all preliminary calculations indicate the core remains covered and does not heat up. Uncertainty evaluation is done in this case using a much simpler [[]]. This approach does not make any claims on variation of parameters, but does claim to provide a limiting-case evaluation.

The specific plant conditions ranged and their limits are as identified in the following table, however, no plant parameter uncertainties have been considered.

Table 3.14.1
Uncertainty Considerations

Quantity	Control of Initial Condition	Range of Conditions	Consideration of Uncertainty about the Initial Conditions
[[

]]

Unlike prior reviewed and approved applications of the TRACG methodology, the application of TRACG to the ESBWR LOCA event does not utilize a rigorous statistical methodology to combine uncertainties. The model and plant parameters (indicated in Table 1) are determined through sensitivity studies. [[

]]. The calculation result is considered successful based on the minimum static head in the chimney, thus indicating the core remains covered and there is no heatup of the fuel.

Additionally, the containment response is evaluated by a bounding calculation in [[

]]. The bounding calculation is compared to the design conditions to establish that sufficient margin exists to the containment design pressure and temperature.

The staff notes that no previous “realistic” plant evaluation has incorporated the reactor coolant system and containment system into a single computer code calculation. Doing so raises a question as to whether or not the uncertainty analysis that is performed to assess uncertainties in the 10 CFR 50.46 acceptance criteria should also include uncertainties in the containment aspect of the calculation. The current GENE TRACG hybrid analysis applies a pseudo uncertainty analysis, as discussed previously, to the reactor coolant system alone. The containment system is treated in a bounding way as also discussed previously. The question of performing a combined uncertainty analysis should be examined more closely at the design certification stage. This view is strengthened by a statement made by GENE in response to a staff RAI. GENE stated, “The precise origin of the tabulated values that are referred to as the

[[]] is not known. There is reason to believe...that these values were obtained by merging the separate results from [[]].” Using data of unknown provenance for design basis calculations is questionable. This is especially troubling since the [[]] data is the least conservative of the available curves in the literature. If the containment portion of the calculation is being performed as a bounding calculation, then the more conservative models of [[]] would be more appropriate to use. At the design certification phase, GENE should perform the analyses for the ESBWR using the appropriate models and supportable data bases.

GENE is not consistent with this step in the CSAU approach for the LOCA/ECCS application of the TRACG code, but the staff finds the GENE method acceptable in light of the predicted lack of core uncover. Should it be found during the design certification review of the ESBWR system that core uncover does occur, the staff will revisit the method of uncertainty combination and statistical methodology for the LOCA/ECCS application.

4.0 CONFIRMATORY ITEMS

In the course of conducting the review of TRACG for applicability to the ESBWR LOCA, several items were identified as needing confirmation at the design certification stage. These items do not affect the applicability or capability of the code, but do address the response of the plant design, and adequacy of the documentation.

- 1) The PIRT at the design certification stage should include the long-term cooling phase of the LOCA since the long-term cooling phase is highly design dependent. Should it be found that unreviewed phenomena occur during the long-term cooling phase, the appropriate models and correlations in the TRACG code will be revisited by the staff.
- 2) During the design certification review, the staff will verify that the TRACG application procedures conservatively calculate the collapsed water level in the chimney above the hot channel for the three break locations, MSLB, BDLB and GDLB.

Reference 11, Table 2.4-2 indicates that the GDLB results in the lowest static head in the chimney of the three break locations examined, the GDCS line, the main steam line, and the bottom drain line. At the design certification stage, GENE will need to provide supporting analyses for a spectrum of break locations to demonstrate that there is no core uncover for the possible break locations. Should core uncover occur, review of the TRACG code will be revisited to determine the adequacy of the applicable models and correlations

The procedures should be applicable to both short term and long term LOCA events (i.e., up to 72 hours).

- 3) GENE has committed to incorporate the missing definition for E_p , and new equations for the transition criterion between churned turbulent and annular flow, including the drift velocity term in updated code model description documentation.

- 4) The description of the TRACG model, Reference 10, will be updated to reflect all current models and correlations, thereby providing a level of detail consistent with a stand-alone document.
- 5) Further investigations are needed to conclusively determine the sound in the PANTHERS-IC testing that may have been due to water hammer, and to confirm its prevention in the ESBWR (e.g., by changing the hardware design of the IC inlet line or the startup procedure).
- 6) The PANTHERS-IC testing was terminated when leakages were detected in the IC upper header. As a result, the leakage issue was never resolved, and is an IC structural integrity issue that needs to be resolved for the ESBWR design certification.
- 7) During the design certification review stage, the ECCS baseline model should include the scram delay time and the 2 percent power measurement uncertainty.
- 8) During the design certification stage, separate modeling of the vessel shield, the reflective thermal insulation layer, and the air gap from the lumped heat structure will be necessary.
- 9) Nodalization studies will be necessary at design certification to calculate the minimum water level in the chimney partition.
- 10) The assumption of the loss of feedwater flow used by GENE is not conservative. Therefore the existing GENE MSLB model and the current analysis approach underestimates the maximum containment pressure and temperature. At the design certification phase, this should be resolved.
- 11) Without detailed feedwater heater system design information, both the staff and GENE had to make assumptions about the mass and energy discharge from the feedwater heater system. The staff believes that the bounding containment peak pressure and temperature need to be evaluated during the design certification stage after the feedwater heater system design is finalized. If the evaluation indicates that the code application range is exceeded or a new scenario, such as wetwell flooding, has not been examined during the preapplication stage, the staff may choose to review the TRACG code for such new use.
- 12) The quick closure of the MSIVs while control rods are being inserted may increase the total core power due to void collapse. At the design certification stage, GENE should evaluate the effects of void collapse for the GDCCS and BDLB LOCA cases.
- 13) During the staff's earlier review of the SBWR, work that GENE relies on for the ESBWR, the staff noted that GENE had not evaluated more traditional integral containment tests such as the Marviken tests, the Carolinas Virginia Tube Reactor test 3 without sprays,

and the Battelle- Frankfurt Model Containment tests C-13 and C-15, for MSLBs. In response to staff RAI 317.1, GENE agreed to perform assessments of TRACG to model containment performance against integral test data that is publicly available for International Standard Problems where the test facilities and tests are well defined. The tests to be analyzed will be specified later, and the analysis will be completed during the design certification review.

The staff also requested that GENE provide a plan and schedule to assess the ability of TRACG to model containment performance against additional separate effects tests. Separate effects tests that should be considered include the Wisconsin Flat Plate condensation tests, (References 36, 37, and 38). In response to staff RAI 317.2, GENE agreed to perform assessments of TRACG to model containment performance against separate effects test data that is publicly available for International Standard Problems where the test facilities and tests are well defined. The tests to be analyzed will be specified later, and the analysis will be completed during the design certification review.

- 14) GDACS gas space and the wetwell vent should be modeled correctly during the design certification stage.
- 15) During the design certification review, if the ECCS evaluation model is used beyond 2000 seconds, additional VESSEL levels need to be added on top of the existing [[]], and the pool needs to be modeled in the same fashion as is done for containment/LOCA modeling.
- 16) Prior to submission of the final design analyses in support of design certification, GENE should perform a review of the appropriateness of the [[]] factors and the liquid/vapor interface heat transfer used in the containment modeling.
- 17) Prior to performing the final design analyses at the design certification stage, GENE should perform a thorough evaluation of the ESBWR design records and TRACG ESBWR model development records to substantiate that the TRACG models and correlations are consistent with the final design requirements and intended application.
- 18) At the design certification stage, GENE should examine further whether or not an uncertainty analysis can be performed on the combined reactor coolant system/containment system calculation rather than treating the containment aspect of the ECCS LOCA calculation in a bounding way. The uncertainty analysis methodology should be applicable to both short term and long term LOCA events (i.e., up to 72 hours).
- 19) The actual design configuration of the PCCS vent system, especially the vent submergence, may influence the amount of steam condensed in the SP. Therefore, during the design certification review, the staff will confirm that steam entering the SP through the PCCS vent, as designed, will perform as expected to condense steam entering the SP.

- 20) This safety evaluation is based on the 4000 MWth ESBWR reference design as described in Reference 15. At the design certification stage, GENE should demonstrate that the reference design as described in Reference 15 has not been altered in such a way as to affect the staff's conclusions of this report. Significant changes in the design that challenge the conclusions of this report will result in the staff reevaluating the applicability of the TRACG code.

5.0 CONCLUSIONS

Test Program

The **full-size component** test data from the PANTHERS/PCC and PANTHERS/IC testing programs cover the range of the operational conditions expected in the design-basis LOCAs in the ESBWR. These data are deemed to be adequate for validating the TRACG code regarding the PCCS and ICS performance in the ESBWR, with the understanding that a PCCS condenser in the ESBWR has approximately 35 percent more heat removal capability compared to the PANTHERS/PCC condenser and an ICS condenser (with two identical modules of tubes) has twice the heat removal capability as the PANTHERS/IC condenser (with only one module of tubes).

The **integral systems** test data from the GIST, GIRAFFE helium, GIRAFFE systems interactions, PANDA M-series, and PANDA P-series test programs as a whole cover a range of the late blowdown phase, GDCS phase, and long-term cooling phase of the accidents. Strengths and weaknesses of the individual test programs are identified and evaluated. The staff has reviewed the test programs and results and concludes that the weaknesses (including some phenomenon distortions) in general do not invalidate the overall reactor vessel and containment response in a LOCA shown by TRACG. The combined data from the GIST, GIRAFFE, and PANDA integral systems tests are generally expected to cover the LOCA phenomena and processes defined in the PIRTs for the late blowdown phase, GDCS phase, and long-term cooling phase.

The GENE test programs, as set forth in detail above, lack an integral test facility in the ESBWR configuration, and the PCCS tests are not full scale to the ESBWR design. These weaknesses in the test data will increase overall uncertainty in plant calculations. However, the design certification analysis is not anticipated to result in uncovery of the ESBWR core during a LOCA based on the margin demonstrated in the calculated results.

Independent Analyses

The staff's independent analyses of the reactor coolant system and containment behavior under a LOCA, using the GENE TRACG code and the staff's TRACE/CONTAIN code, indicate that beyond 600 seconds, TRACG and TRACE/CONTAIN provide consistent results. While differences occur in the short time period within 600 seconds, the codes indicate the same trends and predict the same phenomena. At this time, those differences can not be fully

explained as the TRACE code is still in the developmental stage and has not yet been fully assessed.

Scaling

The staff concludes that GENE demonstrated that there are relevant data sufficient to qualify TRACG in its simulation of the phase for which the scaling analysis was completed. The phase for which this has been done, the GDCS injection phase, is indeed the most important period of the transient. Conservative, bounding analyses have been employed for the remainder of the LOCA event. The rigor of the analyses is not at issue, but rather the completeness of the analysis. As a part of this review, the staff has determined that it is acceptable for GENE to perform a rigorous scaling analysis limited to the most important phase of the LOCA event, and in terms of the most critical variable (core level), thereby demonstrating that the scaling analysis tools are correct while the scaling analysis itself may be incomplete. GENE has been fully responsive to the staff concerns regarding the scaling analysis and methodology.

Uncertainty Analysis

The staff concludes, based on review of the GENE uncertainty analysis, that GENE is not consistent with this step in the CSAU methodology approach for the LOCA/ECCS application of the TRACG code. However, as set forth in Section 3.14 above, the staff finds the GENE method acceptable in light of the margins in the design as indicated in the predicted lack of core uncover and heatup. Should it be found during the design certification review of the ESBWR system that core uncover does occur, the staff will revisit the method of uncertainty combination and the associated statistical methodology for the LOCA/ECCS application.

Assumptions

The assumption of the loss of feedwater flow used by GENE for the current stage in the design is not conservative, resulting in underestimation of the maximum containment pressure and temperature. Although there is adequate margin in the prediction of containment pressure and temperature, the feedwater flow assumption needs to be justified at the design certification phase.

TRACG Applicability and Overall Conclusion

The staff concludes, based on the above discussion, that TRACG, including the application methodology, is an acceptable evaluation model for ESBWR Loss-of-Coolant Accident analyses as presented in NEDC-33083P, *TRACG Application for ESBWR*. The staff therefore concludes that TRACG is acceptable for referencing during the design certification review of the ESBWR, provided the conditions specified in this safety evaluation are met. Section 4 of this report identifies those items that should be addressed at the design certification stage as part of the application of TRACG to the ESBWR design.

NRC Criteria

If the NRC's criteria or regulations change so that its conclusions about the acceptability of the report are invalidated, GENE or the applicant referencing the report, or both, will be expected to revise and resubmit its respective documentation, in accordance with 10 CFR 52.47, or submit justification for the continued effective applicability of the report without revision of the respective documentation.

6.0 ACRONYMS

ABWR	Advanced Boiling Water Reactor
AC	Alternating Current
ADS	Automatic Depressurization System
ANS	American Nuclear Society
ANSI	American National Standards Institute
AOO	Anticipated Operational Occurrence
ATWS	Anticipated Transient without Scram
BDLB	Bottom Drain Line Break
BOP	Balance of Plant
BWR	Boiling Water Reactor
CCFL	Counter-Current Flow Limit
CHF	Critical Heat Flux
CSAU	Code Scaling Applicability and Uncertainty
DBA	Design Basis Accident
DC	Direct Current
DPV	Depressurization Valve
DW	Dry Well
ECCS	Emergency Core Cooling System
ECI	Exterior Component Interface
ESBWR	Economic Simplified Boiling Water Reactor
GDC	General Design Criteria
GDCS	Gravity-Driven Cooling System
GDLB	GDCS Line Break
GE	General Electric Company
GENE	General Electric Nuclear Energy
GEXL	General Electric Critical Quality Boiling Length Correlation
GIST	Gravity-driven Integral Systems Test
H2TS	Heirarchical Two-Tiered Scaling
HVAC	Heating, Ventilation and Air Conditioning
IC	Isolation Condenser
ICS	Isolation Condenser System
KSP	Kuhn-Schrock-Peterson
LHGR	Linear Heat Generation Rate
LOCA	Loss-of-Coolant Accident
MCPR	Minimum Critical Power Ratio
MSIV	Main Steam Isolation Valve
MSLB	Main Steam Line Break
NPP	Nuclear Power Plant
OD	Outside Diameter
PCC	Passive Containment Cooling
PCCS	Passive Containment Cooling System
PCT	Peak Cladding Temperature
PIRT	Phenomena Identification and Ranking Table

PSTF	Pressure Suppression Test Facility
QA	Quality Assurance
RAI	Request for Additional Information
RPV	Reactor Pressure Vessel
SBWR	Simplified Boiling Water Reactor
SER	Safety Evaluation Report
SIET	Societa Informazioni Esperienze Termoidrauliche
SP	Suppression Pool
SRP	Standard Review Plan
SRV	Safety Relief Valve
SSAR	Standardized Safety Analysis Report
TAF	Top of Active Fuel
TAPD	Testing and Analysis Program Description
VB	Vacuum Breaker
V-S	Vierow-Schrock
WW	Wet Well

7.0 REFERENCES

1. NEDE-32906P, Rev. 0, *TRACG Application for Anticipated Operational Occurrences (AOO) Transient Analyses*, January 2000.
2. NEDE-32906P Supplement 1, *TRACG Application for Anticipated Transient Without Scram Transient Analysis*, September 2002.
3. Safety Evaluation Report by the Office of Nuclear Reactor Regulation for NEDE-32906P, *TRACG Application for Anticipated Operational Occurrences (AOO) Transient Analyses*, June 2002.
4. Safety Evaluation Report by the Office of Nuclear Reactor Regulation for NEDE-32906P, Supplement 1, *TRACG Application for Anticipated Transient Without Scram Transient Analyses*, August 2003.
5. NUREG/CR-5249, *Quantifying Reactor Safety Margins: Application of Code Scaling Applicability, and Uncertainty Evaluation Methodology to a Large-Break, Loss-of-Coolant Accident*, December 1989.
6. Draft Regulatory Guide, DG-1120, *Transient and Accident Analysis Methods*, U.S. NRC, December 2000.
7. Draft Standard Review Plan, Section 15.0.2, *Review of Analytical Computer Codes*, U.S. NRC, December 2000.
8. Regulatory Guide 1.157, *Best-Estimate Calculations of Emergency Core Cooling System Performance*, May 1989.
9. NEDE-32176P, Rev. 1, *TRACG Model Description*, February 1996.
10. NEDE-32176P, Rev. 2, *TRACG Model Description*, December 1999.
11. NEDC-33083P, *TRACG Application for ESBWR*, November 2002.
12. NEDC-33079P, *ESBWR Test and Analysis Program Description, Supplement 1 - Discussion of PIRT Parameters*, August 2002.
13. NEDC-33080P, *TRACG Qualification for ESBWR*, August 2002.
14. NEDC-33081P, *ESBWR Test Report*, August 2002.
15. NEDC-33084P, Revision 1, *ESBWR Design Description*, August 2003.
16. NEDC-32752P, *TRACG Qualification for SBWR*, August 2002.

17. NEDC-32606P, *SBWR Testing Summary Report*, August 2002.
18. McAdams, W. H., *Heat Transmission*, 3d ed., McGraw-Hill Book Company, Inc., New York, 1954.
19. NEDE-32178P, Rev.1, *Application of the TRACG Model to SBWR Licensing Safety Analysis*, 1998.
20. Kuhn, S. Z., V. E. Schrock, and P. F. Peterson, *Final Report on U. C. Berkley Single Tube Condensation Studies*, University of California, Berkley Report UCB-NE-4201, August 1994.
21. Robbins, C. H., *Tests of the Humboldt Bay Pressure Suppression Containment*, GEAP-3596, November 1960.
22. *Pressure Suppression Test Program*, PG&E, Bodega Bay Atomic Power Unit 1 Exhibit 1, Preliminary Hazards Summary Report, December 1962.
23. NEDE-13442P-01, *Mark II - Pressure Suppression Test Program*, May 1976.
24. NEDM-13377, *Mark III Confirmatory Test Program*, Phase I - Large Scale Demonstration Tests, Test Series 5701 through 5703, October 1974.
25. Holman, J. P., *Heat Transfer*, 3rd Edition, McGraw-Hill Book Company, Inc., New York, 1972.
26. Collier, J. G., *Convective Boiling and Condensation*, McGraw-Hill Book Company, Inc., New York, 1972.
27. NEDC-32301, *Single Tube Condensation Test Program*, March 1994.
28. Forster, H. K., and N. Zuber, *Dynamics of Vapor Bubbles and Boiling Heat Transfer*, AIChE Journal, pp 531-535, 1955.
29. COMPRES Report ED45913, *SBWR Vacuum Breaker (VB) Prototype Experimental Qualification General Test Report*, October 1994.
30. NEDE-23785-PA, Rev. 1, *The GESTR-LOCA and SAFER Models for the Evaluation of the Loss-of-Coolant Accident, Volume III: SAFER/GESTR Application Methodology*, October 1984.
31. Fujii, T., et al., *Experimental Study of Performance of a Hybrid Baffle Plate for the Water Wall Type Passive Containment Cooling System*, Nuclear Technology, Vol. 112, October 1985.

32. Kataoka, Y., et al., *Thermal-Hydraulic Characteristics and Heat Removal Capability of Containment Cooling System with External Water Wall*, Nuclear Science and Technology, 27[9], pp 802-814, September 1990.
33. Uchida, H., A. Oyama, and M. Togo, *Evaluation of Post-Incident Cooling Systems of Light Water Power Reactors*, Third International Conference on the Peaceful Uses of Atomic Energy, Vol. 13, Geneva, Switzerland, 1964.
34. NEDE-32177P, Rev. 2, *TRACG Qualification*, January 2000.
35. *Containment Configuration Data Book*, 25A5044, Rev. 1, November 1992.
36. Huhtiniemi, I. K., and M. L. Corradini, *Condensation in the Presence of Noncondensable Gases*, Nuclear Engineering Design, 141, pp 429-446, 1993.
37. Siddique, M., *The Effects of Noncondensable Gasses on Steam Condensation Under Forced Convection Conditions*, MIT, January 1992.
38. Lian, K., *Experimental and Analytical Study of Direct Contact Condensation of Steam and Water*, MIT, May 1991.
39. ANSI/ANS-5.1, Decay Heat Standard, 1994.
40. NEDC-33082P, *ESBWR Scaling Report*, December 2002.
41. Tills, J., *Letter Report on the CONTAIN SBWR Plant Assessment*, Sandia National Laboratory, June 19, 1994.
42. Murata, K. K., et al, *Code Manual for CONTAIN 2.0: A Computer Code for Nuclear Reactor Containment Analysis*, Sandia National Laboratory, NUREG/CR-6533, June 1997.
43. Tills, J., *Letter Report on PCCS Modeling for SBWR*, Sandia National Laboratory, March 1994.
44. Tadios, E. L., *CONTAIN Model for the GIRAFFE Passive Heat Removal Test Facility*, Sandia National Laboratory, June 29, 1995.
45. Tills, J., *Analysis of the GE PANTHERS Tests Using the CONTAIN Code*, Sandia National Laboratory, June 20, 1996.
46. NEDC-33082P, Rev. 0, *ESBWR Scaling Report*, December 2002.
47. NEDC-32288P, Rev. 1, *Scaling of the SBWR Related Tests*, October 1995.

48. NEDC-32391P, Rev. 1, *SBWR Test and Analysis Program Description*, April 1995.
49. NUREG/CR-5809, *A Hierarchical, Two-Tiered Scaling Analysis*, November 1991.
50. Letter from T.R. Quay, USNRC, to J.E. Quinn, *GE Nuclear Energy, Staff Review of GE's Report NEDC-32288P, Revision 1, Scaling of SBWR Related Tests Related to Containment Area*, April 24, 1996 (Accession No. 9906030224).

Technical Evaluation Reports

51. Barber, D. A., *ESBWR LOCA Confirmatory Analysis*, Task Order 29, Information Systems Laboratories, Inc., October 2003.
52. Han, J., *ESBWR PIRT, Test and Analysis Program Description, and Full-Size Component Testing Programs and Integral Testing Programs*, NRC Office of Nuclear Regulatory Research, October 2003.
53. Krotiuk, W., *Scoping Analysis of a Main Steam Line Break in the GE ESBWR Containment Using CONTAIN*, NRC Office of Nuclear Regulatory Research, November 2003.
54. Rohatgi, U. S., L. Cheng, and J. Jo, *TRACG Model Description, NEDE-32176P, Rev. 2*, Brookhaven National Laboratory, October 2003.
55. Cheng, L., J. Jo, and U. S. Rohatgi, *TRACG Qualification, NEDE-32177P, Rev. 2*, Brookhaven National Laboratory, October 2003.
56. Jo, J., U. S. Rohatgi, and L. Cheng, *TRACG Qualification for ESBWR, NEDE-33080P, Rev. 0*, Brookhaven National Laboratory, October 2003.
57. Cheng, L., J. Jo, and U. S. Rohatgi, *TRACG Application for ESBWR, NEDE-33083P*, October 2003.
58. Staudenmeier, J., et al., *ESBWR TAPD, PIRT, Scaling, and Testing*, NRC Office of Nuclear Regulatory Research, January 2004.

Requests for Additional Information

Author	Description	Date
A. Cabbage	Request for Additional Information Letter No. 1 Related to ESBWR Pre-application Review	May 16, 2003
A. Cabbage	Request for Additional Information Letter No. 2 Related to ESBWR Pre-application Review	May 20, 2003
A. Cabbage	Request for Additional Information Letter No. 3 Related to ESBWR Pre-application Review	May 30, 2003
A. Cabbage	Re-issuance of Request for Additional Information Letter No. 4 Related to ESBWR Pre- application Review	July 25, 2003
A. Cabbage	Request for Additional Information Letter No. 5 Related to ESBWR Pre-application Review	July 17, 2003
A. Cabbage	Request for Additional Information Letter No. 6 Related to ESBWR Pre-application Review	July 17, 2003
A. Cabbage	Request for Additional Information Letter No. 7 Related to ESBWR Pre-application Review	July 30, 2003
A. Cabbage	Re-issuance of Request for Additional Information Letter No. 8 Related to ESBWR Pre- application Review	August 19, 2003
L. Fields	Re-issuance of Request for Additional Information Letter No. 9 Related to ESBWR Pre- application Review	September 11, 2003

GENE Responses to Requests for Additional Information

Author	Title/Description	Document Date
A. Rao	Responses to Request for Additional Information (RAI) numbers (9, 16-24, 113-143, 213, 214, 234, 236, 257, 258, 266, 275, 276, 279 and 281) for ESBWR Pre-application Review.	July 31, 2003

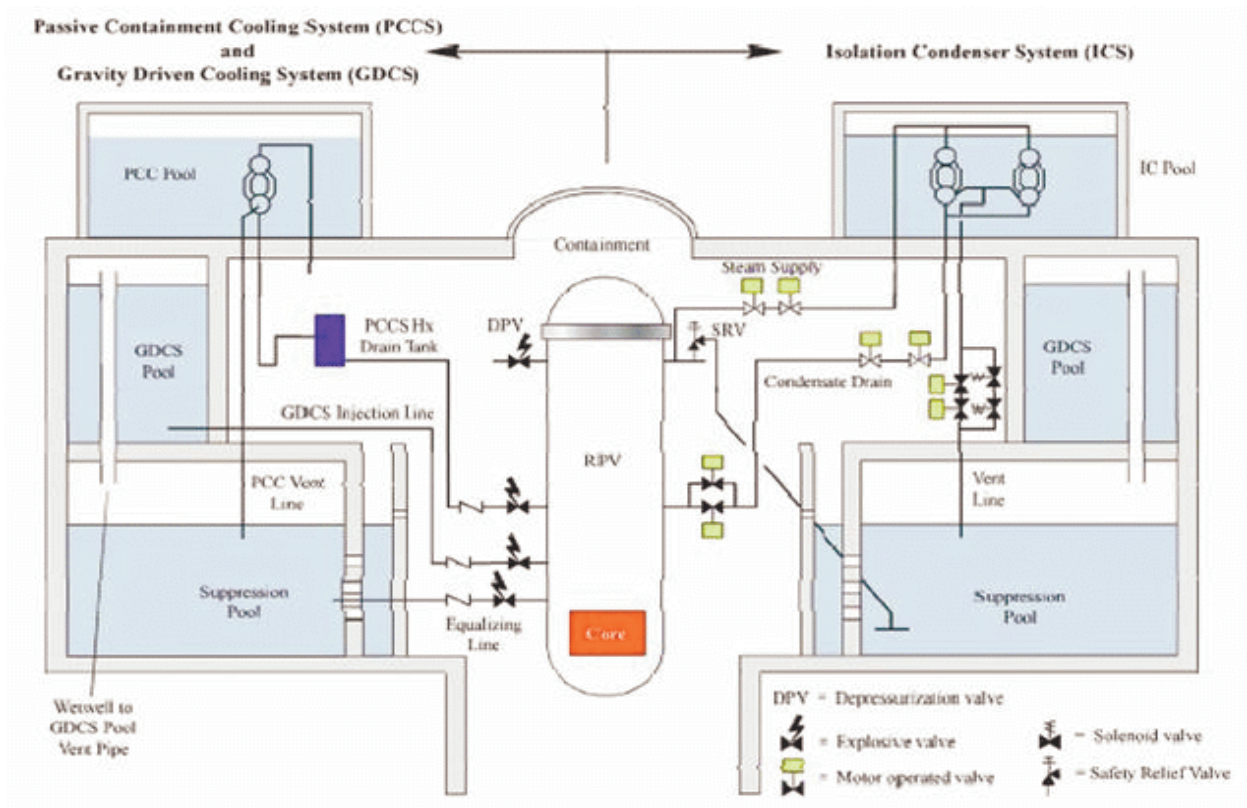
A. Rao	Response to Request for Additional Information Numbers (187, 190, 191, 195, 202, 220, 225, 231, 232, 272, 296, 297, 327, 334-338, 345, 347, 349-359, 371-376, 378, & 379) for ESBWR Pre-Application Review.	August 8, 2003
A. Rao	Response to Request for Additional Information (RAI) numbers (13, 14, 28-30, 33, 34, 36-44, 46, 49-53, 55, 57-59, 61-64, 66, 68, 69, 72-76, 78, 80, 81, 83-85, 88, 93, 96, 98, 99, 102-104, 107, 108, 110-112, 147-150, 153-158, 163, 165, 166, 168-175, 178-182, 185, 186, 188, 189, 192-194, 196-201, 203-212, 215-219, 221-224, 226-230, 233, 235, 237-256, 263, 265, 267-270, 273, 274, 278, 280, 283-285, 287-289, 291, 300, 302, 303, 318, 320, 322, 328, 332, 340-344, 348, 361, 362, 364-370, 377, 386, 407, 409-413) for ESBWR Pre-application Review.	August 18, 2003
A. Rao	Response to Request for Additional Information (RAI) numbers (7 and 8) for ESBWR Pre-application Review.	August 15, 2003
S. Delvin	Response to Request for Additional Information Numbers (1-5, 10-12, 25-27, 31, 32, 144-146, 151, 152, 160, 167, 177, 262, 277, 290, 294, 308, 312-315, 346, 360, 363, 380, 381, 383-385, & 389-405) for ESBWR Pre-Application Review.	August 20, 2003
A. Rao	Response to Request for Additional Information Numbers (161, 162, 164, 176, 183, 184, 286, 292, 293, 295, 301, 323, 325, 339, & 382) for ESBWR Pre-Application Review.	August 22, 2003
A. Rao	Re-transmittal of Response to Request for Additional Information (RAI) numbers (6, 15, 35, 45, 47, 48, 60, 65, 67, 77, 89-92, 94, 95, 97, 105, 159, 264, 271, 298, 299, 304, 305, 307, 310, 317, 321, 324, 326, 329, 331, 387, 388, 406, and 408) for ESBWR Pre-application Review.	September 5, 2003
S. Delvin	Response to Request for Additional Information (RAI) 330 for ESBWR Pre-application Review.	September 3, 2003
S. Delvin	Response to Request for Additional Information (RAI) Nos. (54, 79, 100, 101, 109, 259, 282, 309, 311, 333, and 383) for ESBWR Pre-Application Review.	September 5, 2003
A. Rao	Response to Request for Additional Information (RAI) numbers (7, 8, 106 and 177) for ESBWR Pre-application Review.	September 12, 2003
A. Rao	Response to Request for Additional Information (RAI) numbers (70, 71, 82, 86, 87, 316, and 318) for ESBWR Pre-application Review.	September 16, 2003

A. Rao	Response to Request for Additional Information (RAI) numbers (25, 306, and 319) for ESBWR Pre-application Review.	September 18, 2003
A. Rao	Response to Request for Additional Information (RAI) Number 56 for ESBWR Pre-Application Review.	September 19, 2003
S. Delvin	Response to Request for Additional Information (RAI) numbers (306 and 339) for ESBWR Pre-application Review.	September 24, 2003
S. Delvin	Response to Request for Additional Information (RAI) numbers (7 and 8) for ESBWR Pre-application Review – Supplementary Information.	October 2, 2003
S. Delvin	Response to Request for Additional Information (RAI) numbers (117.2, 306, 314.1, 322, 323.4, 329, and 406) for ESBWR Pre-application Review - Supplementary Information	October 13, 2003
S. Delvin	Response to Request for Additional Information (RAI) numbers (15, 259, 286, and 292) for ESBWR Pre-application Review - Supplementary Information.	October 20, 2003
A. Rao	Response to Request for Additional Information (RAI) numbers (322 and 406) for ESBWR Pre-application Review - Supplementary Information	October 23, 2003
A. Rao	Response to RAI 339 - Supplementary information	November 3, 2003
S. Delvin	Response to RAI 406 additional supplementary information	November 4, 2003
S. Delvin	Response to Request for Additional Information (RAI) on Scaling Responses for ESBWR Pre-application Review – Additional Supplementary Information.	November 6, 2003
S. Delvin	Response to Request for Additional Information (RAI) on Model LTR NEDE-32176 (Rev 1 and 2) and RAI number (330.4) for ESBWR Preapplication Review – Additional Supplementary Information.	November 7, 2003
S. Delvin	Response to Request for Additional Information (RAI) Number (25) for ESBWR Pre-application Review – Additional Supplementary Information. (Errata to TRACG qualification for ESBWR)	November 12, 2003

S. Delvin	Response to Request for Additional Information (RAI) Number (406) for ESBWR Pre-application Review – Additional Supplementary Information.	November 14, 2003
S. Delvin	Response to Request for Additional Information (RAI) Number (406) for ESBWR Pre-application Review – Supplementary Information regarding Identification of changes to TRACG04.	November 19, 2003
S. Delvin	Response to Request for Additional Information (RAI) number (330.4) for ESBWR Pre-application Review – Additional Supplementary Information Regarding TRACG Input Deck for PSTF Test 5807-29.	November 21, 2003
R. Gamble	Response to Request for Additional Information (RAI) No. 183 for ESBWR Pre-application Review - Supplementary Information.	March 1, 2004
R. Gamble	Response to Requests for Additional Information (RAIs) Related to TRACG Calculations for the GDCS Line Break.	March 3, 2004
R. Gamble	Response to RAI No. 183 for ESBWR Pre-application Review - Supplementary Information With Revised Calculation.	March 16, 2004
R. Gamble	Response to Request for Additional Information (RAI) Number 183 for ESBWR Pre-application Review - Supplementary Information with Parametric Long-Term Calculation for GDCS Line Break	April 12, 2004
R. Gamble	Update of ESBWR TRACG Application Cases for NEDC-33083P Using the 9-Apr-2004 Program Library Version of TRACGO4	June 2, 2004
R. Gamble	Update of ESBWR TRACG Qualification for NEDC-32725P and NEDC-33080P Using the 9-Apr-2004 Program Library Version of TRACGO4	June 2, 2004
R. Gamble	Response to Additional RAIs on ESBWR PCCS Modeling for TRACG Calculations	June 18, 2004
R. Gamble	Description of Changes in TRACG4 Between Original Version and April 9, 2004 Program Library Version	July 7, 2004
R. Gamble	Response to Additional RAIs on TRACG Calculations for GDCS Line Break	July 9, 2004

8.0 FIGURES

Figure 3.0.1 ESBWR Layout
(Note: Figure is not to scale)



PIRT Process

Top-Down Process Bottom-Up Process

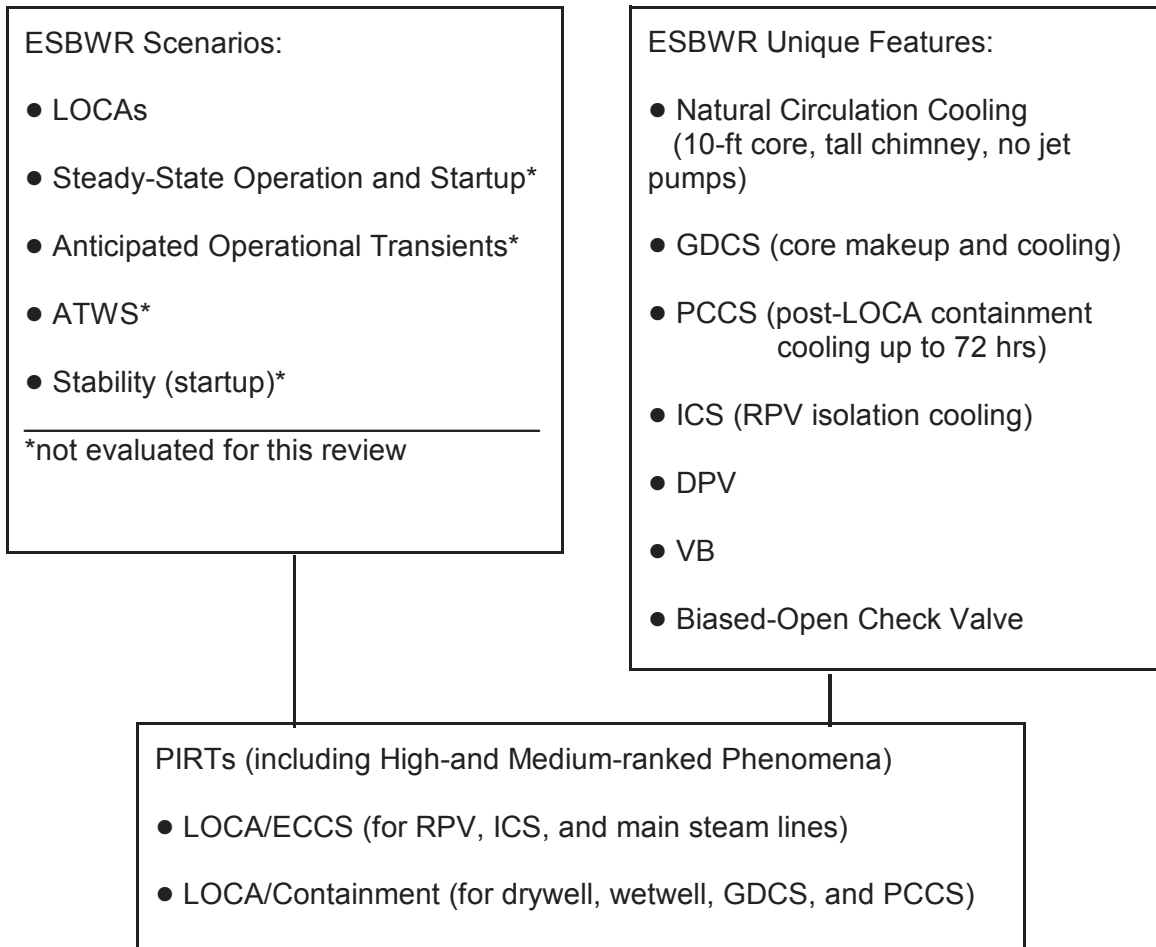


Figure 3.3.1 - PIRT Process

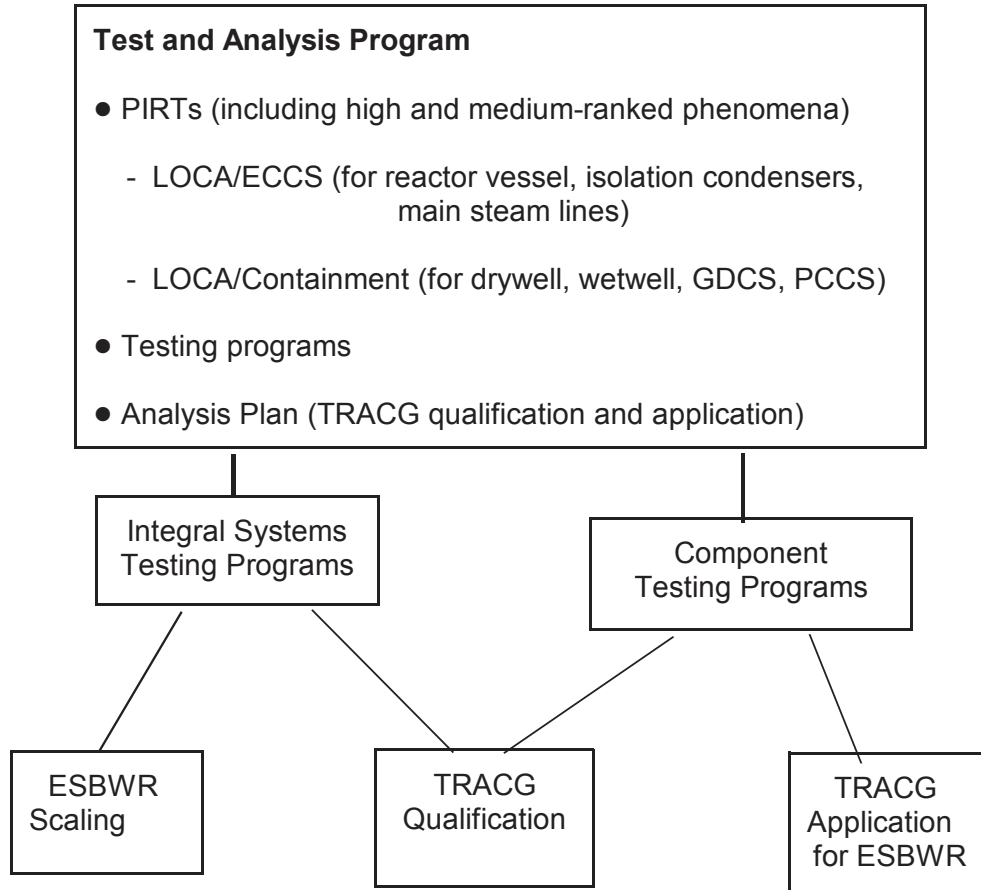


Figure 3.7.1.1 - Test and Analysis Program

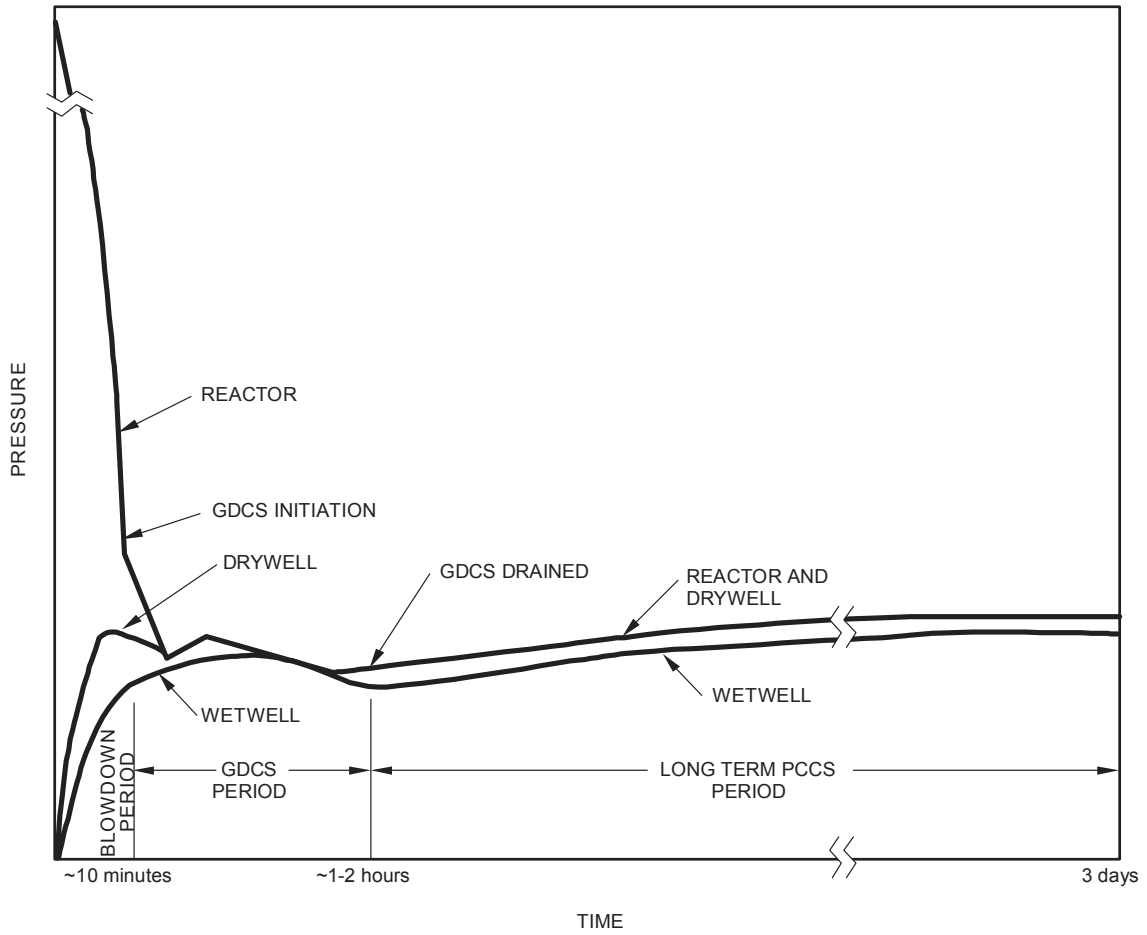


Figure 3.10.1 Time Phases of LOCA Event

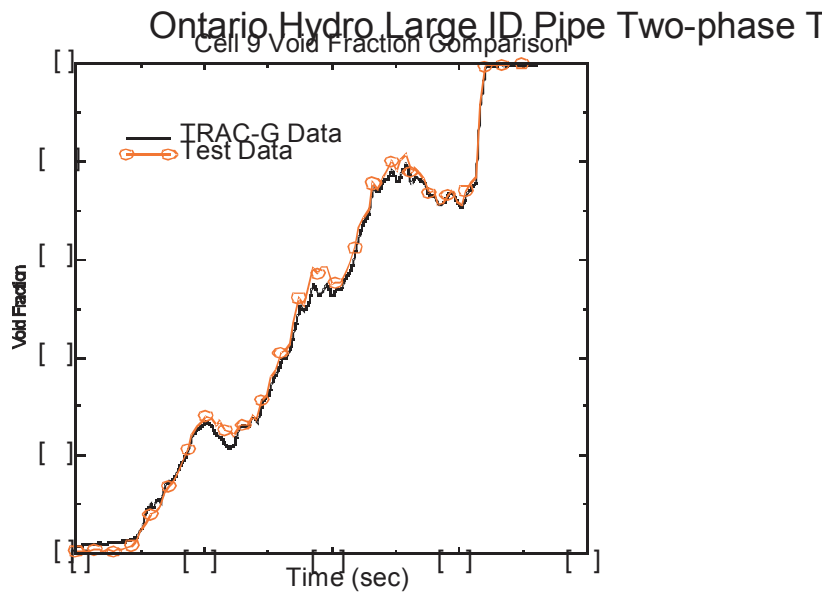


Figure 3.7.2.1 Ontario Hydro Large Pipe Two-phase Flow Testing - Void Fraction

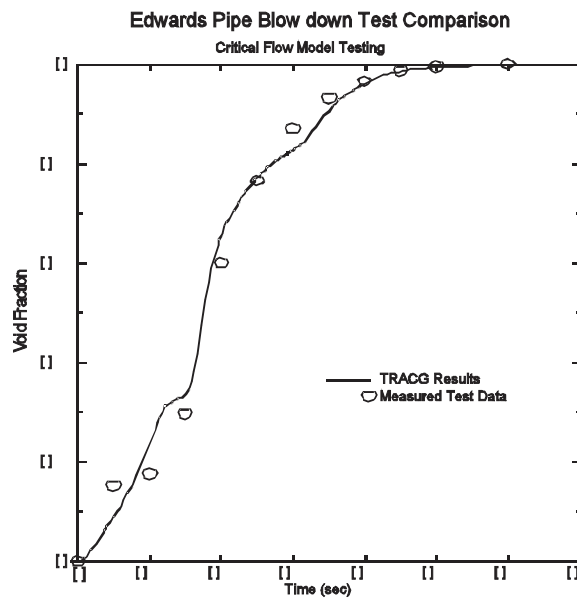


Figure 3.7.2.2 Edwards Pipe Blow Down Test - Void Fraction.

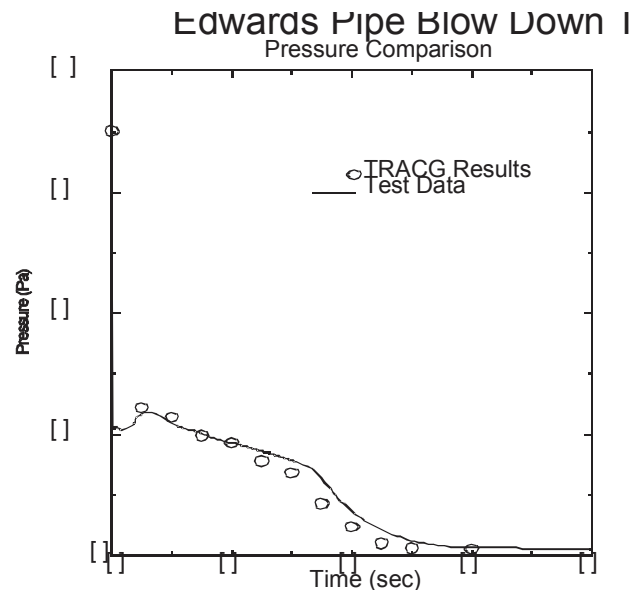


Figure 3.7.2.3 Edwards Pipe Blow Down Test - Pressure

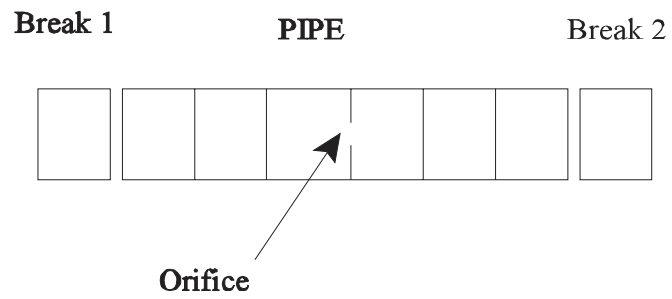


Figure 3.7.2.4 Kinetic Energy Verification Test Problem Nodalization

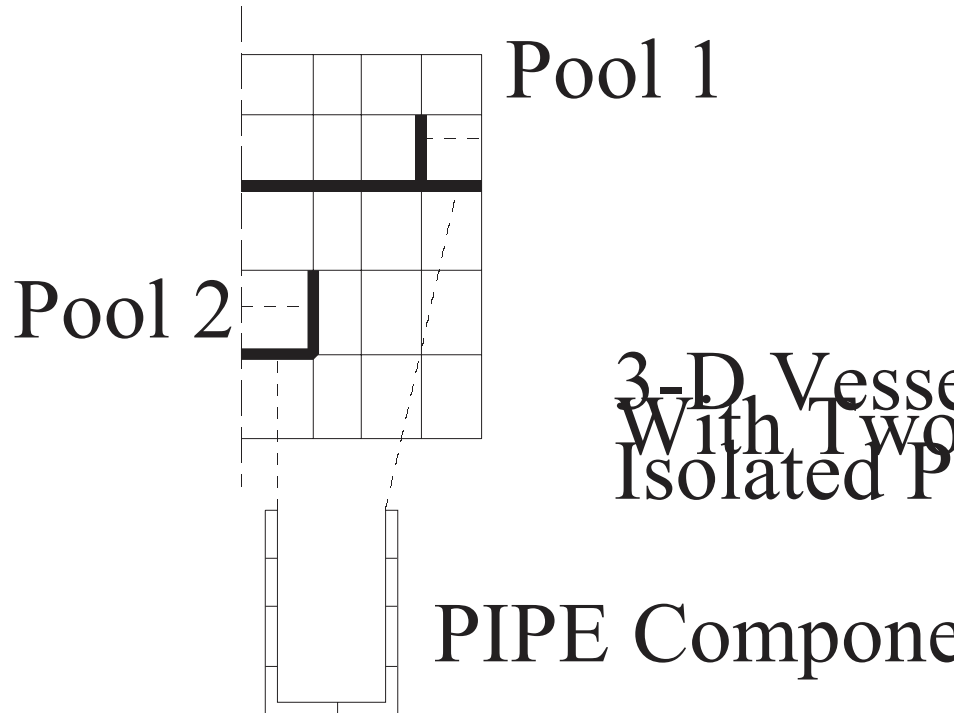


Figure 3.7.2.5 Gravity Head Preservation Verification Test.

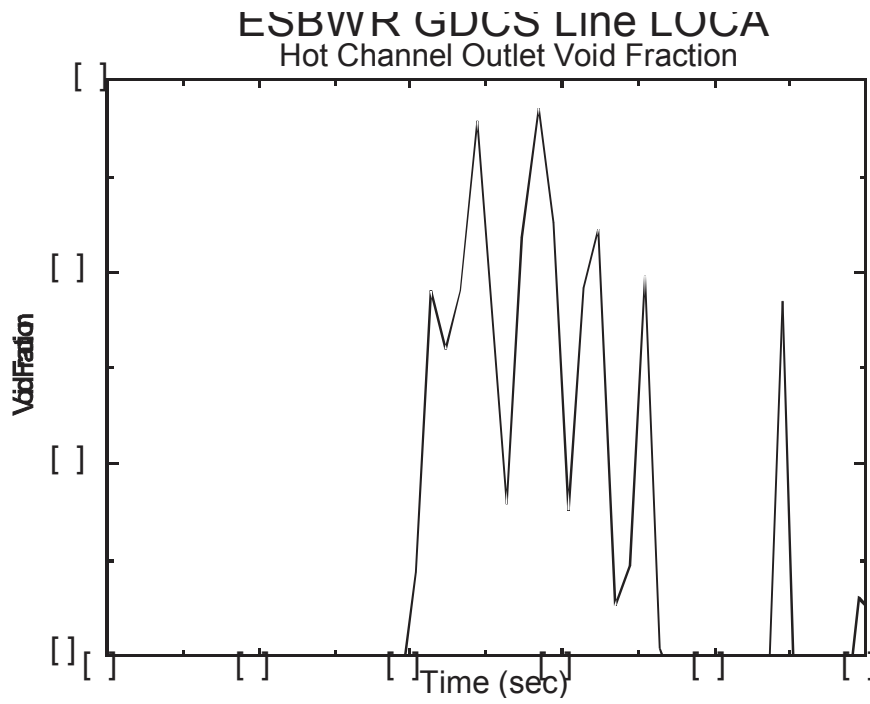


Figure 3.7.2.6 Hot Channel Void Fraction During Blowdown.

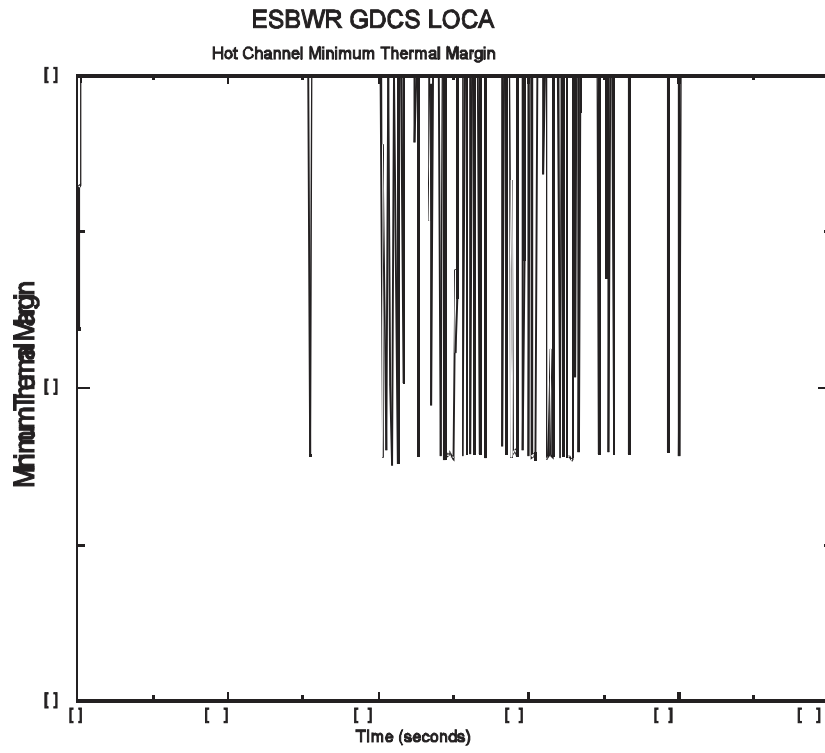


Figure 3.7.2.7 Hot Channel Minimum Thermal Margin During GDCS Line Break LOCA.

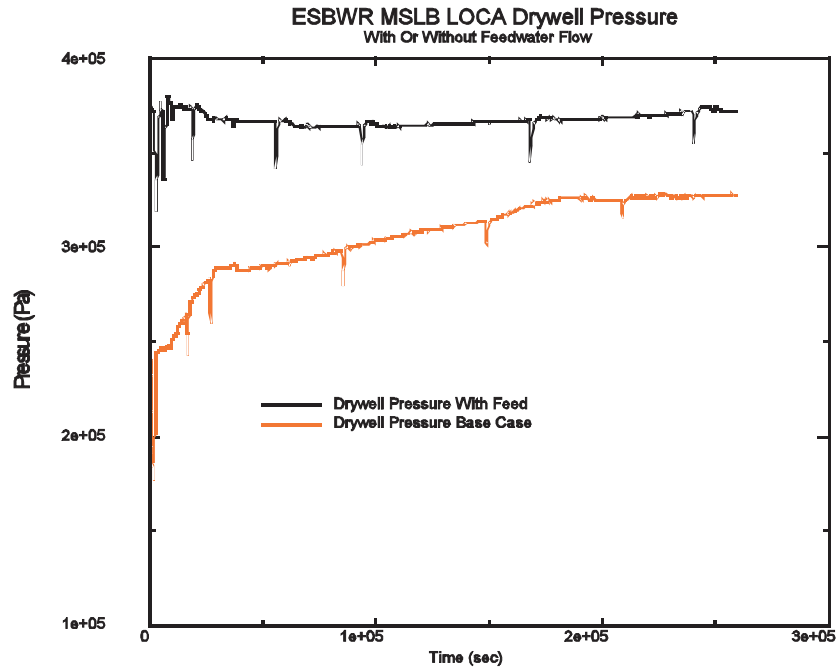


Figure 3.7.2.8 Drywell Pressure With or Without Feedwater Mass And Energy.

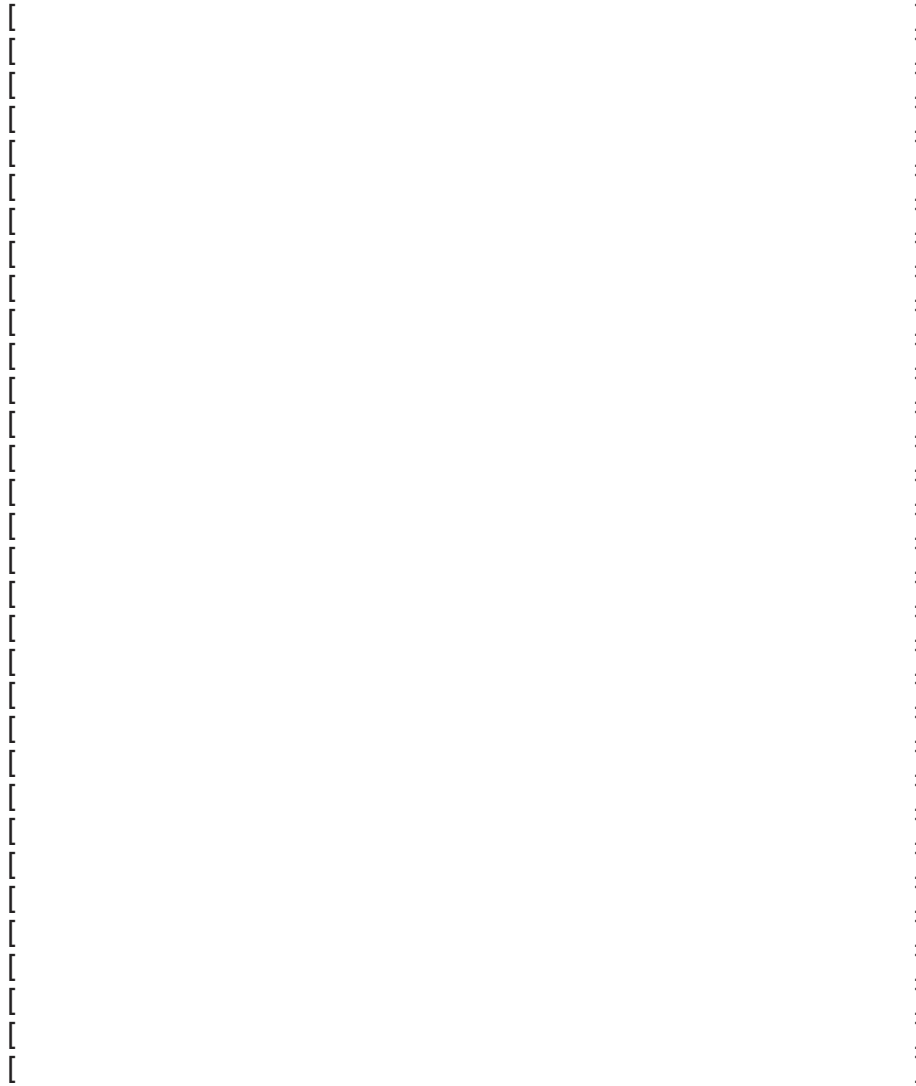


Figure 3.7.2.9 : TRACE ESBWR Reactor Vessel Model

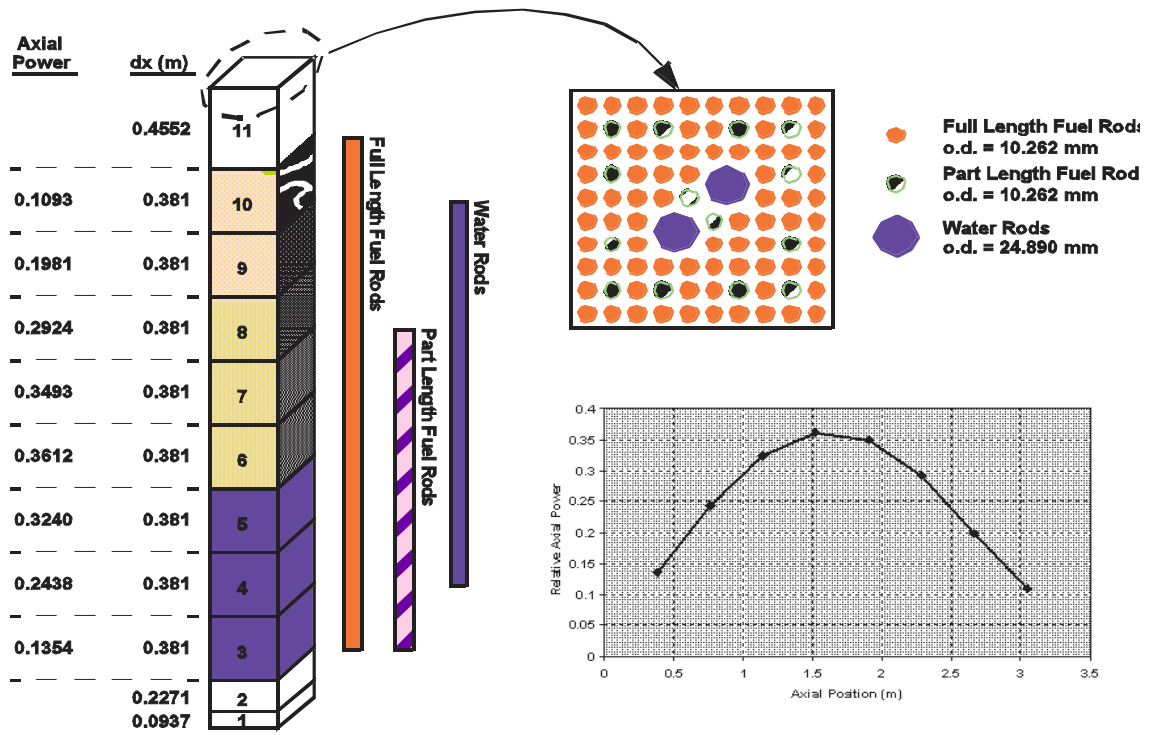


Figure 3.7.2.10 TRACE Fuel Channel Model.

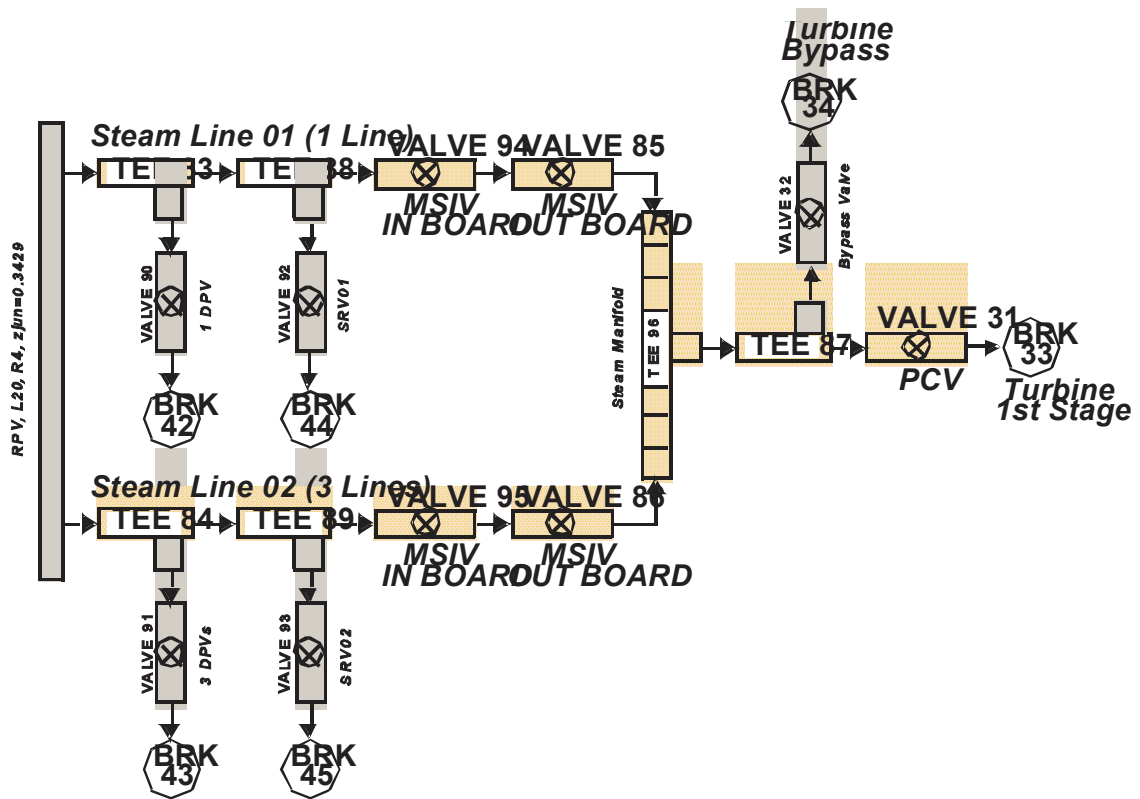


Figure 3.7.2.11 TRACE ESBWR Main Steam Line.

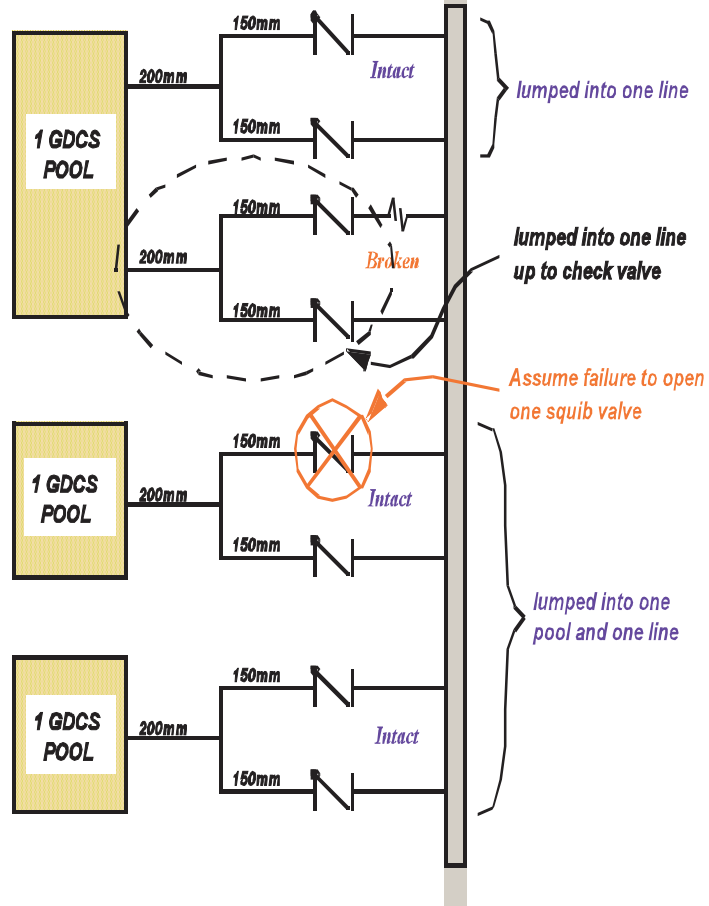


Figure 3.7.2.13 GDCS Line Break Model.

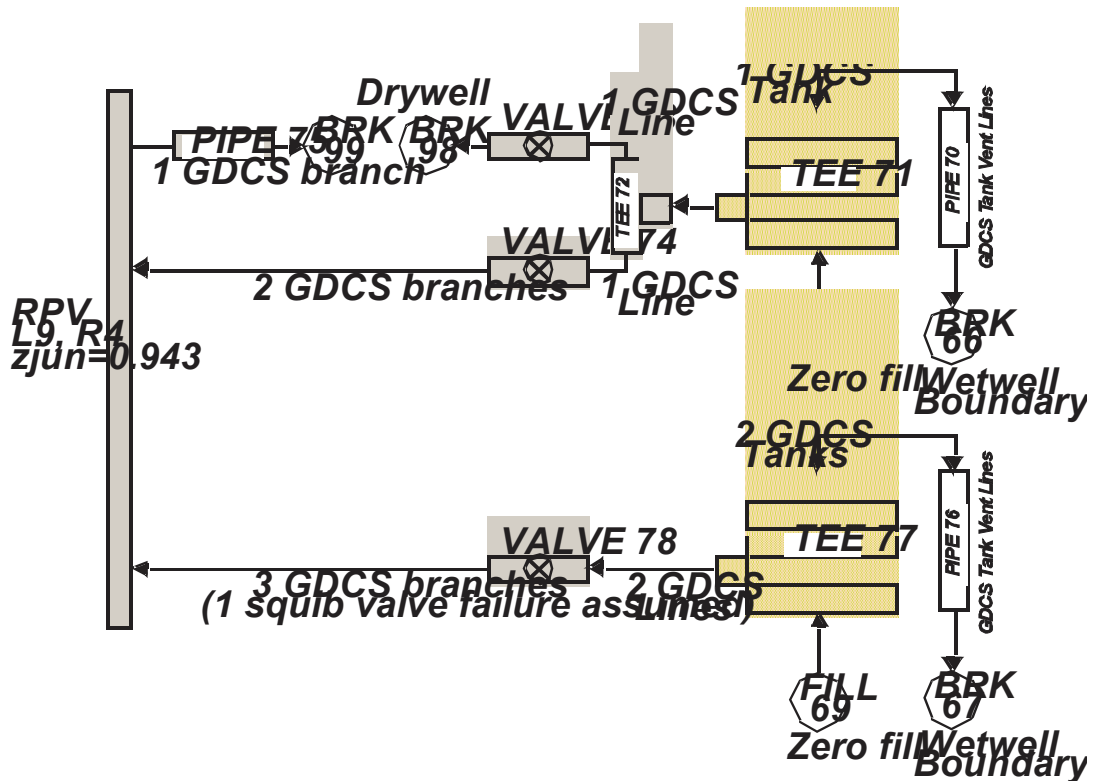
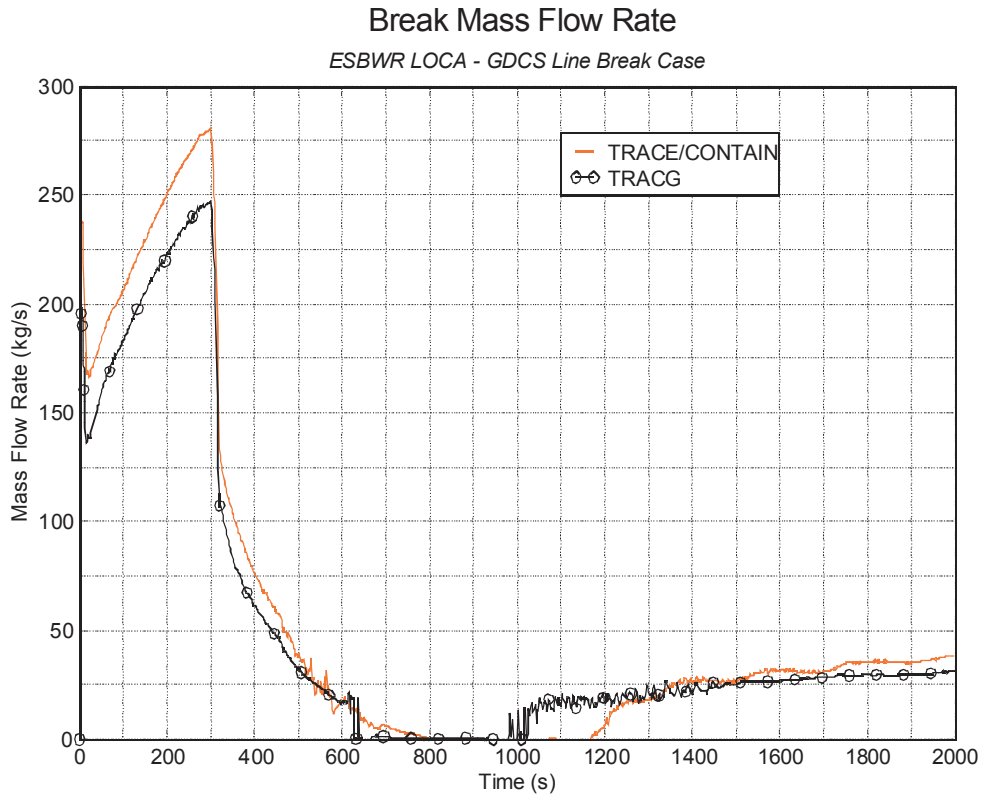
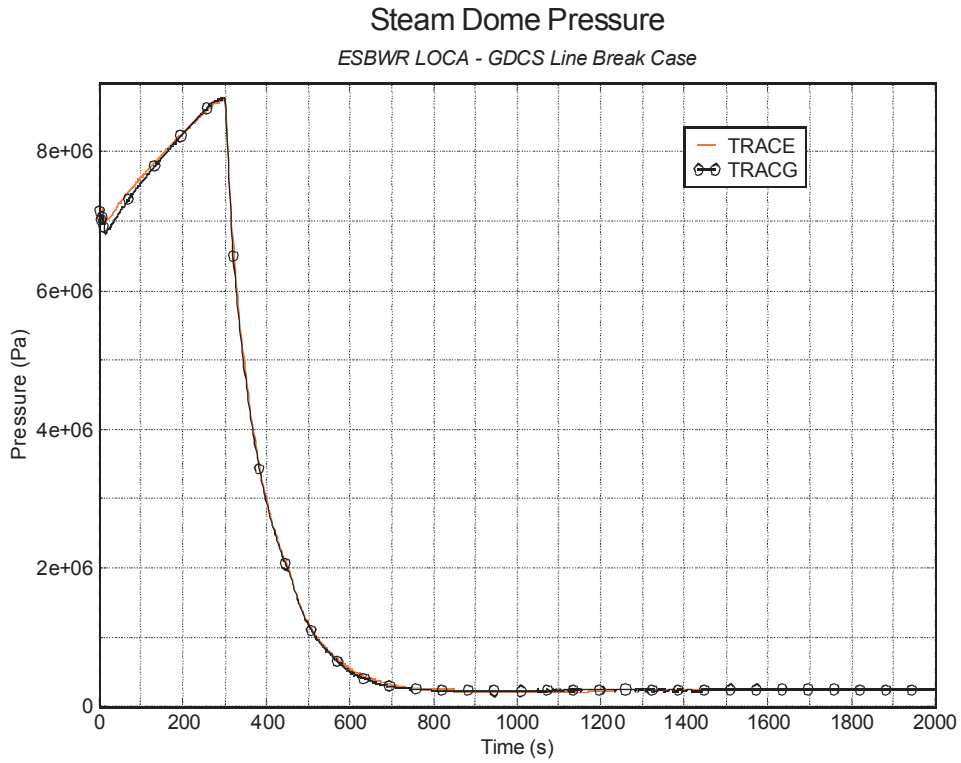


Figure 3.7.2.14 Nodalization of GDCS for the GDCS line Break LOCA Case.



Sat Aug 14 10:05:58 2004

Figure 3.7.2.15 GDCS Line Break Mass Flow Rate.

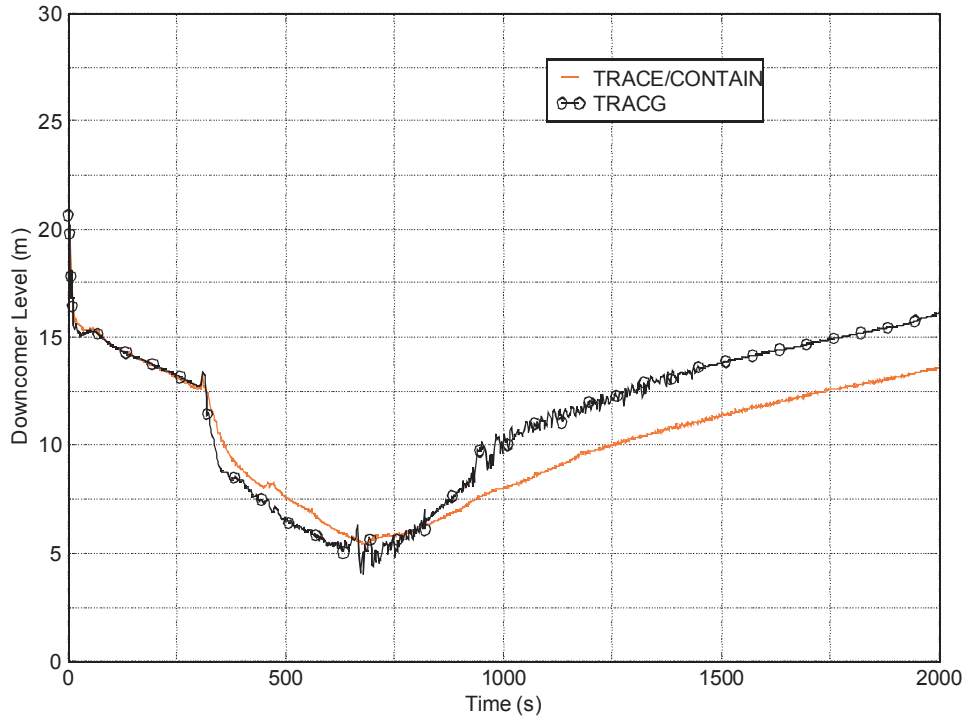


Tue Aug 10 11:57:23 2004

Figure 3.7.2.16 GDCS Line Break Dome Pressure.

Downcomer Collapsed Liquid Level

ESBWR LOCA - GDCS Line Break Case

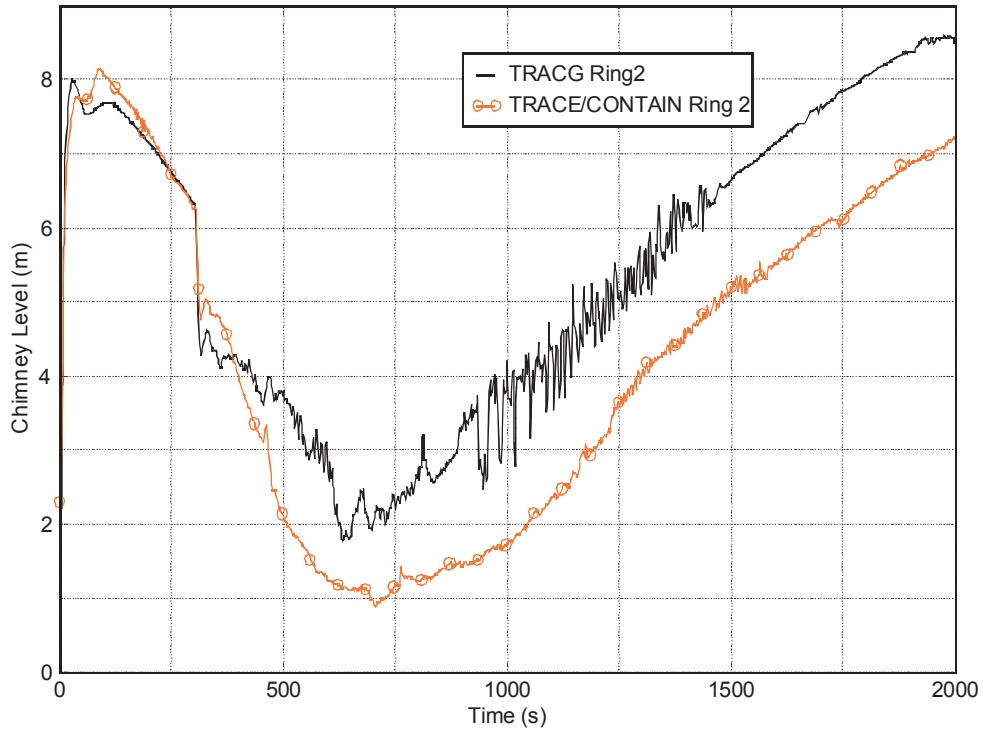


Tue Aug 10 12:06:02 2004

Figure 3.7.2.17 Downcomer Water Level.

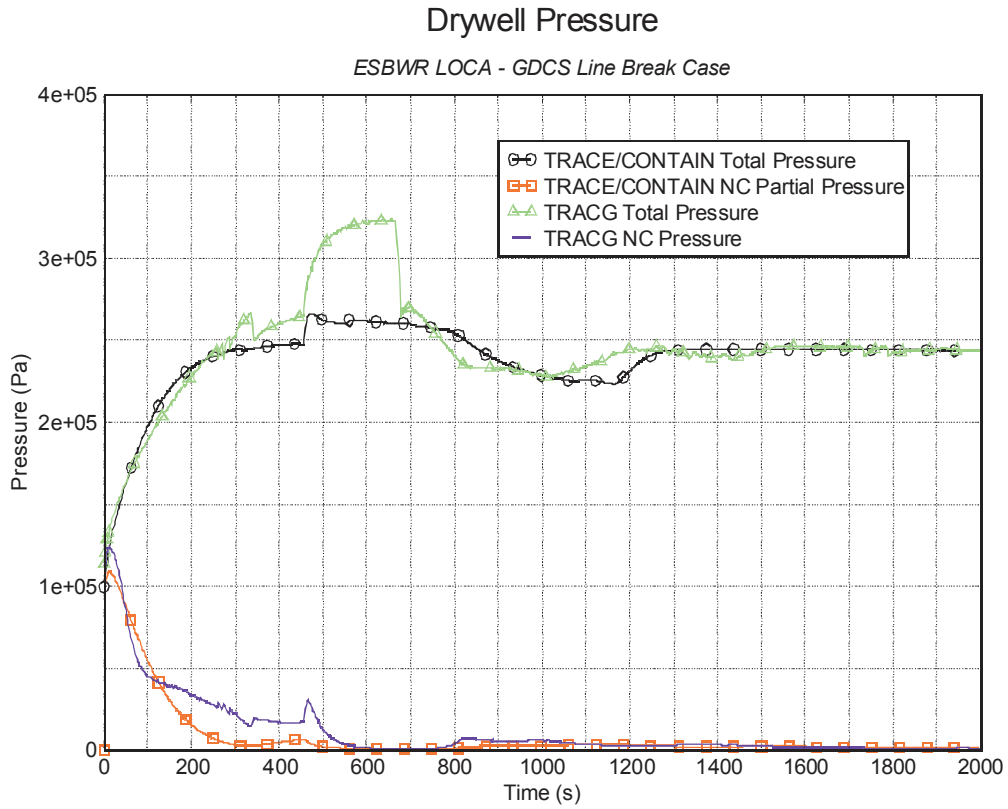
Chimney Collapsed Liquid Level

ESBWR LOCA - GDCS Line Break Case



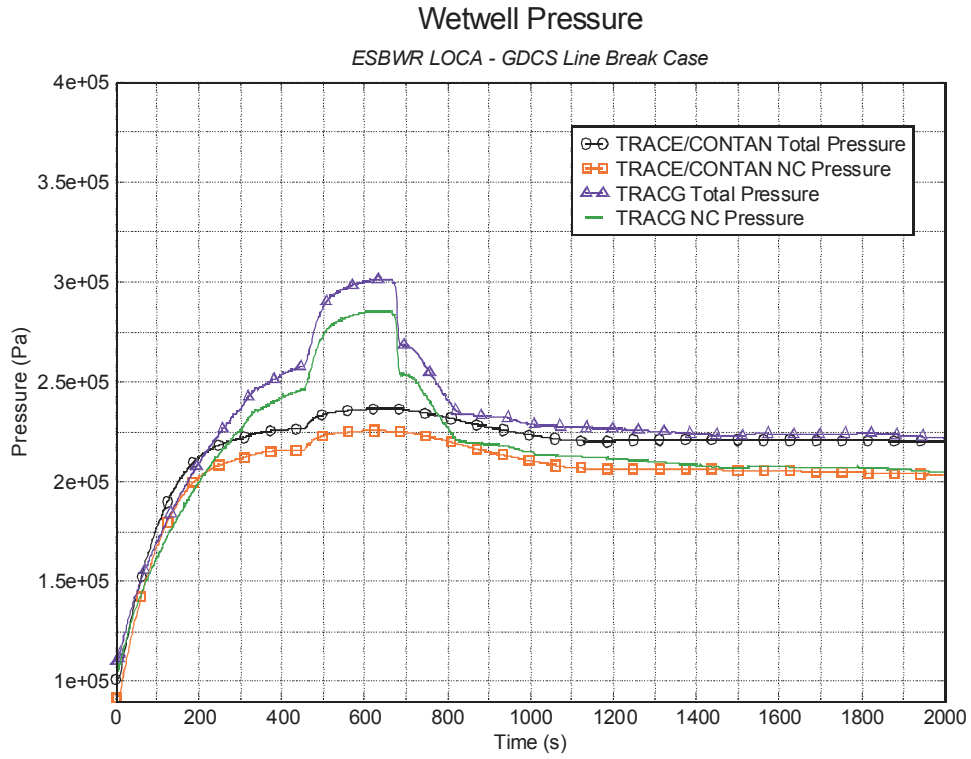
Tue Aug 10 12:15:53 2004

Figure 3.7.2.18 Collapsed Water Level in the Chimney.



Sat Aug 14 10:12:59 2004

Figure 3.7.2.19 Drywell Total Pressure and Non-Condensable Partial Pressure.

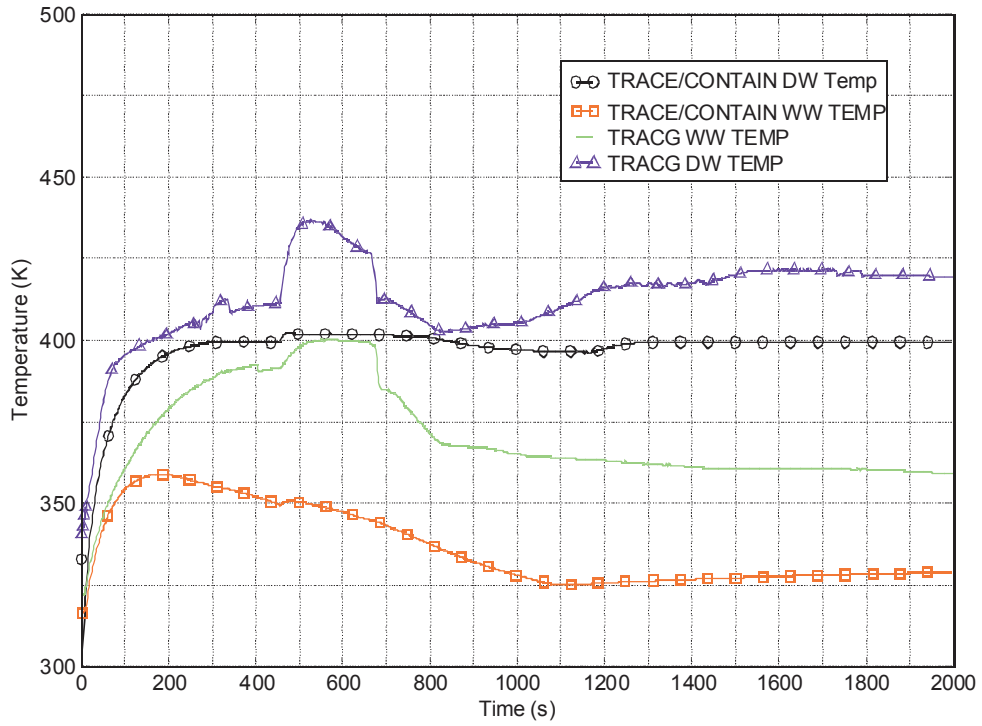


Sat Aug 14 10:20:14 2004

Figure 3.7.2.20 Wetwell Total Pressure and Non-Condensable Partial Pressure.

Drywell and Wetwell Gas Temperature

ESBWR LOCA - GDCS Line Break Case

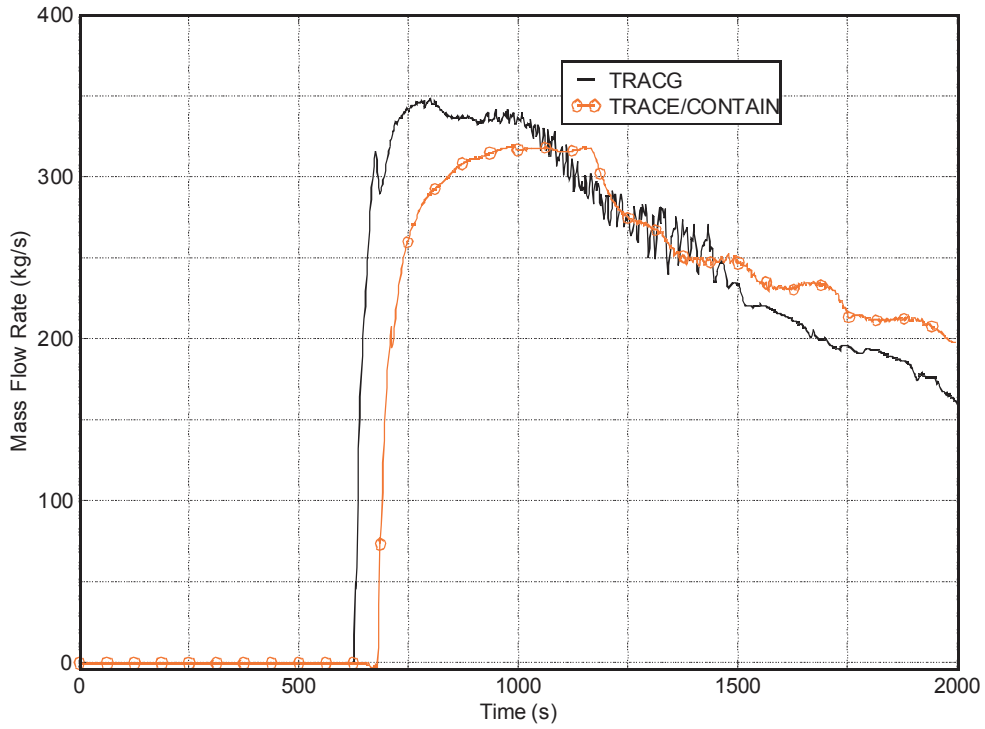


Sat Aug 14 11:26:48 2004

Figure 3.7.2.21 Drywell and Wetwell Atmosphere Temperature.

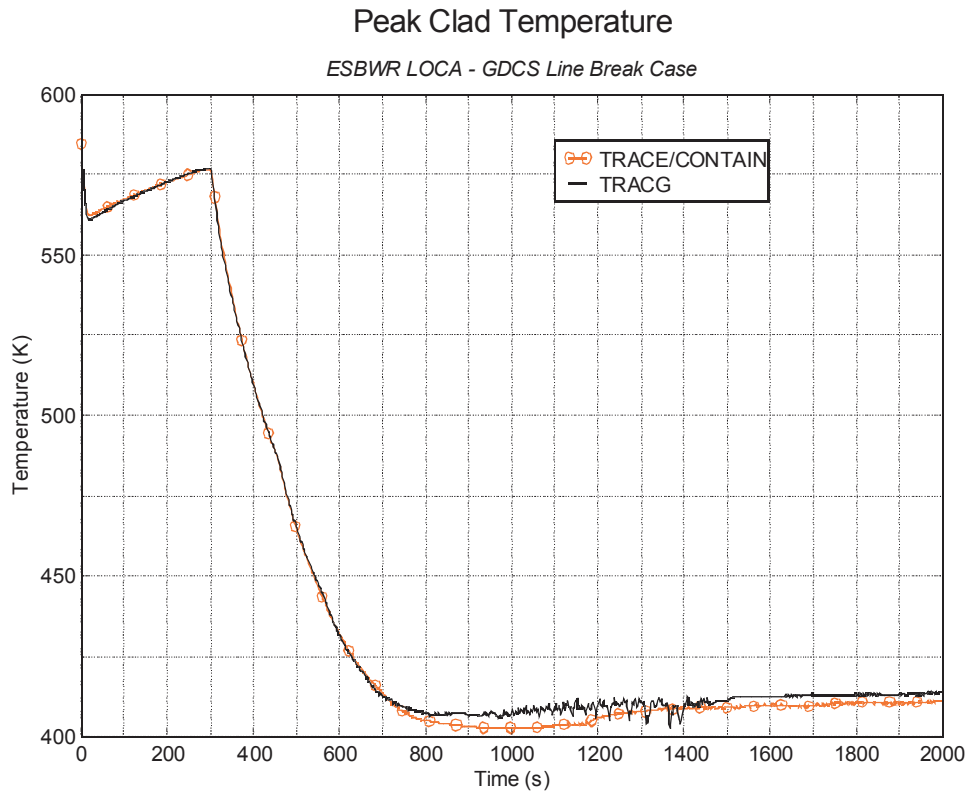
Total GDCS Injection Mass Flow Rate

ESBWR LOCA - GDCS Line Break Case



Fri Aug 13 10:41:06 2004

Figure 3.7.2.22 GDCS Mass Flow Rate



Fri Aug 13 11:09:01 2004

Figure 3.7.2.23 Peak Cladding Temperature

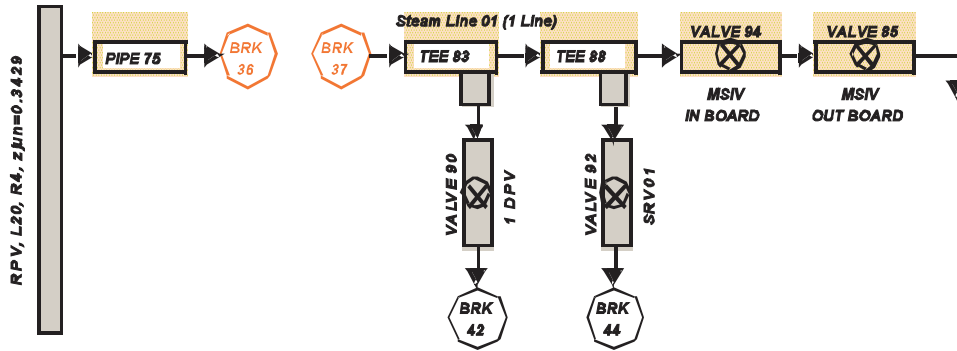
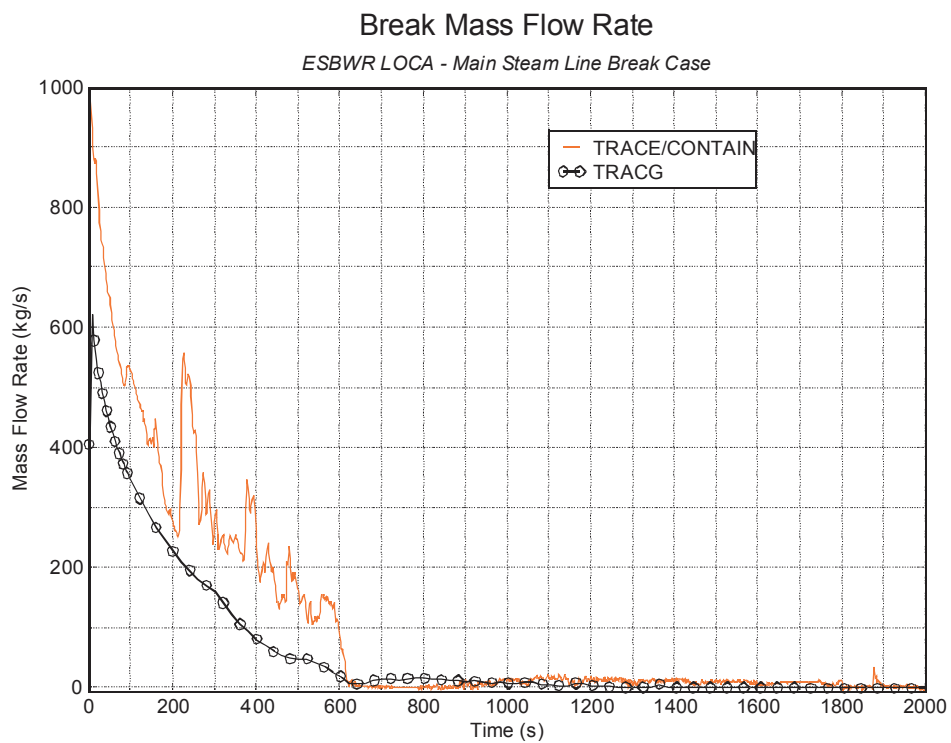
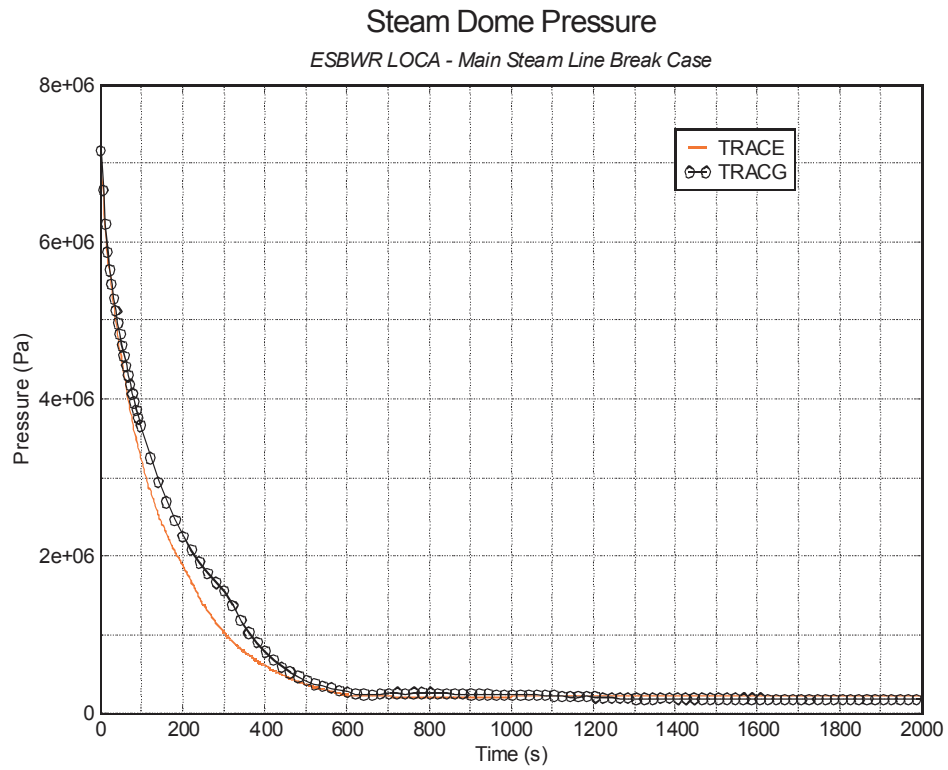


Figure 3.7.2.24 MSLB Broken Steam Line Nodalization.



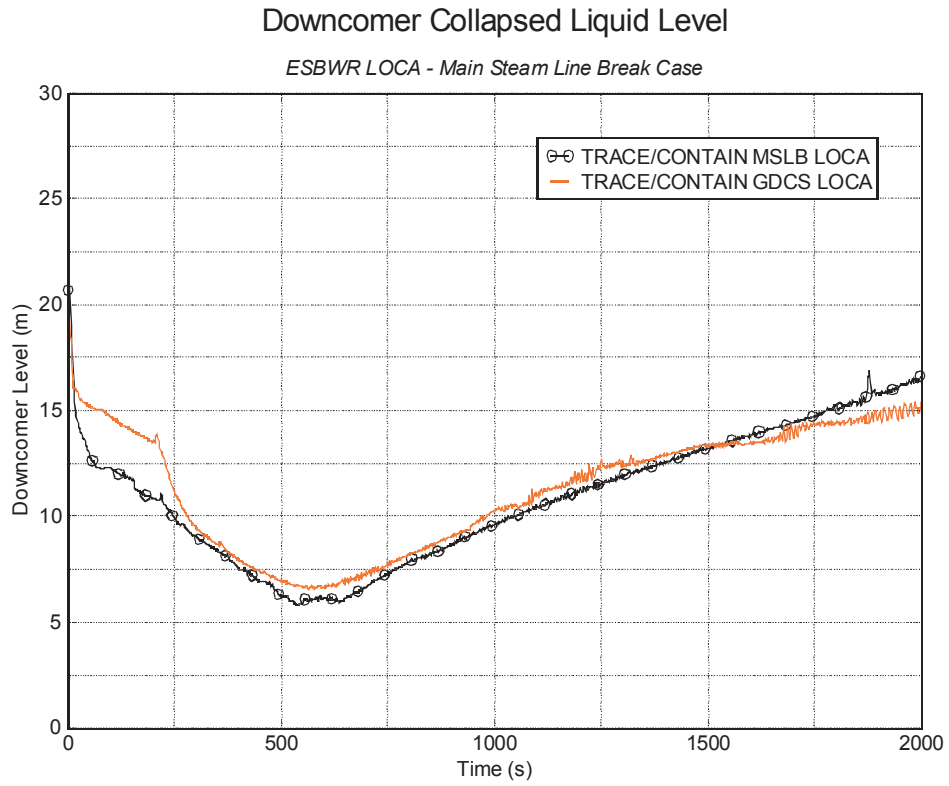
Sat Aug 14 12:05:25 2004

Figure 3.7.2.25 MSLB Break Mass Flow Rate.



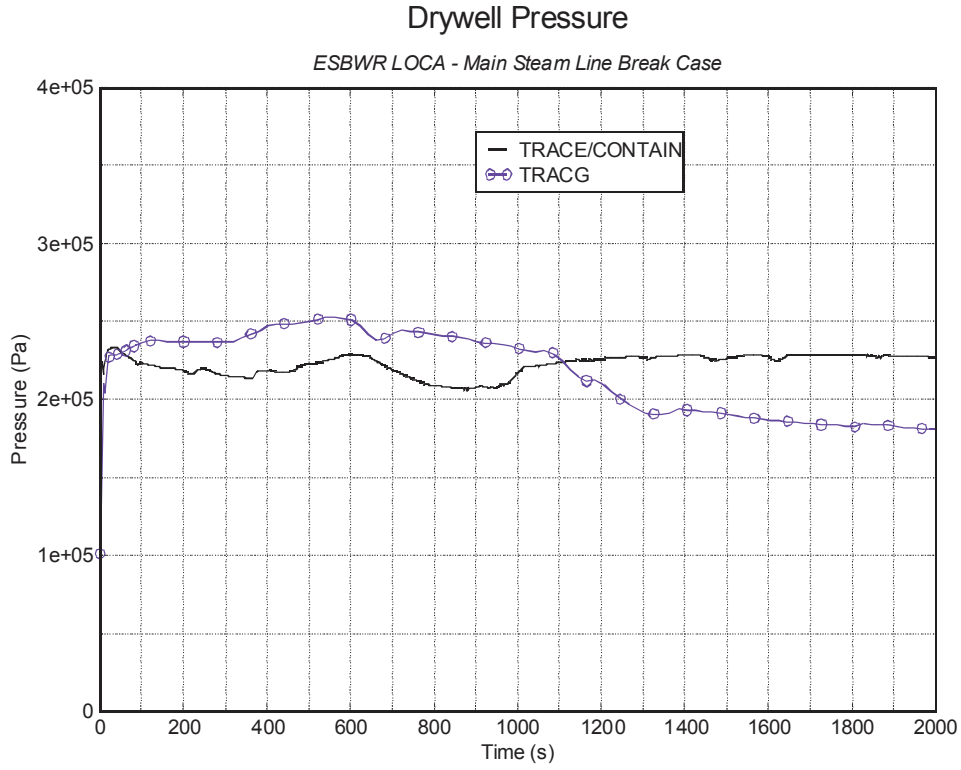
Sat Aug 14 12:20:35 2004

Figure 3.7.2.26 MSLB Steam Dome Pressure.



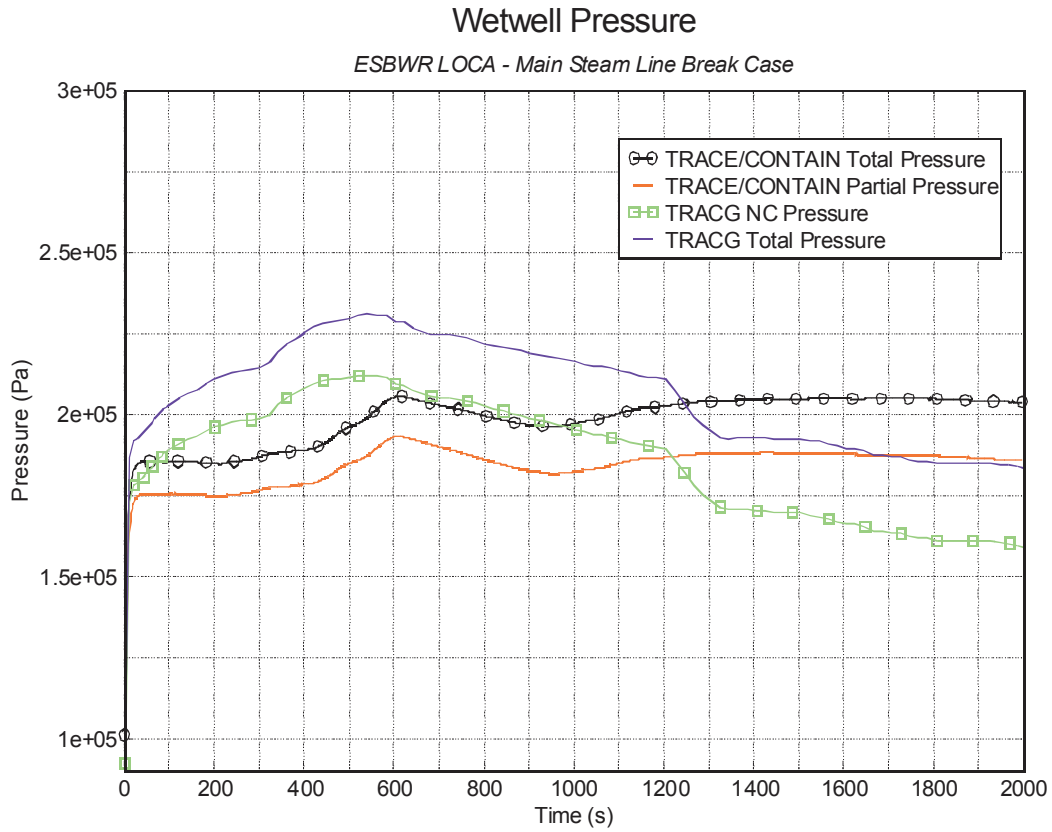
Sat Aug 14 12:40:53 2004

Figure 3.7.2.27 MSLB and GDCS LOCA Downcomer Water Level.



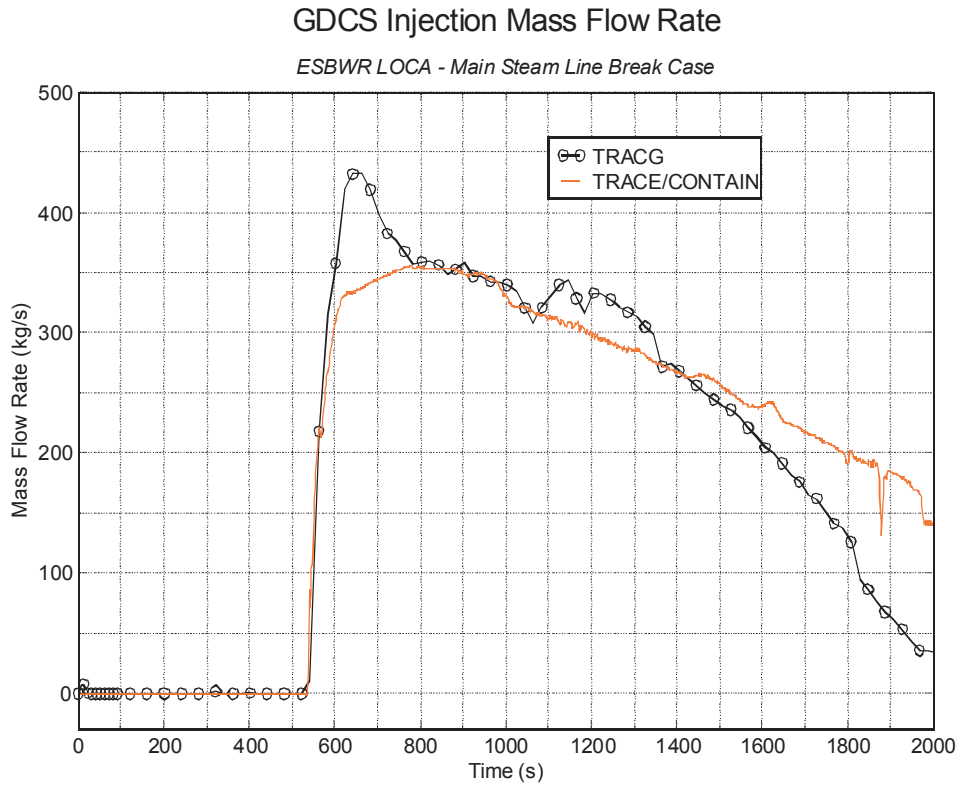
Sat Aug 14 12:50:54 2004

Figure 3.7.2.28 MSLB Drywell Total Pressure.



Sat Aug 14 13:18:17 2004

Figure 3.7.2.29 MSLB Wetwell Total Pressure And Noncondensable Partial Pressure.

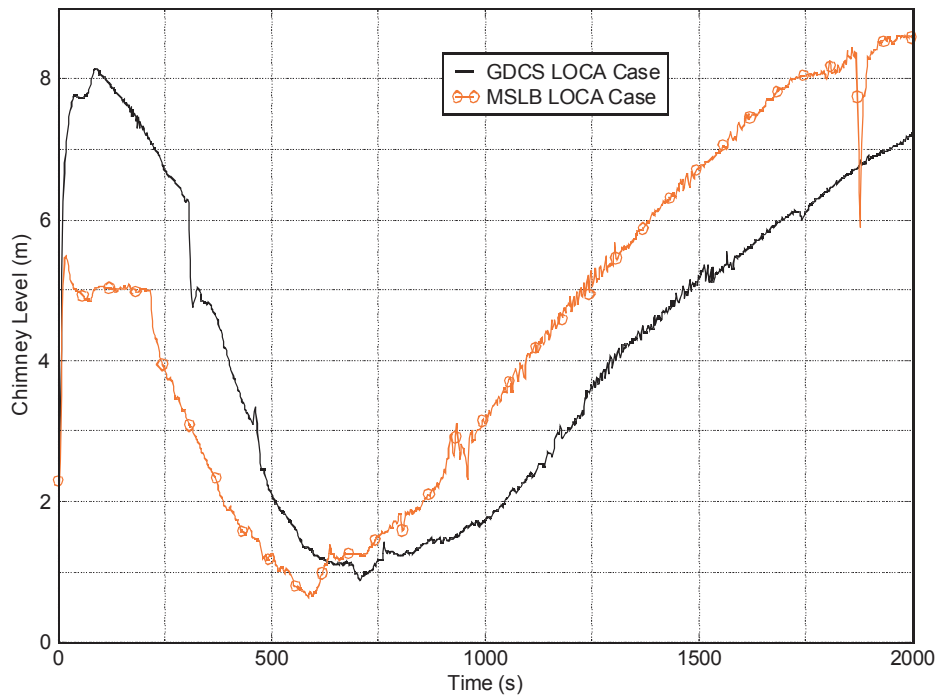


Sat Aug 14 13:56:49 2004

Figure 3.7.2.30 MSLB GDCS Line ECCS Injection Mass Flow Rate.

Chimney Collapsed Liquid Level

ESBWR LOCA - MSLB&GDCS Break Case

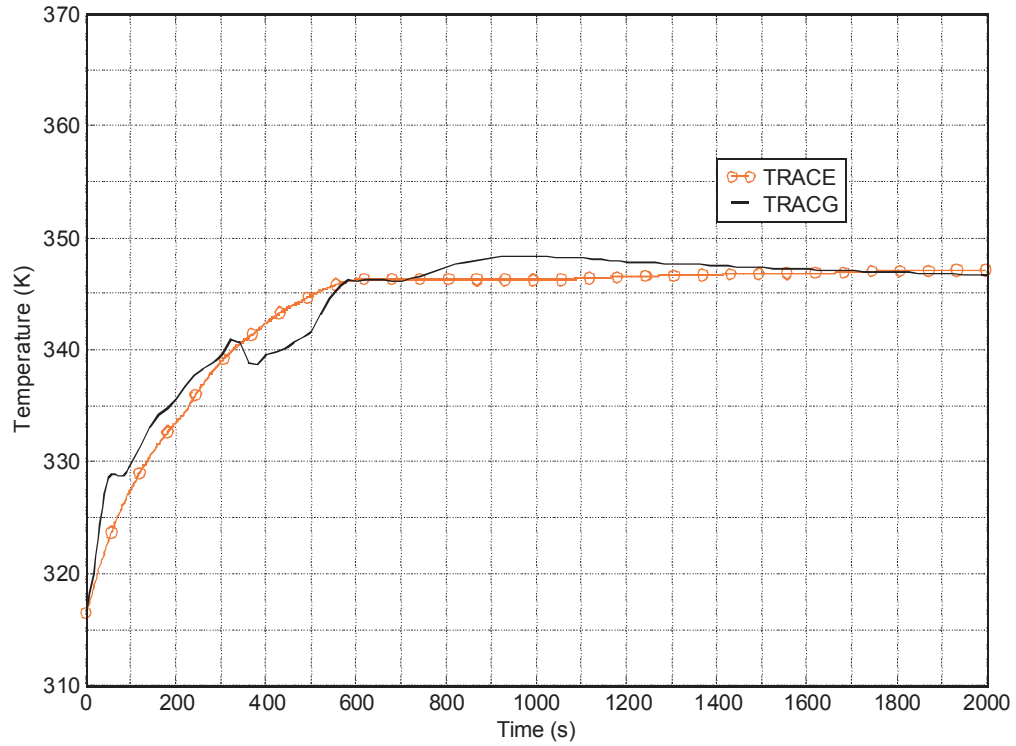


Sat Aug 14 14:13:00 2004

Figure 3.7.2.31 MSLB and GDCS LOCA Chimney Collapsed Water Level

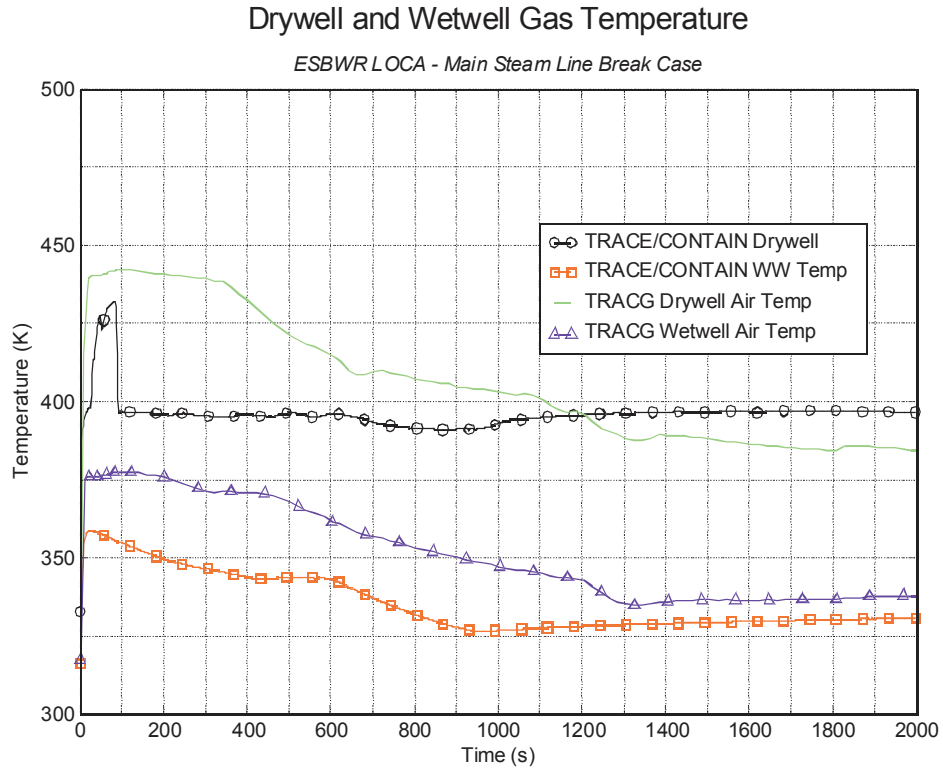
Wetwell Liquid Temperature

ESBWR LOCA - Main Steam Line Break Case



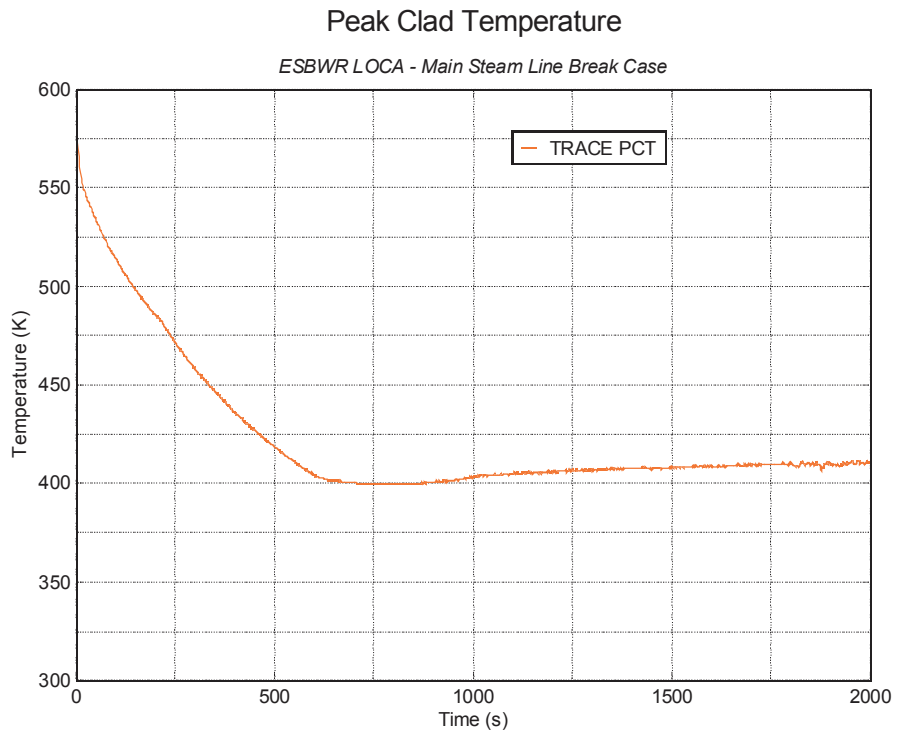
Sat Aug 14 14:21:39 2004

Figure 3.7.2.32 MSLB LOCA Wetwell Liquid Temperature.



Sat Aug 14 14:36:18 2004

Figure 3.7.2.33 MSLB LOCA Drywell And Wetwell Vapor Temperature.



Sat Aug 14 14:02:36 2004

Figure 3.7.2.34 MSLB LOCA Peak Cladding Temperature. Figure

GE ESBWR Bottom Drain Line Break Core Average Channel Void Fraction

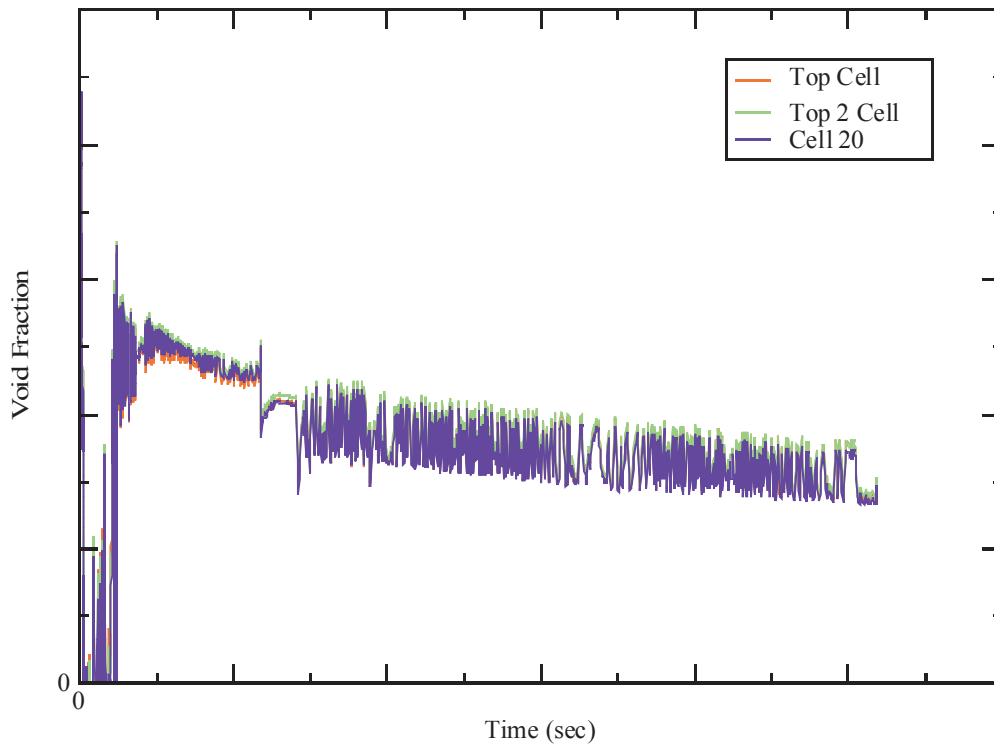


Figure 3.7.2.35 BDLB LOCA Core Average Channel Void Fraction.